SORPTION STUDIES

OF

ACID DYES ON CHITOSAN

By

Yu-Chiu Wong

A Thesis of the Degree of Master of Philosophy

Institute of Textiles and Clothing

THE HONG KONG POLYTECHNIC UNIVERSITY

2002

DECLARATION

I hereby declare that this thesis entitled "Sorption Studies of Acid Dyes on Chitosan" has not been, either wholly or in part, previously submitted to any other institution for a degree or other qualification, and contains no material previously published or written by another person, except where due reference is made in the text.

Yu-Chiu, Wong

ACKNOWLEDGEMENT

I would like to express my sincerest gratitude to my supervisors, Dr. Y.S. Szeto and Dr. G. Mckay for their constant guidance, critical discussion and invaluable comments in the course of research and writing up the thesis. Their consecutive encouragements and supervision made this research possible.

Thanks also go to the technicians in the Textile Chemistry Laboratory, Mr. W.K. Ho and Ms. C.Y. Lung for their kind assistance in the instrumental and technical support throughout my study.

Finally, I would like to acknowledge the financial support provided by the University Research Grant from the Hong Kong Polytechnic University.

ABSTRACT

The feasibility and capability of chitosan as an adsorbent for the removal of acid dyestuffs, namely, Acid Green 25, Acid Orange 10, Acid Orange 12, Acid Red 18 and Acid Red 73 from aqueous solution have been studied.

The experimental data were analysed using Langmuir, Freundlich, Redlich-Peterson equations for each individual dye. The Langmuir isotherm equation was found to provide the best prediction for the sorption of all five acid dyes for the entire concentration ranges. Based on the Langmuir isotherm analysis, the monolayer adsorption capacities were determined to be equal to 645.1, 922.9, 1006.3, 693.2 and 728.2 mg per g chitosan for Acid Green 25, Acid Orange 10, Acid Orange 12, Acid Red 18 and Acid Red 73, respectively. The difference in capacities may due to the effect of molecular size and the number of sulfonate groups of each dye. The results demonstrated that monovalent and/or smaller dye molecules have superior adsorption capacities due to an increase in dye/chitosan ratio in the system, enabling a deeper penetration of dye molecules to the internal pore structure of chitosan.

Due to the inherent bias in using the correlation coefficient resulting from linearization, alternative single component parameters determined by non-linear regression were employed in this study. Five error functions were used, namely, the sum of the squares of the error (SSE); a hybrid fractional error function (HYBRID); Marquardt's percent standard deviation (MPSD); the average relative error (ARE) and

the sum of the absolute errors (EABS). It was found that the Redlich-Peterson isotherm had the lowest values and provided the best fit to the experimental data.

The monolayer adsorption capacities of chitosan increased with increasing temperature from 25 °C to 60 °C and showed no further increment at 80 °C due to the increased the mobility of the large dye ions and the maximum swelling within the internal structure of the chitosan at 60 °C.

Furthermore, the amount of dye adsorbed increased with decreasing particle size due to the inability of the large dye molecule to completely penetrate into the internal pore structure of chitosan and the increase in active surface area exposure for the adsorption of dyes onto the chitosan.

The reformation of the crystalline region within the chitosan occurs due to an increase in homogeneity of the internal structure of chitosan with higher DD% leading to a decrease in the overall monolayer equilibrium capacities.

The kinetics of acid dye removal were investigated by substituting experiment data into those kinetic models, i.e. the pseudo-first order, the pseudo-second order, the modified second order and the Elovich equations. The sorption kinetics of Acid Green 25, Acid Orange 10, Acid Orange 12, Acid Red 18 and Acid Red 73 onto chitosan can be fully correlated by the Elovich equation. The kinetic model was

determined in accordance with the minimum error function and the agreement between the rate equations and the differentiation of kinetic equations.

TABLE OF CONTENTS

LIST OF TABLES

LIST OF FIGURES

CHAPTER 1: INTRODUCTION

1.1 Background

The treatment of wastewater has long been a major concern of the textile industry. Large quantities of aqueous waste and dye effluents, over 4.4 x 10^6 m^3 per day in Mainland China (Wu *et al.*, 1999), are discharged from the dyeing process with strong persistent color and high BOD loading that is aesthetically and environmentally unacceptable (Annadurai et al, 1997). Synthetic dyes are extensively used in dyeing and printing processes. Many of these dye wastes are toxic and even carcinogenic (Vandevivere, 1998), and this poses a serious hazard to aquatic living organisms. As a result, many governments have established environmental restrictions with regard to the quality of colored effluents and have forced dye houses to decolorize their effluents before discharging.

The total dye consumption of the textile industry worldwide is in excess of 10^7 kg per year and an estimated 90% of this ends up on fabrics. Consequently, approximately one million kg per year of dyes are discharged into waste streams by the textile industry. Dye producers and users are interested in stability and fastness and consequently are producing dyestuffs, which are more difficult to degrade after use (Marc, 1996).

A range of conventional treatment technologies for dye removal has been investigated extensively (Lin & Lin, 1993; Ganesh *et al.*, 1994; Walker & Weatherley, 1997;

Philippe *at al.*, 1998; Chu & Tsui, 1999) such as the tricking filter, activated sludge, chemical coagulation, carbon adsorption and photodegradation processes. Adsorption can handle fairly large flowrates, producing a high quality effluent and does not result in the formation of harmful substances, such as ozone and free radicals during the photodegradation process using UV. Therefore, the aim of this research is to study the removal of colour from effluents using adsorption techniques.

1.2 The Aim of the Research

In this research, the ability of chitosan to remove acid dyes namely, Acid Green 25 (AG25), Acid Orange 10 (AO10), Acid Orange 12 (AO12), Acid Red 18 (AR18) and Acid Red 73 (AR73)by adsorption, has been studied. The sorption capacities of dyes on chitosan have been studied using the adsorption isotherm technique. The experimental data were fitted into Langmuir, Freundlich, Redlich-Peterson equations. Five different error analysis methods are used to determine the isotherms parameters, including: Sum of the squares of errors (ERRSQ); Hybrid fractional error function (HYBRID); Marquardt's percent standard deviation (MPSD); Average relative error (ARE); and Sum of the absolute errors (EABS). The normalization method has been used on the error analysis data to find out the most suitable error equation.

The sorption rates of dyestuffs onto chitosan have been investigated by batch contact time studies. The experimental data were substituted into the reaction kinetic models, which were pseudo-first order equation, modified second order equation and Elovich equation. The best-fit equation was determined by the differential form of the rate

equations and the parameters to determine if the sorption of dyestuffs onto chitosan can be represented in terms of reaction kinetic models.

Based on the sorption capacity and sorption rate of chitosan, the effectiveness of chitosan in wastewater treatment can be evaluated.

CHAPTER 2: LITERATURE REVIEW

2.1 General

A dye may be defined as a colored substance capable of application in aqueous or non-aqueous solution or in aqueous dispersion to a substrate so that the substrate acquires a colored appearance. All organic dye compounds containing an unsaturated group or groups absorb light energy, because the electrons are more mobile and cause resonance, which will cause absorption of the lower energy light in the visible range. The characteristic is promoted by the existence in the molecule of one or more of certain unsaturated groups of atoms called chromophores; the most important of them are shown below:

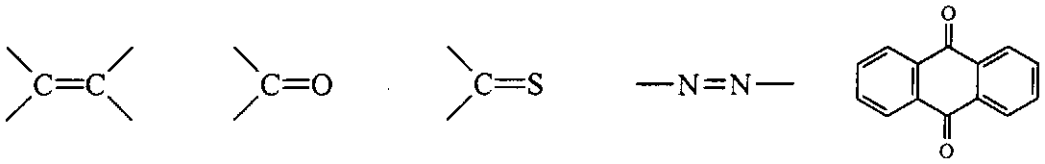

ethylene keto thioketo azo anthraquinone

However, colored molecules (i.e. chromogens) are not dyes unless they contain auxochromes such as amino, substituted amino, hydroxyl, sulphonic groups. Auxochrome constituents do not give rise to strong colors, but have a significant effect on the shade and the solubility character of the chromophoric molecules.

Generally speaking, dyes are classified according to their chemical constitution, or on the basis of their dyeing properties. Consequently, the dyes may be divided into nine classes (Trotman, 1970). These are basic, acidic, direct mordant, sulphur, azoic, vat, disperse and reactive dyes. Only acid dyes of the azo and anthraquinone type, which make up 60-70% of all textile dyestuffs, will be considered in these studies due to their increasing usage recently in industry and since only a limited amount of research on the adsorption of acid dyes on chitosan has been reported.

2.1.1 Dye Chemistry

2.1.1.1 Azo dye

Azo dyes constitute the largest and most varied class of dyestuffs, and they are characterized by the presence in the molecule of one or more azo chromphores (—N=N—), which are linked to sp^2-hybridized carbon atoms. In accordance with the number of such groups the dyes are described as mono, di, tri and poly azo dyes. The azo groups are mainly bound to benzene or naphthalene rings and exist in the trans form. Azo dyes can be further classified in various ways depending on the structure, such as carbocyclic, heterocyclic and metallized azo dyes (Zollinger, 1991).

2.1.1.2 Anthraquinone dye

Anthraquinone dyes are the second most important class next to azo dyes, also one of the oldest types of dyes. Achieving the desired region of the visible spectrum is highly dependent on the positions and strengths of the constituent, amino or hydroxy groups, introduced into the parent compound. In order that an intense colour range

from red to blue can be obtained, anthraquinone dyes are generally characterized by their superior light fastness in comparison with those of many other dye classes. In contrast to the azo dyes, which have no natural counterparts, most of the important natural red dyes are anthraquinones.

2.1.2 Acid Dyes

These dyes are nearly all sodium salts of organic acids and the anion is the active coloured component; in fact, most of them are sulphonic acid salts and some contain carbonyl groups. The acid dyes have a direct affinity towards protein fibres and are the main class used in wool dyeing. The acid dyes can be divided into several groups one of which is the dyes derived from anthraquinone. Many acid dyes, however, will not exhaust on wool at all, unless the dye bath has been acidified, and sometimes Glauber's salt is used as a levelling agent – but the retarding action of salts is only effective at low pH values. With every dye there is a critical pH, above which electrolytes have the reverse effect and promote exhaustion.

2.1.3 Dyes in Effluents

In the textile sector, an estimated 10-20% of dyes (active substance) used is lost in residual liquors through exhaustion and washing operations. For pigments, the rate of loss is about 1-2%, and 10% for paper and leather dyes. All of these, make up to a total of about 30% out of 1.0 billion kg dye consumption as reported in 1994 (Marc, 1996). However, available effluent treatment processes for dye containing effluents are currently capable of removing about half the dyes lost in residual liquors.

Therefore, about 400 tonnes daily, finds its way into the environment, primarily dissolved or suspended in water. Colored organic substances generally impart only a small fraction of the total organic load in a wastewater; however, their high degree of color is easily detectable and detracts from the aesthetic value of river, streams etc. It is a fact, therefore, that as far as the public is concerned, the removal of color from wastewater is often more important than the removal of the soluble colorless organic substances which usually contribute to the major fraction of the biochemical oxygen demand.

2.1.4 Toxicity of Dyestuffs

Toxicity towards humans should be the first property to be ascertained and the crucial factor is the degree of exposure to the manufacturer, the processor, and the end-user. Virtually no toxicity danger threatens the public from dyes used in textiles, papers, leather or pigments. One of the main reasons is that most of the dyes are only slightly toxic to warm-blooded animals, and if properly selected and applied, they are strongly fixed on the material. Toxicity used to be assessed from fairly short duration tests with animals, with growing experimental experience it was later found that there are toxic effects that show up only in the course of long-term studies, continuing throughout the entire life-span of the test animals. This is particularly the case with cancer-causing substances. The list of tests has now grown to include procedures for detecting mutagenic and teratogenic effects. In the light of these new findings, primarily due to carcinogenic effects in animal studies, the number of officially approved dyes is rapidly shrinking. Of particular concern are the effects of dyes on

aquatic organisms, especially fish and algae. Two aspects of aerobic systems were considered; the effects of activated sludge from a typical oxidation system, and the biological oxidation of organic matter in a stream. The effects of dyes on anaerobic systems were also considered. Allen *et al.* (1981) reported the average metal concentration for eight metals in numerous dyes. For almost 900 unmetallised acid, basic and direct dyes, the average concentrations of arsenic, cadmium, cobalt and mercury were reported to be less than 1 ppm. The amounts of chromium, copper, lead and zinc were also reported. Copper and chromium are particularly toxic to the microorganisms present in biological effluent treatment plants, therefore they have to be eliminated to a very large extent. The increasingly tighter controls on effluent discharges in most countries, means that future technology in dyestuffs production, as well as in its application, will bring new basic developments, resulting in considerably smaller amounts of effluents.

2.2 Research on Colour Removal Technologies

Industrial development is pervasively connected with the disposal of a large number of various toxic pollutants that are harmful to the environment, hazardous to human health, and difficult to degrade by natural means. The decolorization of textile wastewater is a worldwide problem to which many diverse technologies have been applied. Methods available for color removal from textile effluents are mainly divided into five categories including physical, electrochemical, photochemical, chemical and biological treatment (Cooper, 1993; Tunay *et al.*, 1996; Philippe *et al.*, 1998; Patricio *et al.*, 1999).

2.2.1 Biological Treatment

In the past, biological treatment systems have been used most extensively for the purification of textile mill wastewater. Under aerobic/anaerobic biodegradation, the chromophore of dyes is readily cleaved and the by-products of aromatic amines are not further metabolized under anaerobic conditions but are readily biodegraded in an aerobic environment (O'Neill *et al.*, 1999; Chang & Lin, 2000). It is noted that most dyes are partially degraded under aerobic/anaerobic conditions less readily, and the rate of degradation is proportional to the structural complexity of the dye molecule, as reported by Sopa *et al.*, (2000). Beydilli *et al.* (1998) demonstrated a fixed-film anaerobic reactor to renovate reactive textile dyebaths and reuse the high salt-containing mixture in the dyeing process. Previous investigations found that there is a trend of more color removal with increased organic loading, which is probably due to the high cellular growth rate and associated color adsorption at higher organic loading rates (Young & Yu, 1997; Grau, 1991).

2.2.2 Chemical Decolourization

Chemical decolorization of the effluent is usually by means of oxidative and reductive degradation process. A variety of oxidizing agents such as chlorine, hydrogen peroxide, ozone and Fenton's reagent were used for decoloration. They have been used to destroy various hazardous aromatic pollutants in solution and chromophoric system of dye molecules.

- The use of chlorinated oxidants, such as chlorine, sodium hypochlorite or chloramines, is effective for color removal and is a low-cost technique (Hamada et al., 1998). However, they are suggested as potentially toxic chlorinated by-products may be formed. Besides, the possibility of the emissions of adsorbable organic halogens (AOXs) including most of the chlorinated monophenolics which may arise from excess chlorine dosage.

- Ozone is a highly powerful oxidizing agent and the oxidation potential of ozone is 1.52 times higher than that of chlorine. The high oxidation potential allows it to degrade most organic dyes (Sarasa *et al.*, 1998; Hsu *et al.*, 1998.). Chu and Ma (2000) reported the direct and indirect ozonation of six textile dyestuffs, including reactive, direct and disperse dyes, in which ozone and hydroxyl radicals generated in the aqueous solution are able to oxidize the dye chromopheres. Nevertheless, the low degradation rate in hydrophobic dyes was considered to be the main drawback.

- Hydrogen peroxide is not a powerful oxidizing agent comparatively, therefore, slower decolourization rate was observed at ambient conditions. There is no decolourization of the textile wastewater with hydrogen peroxide at neutral pH values (Tunay *et al.*, 1996). However, a significant removal efficiency was obtained after 24 hours when the system pH was raised to 12. Furthermore, in the presence of catalysts such as Fe powder (Tang & Chen, 1996) or fly ash (Chaudhuri & Sur, 2000) a faster oxidation rate may result.

- The reduction of bisulfite to dithionite by borohydride, spontaneously dissociates to sulphur dioxide anion radicals which in turn reduce the dye's azo bond is described by Cook (1996). However, Laszlo (1997) discovered the potential drawback of using borohydride and bisulfite is that the treatment of dilute dye solutions results in the generation of large volumes of decolorized wastewater contaminated by boron and potentially toxic aromatic amines.

2.2.3 Photodecomposition of Dye Wastewater

Photofading is one of the important reactions for UV radiation upon dye molecules. The UV light may cause various types of reactions, bringing about structural changes or transformation in dye molecules that might greatly contribute to their degradation in the environment and the photogradation in solution. They can be classified into three principles:

a. Direct photodegradation – processes where degradation proceeds following direct excitation of the pollutant by UV light (Zepp & Cline, 1977)
b. Photooxidation – light-driven oxidation processes principally initiated by active oxidizing species such as singlet oxygen or hydroxyl radicals (Peters & Freeman, 1996).
c. Photoreduction – light-driven reduction processes principally initiated by hydrogen source (Bolton and Cater, 1994).

2.3 Adsorbents

The requirement of adequate adsorptive capacity restricts the choice of adsorbents for practical separation processes to microporous adsorbents with pore diameters ranging from a few to a tenth of angstroms.

2.3.1 Chitin

Chitin is a polymer of the polysaccharide class, a cellulose-like biopolymer containing mainly of β-(1→4)-2 acetamindo-2-deoxy-D-glucose units (Figure 2.1). It is the second most common material distributed in nature, present as an important constituent of the protective cuticle of crustacea and insects, and in the cell walls of some fungi and microorganisms. The processing of shell material to render chitin and then chitosan is illustrated in the flow diagram in Figure 2.2.

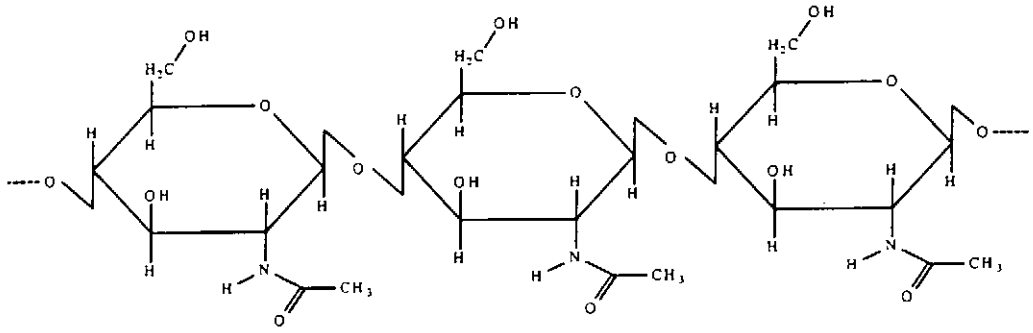

Figure 2.1 Chemical Structure of Chitin

Chitin is an off-white flaky solid substance, which is insoluble in water, dilute acids, cold alkalis of any concentration and most organic solvents. Chitin is the raw material from which another valuable polymer can be formed, such as chitosan.

Chitosan is formed as white solid flakes with a structure unchanged visually from the original purified chitin. Mckay *et al* (1982, 1983) have studied the adsorption isotherms of acid dyes and direct dyes on chitin.

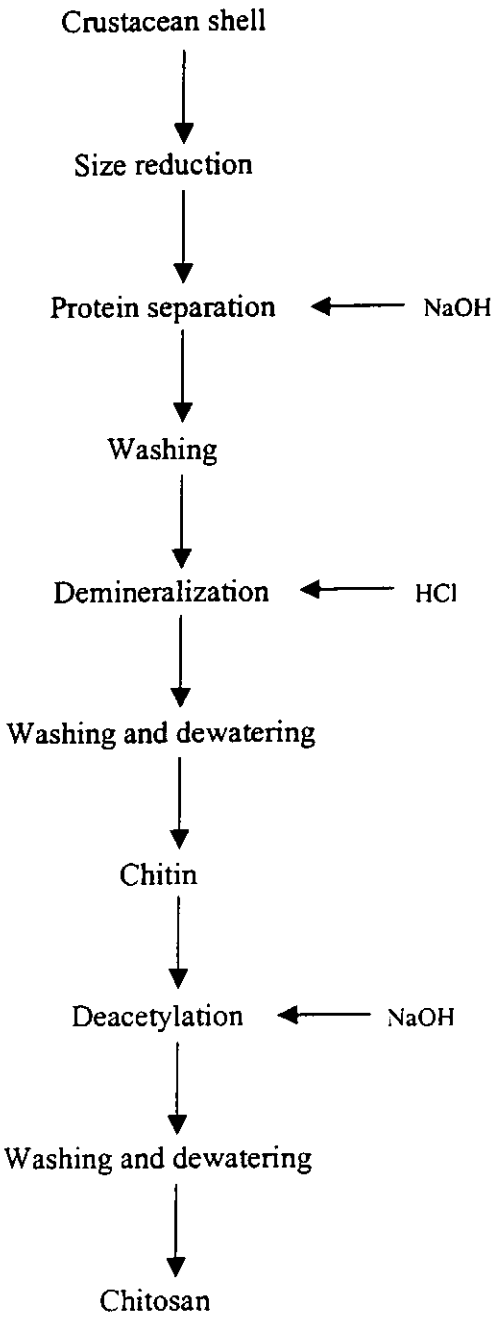

Figure 2.2 Flow Diagram of Chitin and Chitosan Processing

2.3.2 Chitosan

Chitosan is a poly(aminosaccharide) containing mainly of poly (1→4)-2 amino-2-deoxy-D-glucose units (Figure 2.3), usually prepared by the purification and N-deacetylation of chitin with alkaline as shown in Figure 2.2. It is more chemically versatile than cellulose and chitin due to the presence of free amino groups. Furthermore, it is being widely implemented in different industries due to its useful features such as its hydrophilicity, biocompatibility, biodegradability, anti-bacterial properties and high affinity to dyes and some metal ions.

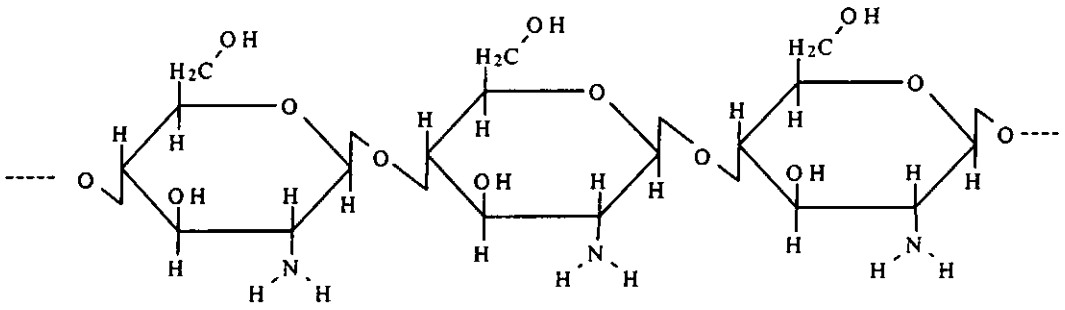

Figure 2.3 Chemical Structure of Chitosan

2.3.2.1 Application Summary of Chitin and Chitosan

The functionality and properties in polymeric, oligomeric and monomeric states of chitin and chitosan lead to great attention in both commercial and scientific development. Table 2.1 lists many of the current and developing applications in the chitin and chitosan field (Mattheus, 1997).

Application	Examples
Water Treatment	Removal of metal ions Flocculant/coagulant Filtration Desalination
Pulp and Paper	Surface treatment Photographic paper Carbonless copy paper Processing additive
Textiles	Finishing treatment Dye fixative Wet-spun filaments Electrospun filaments Decolorizing dye wastewater
Medical	Bandages, sponges Artificial blood vessels Blood cholesterol control Anti-inflammatory Tumor inhibition Anti-viral properties Dental plaque inhibition Burn dressing Artificial skin Eye humor fluid Contact lens Controlled drug release Bone healing treatment
Cosmetics	Make-up powder Nail polish Moisturizers Fixtures Bath lotion Hand cream Toothpaste Shampoo
Biotechnology	Enzyme immobilization Cell recovery Cell immobilization Glucose electrode

Application	Examples
Agriculture	Seed coating Leaf coating Hydroponic fertilizer Controlled agrochemical release
Food	Removal of turbidity from liquids Preservatives Color Stabilization Weight loss products Biodegradable packaging
Chemical production	Oligosaccharides Glucosamine and glucosamine sulfate Chitosan Derivatives
Product separation	Chiral drug separation Bioseparation Pervaporation
Environmental	PCB removal Chemical warfare agent detoxification

Table 2.1 Application Summary of Chitin and Chitosan

2.3.2.2 Sorption of Dyestuffs onto Chitin and Chitosan

Sorption of various dyestuffs onto the chitin and chitosan reported previously demonstrated that the sorption capacities are effected by system parameters such as pH, particle size of sorbent and sorbates, temperature, and initial concentration of sorbate.

Effect of pH

Previous investigations showed that the system pH was one of the prime factors influencing the adsorption of textile dyestuffs on chitin and chitosan. Yoshida *et al.* (1991) demonstrated a feasible technology for the recovery of acid (Acid Orange II) and direct (Brilliant Yellow) dye by using Chitosan Fiber (ChF) and the treatment performance was execellent at pH 6.9. Michelsen *et al. (1993)* showed that for the removal of Navy 106 stack wash water discharge shows the optimum efficiency occurred at pH 4.6 on chitosan. However, adsorption of reactive verifix showed its optimum performance at pH 9.5 and was due to the influence of the intraparticle diffusion rate constant (Kp) and adsorption rate constants. Stefancich *et al (1994)* reported that no interaction was observed between cationic dyes (Neocuproin hydrochloride, Ethidium bromide, Ruthenium Red, 1-(2-pyridilazo)-2-napthhol) and chitosan in the pH range of 5-6. Smith *et al. (1993)* and Shimizu *et al. (1995)* showed that sorption of anionic dyes onto chitosan were related to the protonation of the chitosan's free amino groups at low pH. According to Knorr *(1983)* and Ravi Kumar *et al. (1998),* the dye binding capacity of chitin was stable within a pH range of 2.0-7.0. The same conclusion was made for chitosan in the pH range 7.0 to 5.5, but below 5.5 the chitosan capacity could not be evaluated since chitosan dissolved in the system. It was also suggested that desorption of dyed chitin and chitosan took place at pH > 7.

Effect of particle size

Mckay *et al. (1982)* and Annadurai *et al. (1997)* observed the amount of dyestuffs adsorbed by chitin and chitosan was strongly affected by the particle size of the absorbent. The amount of dye adsorbed increased with decreasing particle size due to the inability of the large dye molecule to penetrate into the internal pore structure of chitin and chitosan. This phenomenon was further proved by Smith *et al. (1993)* in which a series of dyestuffs with same chemical functional group but having a different range of molecular weights were tested. The experimental findings demonstrated that the adsorption capacity of monoazo dyes, named: Mordant Black 17 (m.w.375), Acid Blue 193 (m.w. 479) and Acid Red 1 (m.w. 509) decreased substantially from 9.21 mg/g to 8.43 mg/g and 7.13 mg/g respectively. Annadurai *et. al. (1997)* concluded that specific dye uptake of reactive dye (verofix red) and basic dye (methylene blue) at equilibrium increased by about 10 – 40% with different particle size ranges due to the increase in total surface area made available for adsorption.

Effect of Temperature

Temperature is another prime factor, which affects the adsorption performance. However, the effect of temperature on binding capacity varied among the various dyes. Mckay *et al. (1982)* studied the effect of temperature on the adsorption of four dyestuffs, namely: Acid Blue 25, Acid Blue 158, Mordant Yellow 5 and Direct Red 84 on chitin. The results concluded that the adsorption capacity of direct dye decreased about 53% resulting from the increment of temperature from 20 °C to 80

°C. This is probably due to the desorption mechanism as temperature increased . However, acid dye showed an increase in adsorption capacity from 40 mg/g at 20 °C to 135mg/g at 60 °C. This would be due to the increase in the mobility of the large dye ion and the swelling effect in the internal pore structure of the chitosan enabling deeper penetration of dye molecules. Yoshida *et al. (1991)* indicated that at lower concentration level, the higher temperature, the smaller the amount of adsorption of Brilliant Yellow on chitosan fiber. The amounts of adsorption, however, increase more significantly at high temperature at a higher concentration level. The intrafiber effective diffusivity on the breakthrough curve of ChF-B at 50 °C is about two times larger than that at 25 °C. Apart from these, the adsorption at higher temperature becomes more dependent on intraparticle diffusion, which would be the rate determining step. Therefore at higher temperature, the adsorption rate and the capacity of the reactive dye increase.

Effect of Initial Concentration

Initial dye concentration has been shown to significantly affect the dye-binding capacity of chitin and chitosan performed by Knorr *(1983)* and Ravi Kumar *et al (1998)*. The treatment performance showed that the dye-binding capacity of chitosan was 25-30% greater than chitin at the same initial dye concentration level. Besides, they also found that increase dosage of chitin or chitosan, i.e. four times, to the system would decrease in the dye-binding capacity about 50%. The dye-binding capacity of chitin and chitosan was being enhanced about 25 and 9 times respectively, if the initial dye concentration increase form 0.2 mg/g of chitin to 1.6 mg/g of chitin.

According to Mckay *et al. (1982)*, the film mass transfer coefficients appeared to be independent of initial dye concentration for the adsorption of Mordant Yellow 5 on chitin because there was no apparent difference in the initial gradients. However, the rate of adsorption at the lower initial dye concentration was about 20-50% higher than the rate at the high initial dye concentration. The adsorption of Chitosan Fiber on Acid Orange II and Brilliant Yellow using a column study showed that the amount of the dye adsorbed increased with increase in initial dye concentration due to the increase of the intrafiber effective diffusivity with concentration was reported by Yoshida *et al* (1991, 1993, 1997). Safarik *(1995)* showed that the adsorption of organic polycyclic molecules (Acridine Orange, Congo Red, Safranin O, Neutral Red and Crystal Violet) was a chemical, equilibrated and saturatable mechanism, and therefore adsorption increased with the initial dye concentration, as long as binding sites were not saturated. Almas *et al.* pointed out that the time required to reach equilibrium increased considerably as the initial dye concentration increased for the adsorption of Direct Red 31, no such trend was evident in the adsorption of Reactive Red 73.

2.3.3 Wool Waste

Wool waste discarded from wool manufacturing processes has been used as an adsorbent material for the removal of surfactants and dyestuffs from simulated wastewater (Perineau *et. al.*, 1983). The adsorption isotherms as well as the adsorption kinetics of the surfactants and dyestuffs have both been studied. The

results show that wool waste could be used successfully for wastewater treatment (Perineau *et al.*, 1983)

2.3.4 Bagasse Pith Waste

Bagasse is the waste of sugar mills. It is composed of true fibre, pith and fines, but the true fibre is the only part of real value for pulp and paper. The pith cells are normally removed as completely as possible before pulping. Mckay et al., (1987, 1988) studied the adsorption isotherms and kinetics of the dyestuffs onto bagasse pith in an agitated batch adsorber and fixed-bed systems and the results were fitted to the Langmuir, Freundlich and Redlich-Peterson isotherms.

2.3.5 Activated Carbon

Activated carbons are carbons that generally have a high surface area and complex pore structure resulting from physical or chemical activation processes. The role of activated carbon as an adsorbent material to remove contaminants from liquids and from gases is well established. Adsorption processes involving activated carbon have long been regarded as conventional treatment processes that can remove a multitude of pollutants. Users of activated carbons have often viewed the carbon as a general solution to their effluent problems. Ongoing research has demonstrated that activated carbons and other adsorbent materials can be developed with properties that make them more specific and improve their adsorption characteristics.

2.3.6 Agricultural Waste Materials

Agricultural waste materials such as bagasse pith, sawdust, maize cob rich bran, rice hull, coconut husk fibres, nut shells, soybean and cotton seed hulls have been evaluated for their adsorption properties. These materials have been reported to adsorb different pollutants such as heavy metal ions, dyestuffs and other toxic pollutants (Okieimen *et al.*, 1991; Marshall *et al.*, 1993; Marshall and Johns, 1996). Sawdust waste (Asfour *et al.*, 1985) and bagasse pith (Mckay *et al.*, 1987; Marshall and Champagne, 1995; Marshall and Johns, 1996) have been reported as capable of adsorbing heavy metal ions and dyestuffs from aqueous effluents.

2.3.7 Clay Minerals

The ability of Fuller's Earth to adsorb dyestuffs from aqueous solutions has been studied by Mckay et al., (1985). The adsorption isotherms for the removal dyestuffs by Fuller's Earth and clays have both been studied. The results indicated that Fuller's Earth has considerable potential as an adsorbent material for the removal of dyestuffs in a commercial system (Mckay et al., 1987). El-Geundi, (1991) carried out an analysis of the natural clay and showed that it was composed mainly of kaolinite and montmorillonite, about 51% and 46% respectively. The results demonstrated that natural clay has a good adsorption capacity for the removal of dyestuffs and to an lesser extent heavy metal ions from simulated wastewater.

2.3.8 Maize cob waste

El-Geundi, (1991) reported the feasibility of using maize cob waste as natural adsorbent material for the removal of dyestuffs from simulated wastewater. The experimental results showed that Langmuir, Freundlich and Redlich-Perterson isotherms could be well correlated with the experimental data. Maize cob waste was shown to possess an affinity for dyestuffs of such a magnitude so as to make its use as an adsorbent a possible alternative to the use of more expensive activated carbon.

2.4 Adsorption Systems

Adsorption is a process, which involves the contact of a free aqueous phase with a rigid particulate phase which, has the propensity to selectively remove or store one or more solute present in the solution (Cheremisinoff, 1995). Both batch contacting and column contacting processes are available for sorbent materials with solutions containing dyestuffs. Liquid phase adsorption has been shown to be an effective method for the removal of suspended solids, odors, organic matters, metal ions and dyestuffs by the application of activated carbon (Allen *et al.*, 1992), peat (Mckay *et al.*, 1997), bentonite clay, rice husk, teakwood bark, cotton waste, hair (Mckay *et al.*, 1985, 1986) and maize cob (El-Geundi, 1991) as adsorbents. There may be several mechanisms by which dyestuffs can be removed from a solution and attached to a sorbent particle surface. The mechanism may be due to ion exchange, physical sorption, chemisorption, chemical reaction, lone pair electron sharing or donating, plus a number of other mechanistic processes.

Adsorption systems have been investigated to assess their suitability for application in the field of water pollution control. The cost and performance of product or the mode of application are always of concern to control process efficiency. Sorption equilibrium is established when the concentration of sorbate in the bulk solution is in dynamic balance with that of the interface. An equilibrium analysis is the most important fundamental information required for evaluating the affinity or capacity of a sorbent. However, thermodynamic data can predict only the final state of a system from an initial nonequilibrium mode. It is therefore important to determine how sorption rates depend on the concentrations of sorbate in solution and how rates are affected by sorption capacity or by the character of the sorbent from the kinetic point of view. From the kinetic analysis, the solute uptake rate, which determines the residence time required for completion of the sorption reaction, may be analyzed and established.

2.4.1 Equilibrium Isotherm Models

In studies of adsorption systems, success has been achieved in describing the adsorption behavior by several equilibrium isotherm models. In 1918, Langmuir suggested a theory to describe the monolayer adsorption of homogeneous surfaces. The equation was first developed by Butler and Ockrent (1930) to describe the adsorption equilibrium in competitive multicomponent systems and is based on the same assumptions as the Langmuir equation for single adsorbates.

Freundlich (1906) suggested a model to describe the adsorption properties of heterogeneous systems. This model has been widely applied in heterogeneous adsorption systems especially for organic compounds and highly interactive species on activated carbon. In order to describe the Freundlich type multicompont isotherm, Sheindorf *et al.* (1982) tested some well-known relationships from the studies of Jain and Snoeyink (1973) and Radke and Prausnitz (1972). They obtained satisfactory agreement with measured data and used their results to create a generalized multicomponent isotherm of the Freundlich type where the isotherm coefficients can be determined from the monocomponent isotherm for solid aqueous system such as the adsorption of water pollutants on activated carbon.

The other popular isotherm was proposed by Redlich and Peterson (1959). This isotherm is quite similar to the Langmuir isotherm but it has a power factor in the equation.

The Toth isotherm (1971) derived from the potential theory has proven applicable to systems of phenolic compounds on carbon. This isotherm has been shown to be particularly applicable for heterogeneous adsorption. It assumes asymmetrical quasi-Gaussian energy distribution with widened lift-hand side adsorption energy. The Dubinin-Radushkevich (1947) isotherm is based on the potential theory of adsorption for adsorbents with an energetically non-uniform surface where adsorption interaction is due to dispersion forces.

In this study, only Langmuir, Freundlich and Redlich-Peterson isotherm models will be considered.

2.4.2 Batch Kinetic Models

The study of adsorption reaction kinetics is usually assessed in terms of the reaction order of the adsorption process. The experimental results are substituted into the most widely used kinetic reaction models to determine the sorption mechanism by the 'best fit' procedure.

2.4.2.1 Lagergren Equation

Lagergren (1898) suggested a first-order reaction equation for the sorption of liquid/solid systems based on solid capacity. This equation is the most widely used adsorption rate equation in liquid phase studies.

2.4.2.2 Elovich Equation

The Elovich equation has been successfully used for predicting the chemisorption of adsorbates. Juang and Ju (1998) described the kinetics of the sorption of Cu-EDTA chelated anion on cross-linked, polyaminated chitosan beads by the Elovich equation.

2.4.2.3 Ritchie and Modified Second Order Equation

Ritchie (1977) suggested an alternative model to the Elovich equation for the kinetics of adsorption of gases on solids. The author suggested that the rate of adsorption

depended solely on the number of surface sites, which are occupied by each molecule of adsorbed gas. This model shows that the experimental data that was originally interpreted using the Elovich equation can also be fitted into this model to provide a satisfactory result. To compare the chemisorption aspects of these two models Ungarich and Aharoni (1981) discussed the distinction between Elovichian and Ritchie's second-order equation. The Ritchie equation has been modified for use in this study. The coverage of the sorbent surface at the beginning of the sorption process is assigned a nominal amount of surface coverage. The reasons behind this assumption are discussed later, and therefore, the Ritchie equation was rearranged to obtain the modified second equation.

CHAPTER 3: MATERIALS AND METHODS

3.1 MATERIALS

3.1.1 Adsorbent

The adsorbent used in this research is a powdered form of chitin purchased from Sigma Chemical Company. This chitin is described by the supplier as a practical graded material extracted from crab shells. All raw chitin was dried at 75 °C in an oven for 6 hours and then was sieved into discrete particle size range from 355-500 μm.

3.1.2 Adsorbate

Five different commercial available textile dyestuffs were used in the study including four azo dyes (AO10, AO12, AR18 and AR73) and one anthraquinone dye (AG25). Those selected dyestuffs are commonly used in dye house nowadays and regarded as dye contaminants in the discharged effluent. All dyestuffs were purchased from Aldrich Chemical Co. and used without any further purification process. The characteristics and chemical structures of the selected dyestuffs are listed in Table 3.1 and Figure 3.1 respectively.

Table 3.1: The Physical and Chemical Characteristics of Selected Dyestuffs

Generic Name	Abbrev.	Commercial Name	Purity (%)	Chromophore	F.W.	$\lambda_{max.}$ (nm)
C.I. Acid Green 25	AG25	Acid Green 25	75	Anthraquinone	622.6	642
C.I. Acid Orange 10	AO10	Orange G	80	Monoazo	452.4	475
C.I. Acid Orange 12	AO12	Crocein Orange G	70	Monoazo	350.3	482
C.I. Acid Red 18	AR18	New Coccine	75	Monoazo	604.5	506
C.I. Acid Red 73	AR73	Brilliant Crocein MOO	70	Diazo	566.5	510

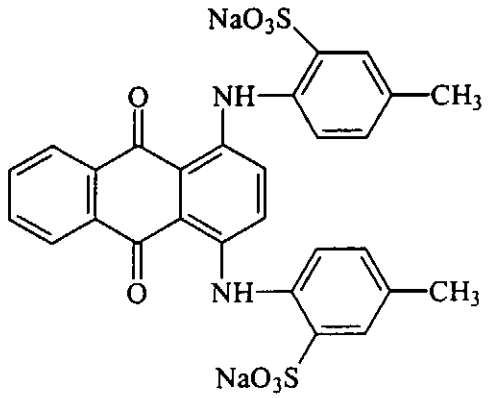

C. I. Acid Green 25 (AG25)

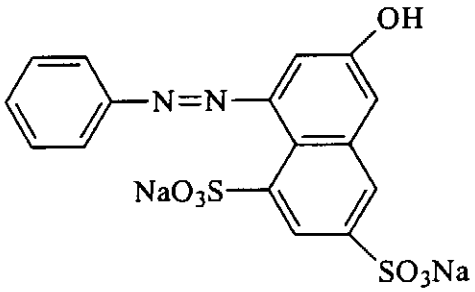

C. I. Acid Orange 10 (AO10)

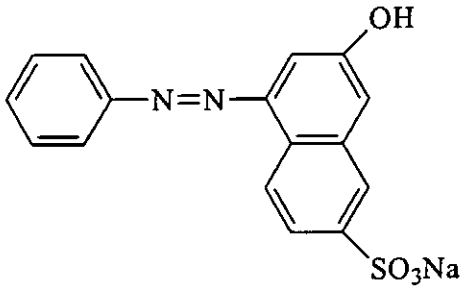

C. I. Acid Orange 12 (AO12)

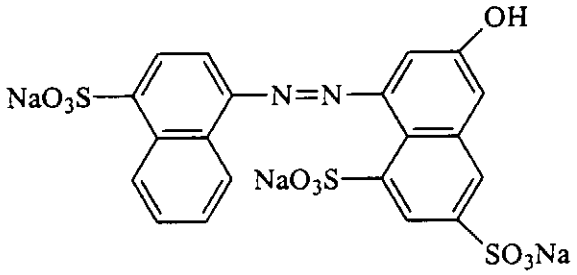

C. I. Acid Red 18 (AR18)

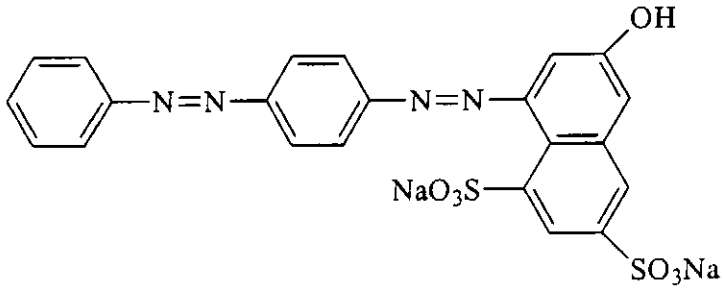

C. I. Acid Red 73 (AR73)

Figure 3.1: The Molecular Structures of the Five Selected Dyestuffs

3.2 Methods

3.2.1 Preparation of Chitosan

The sieved chitin was deacetylated to chitosan with different degree of deacetylation (DD) by using 48% sodium hydroxide solution (w/w) at 100 °C under nitrogen atmosphere for 1-hour periods. Then, the products were washed with deionized water completely, dried at 70 °C in an oven overnight and sieved again into several particle size ranges from 125 – 250, 250 – 355 and 355- 500 μm. The fractions were further dried in vacuum oven for one day and stored in a dessicator. The degree of deacetylation of different chitosans characterized by ^{1}Hnmr method is summarized in Table 3.2.

Table 3.2: Preparation of chitosan with different degrees of deacetylation (DD%)

Treatment Time, (1-hour period)	Degree of Deacetylation (%)
1	53
2	72
3	87
4	95

3.2.2 Concentration Measurement and Calibration

In order to calculate the concentration of the sample from each experiment, a calibration curve of each dye was first prepared. For each dye, five different

concentrations were prepared and the absorbance was measured using a Perkin-Elmer UV/VIS Spectrophotometer Lambda 18 over a range from 400 nm – 700 nm. The calibration checks were carried out in duplicate. Then, the maximum absorbance of each dye was plotted with concentrations. The calculation curves of the five selected dyes are shown in Figure 3.2 – 3.6.

From these results, the concentrations of the dye samples can be calculated with the following equations and constants for calculations which are summarized in Table 3.3.

AG25 : Dye Concentration (mmol/L) = Maximum Absorbance / k_{AG25} (3.1)

AO10 : Dye Concentration (mmol/L) = Maximum Absorbance / k_{AO10} (3.2)

AO12 : Dye Concentration (mmol/L) = Maximum Absorbance / k_{AO12} (3.3)

AR18 : Dye Concentration (mmol/L) = Maximum Absorbance / k_{AR18} (3.4)

AR73 : Dye Concentration (mmol/L) = Maximum Absorbance / k_{AR73} (3.5)

Table 3.3: Constants for calculations of dye concentrations of selected dyes

Name of Dye	Constant, *k*
Acid Green 25 (AG25)	16.650
Acid Orange 10 (AO10)	22.019
Acid Orange 12 (AO12)	23.098
Acid Red 18 (AR18)	25.928
Acid Red 73 (AR73)	40.907

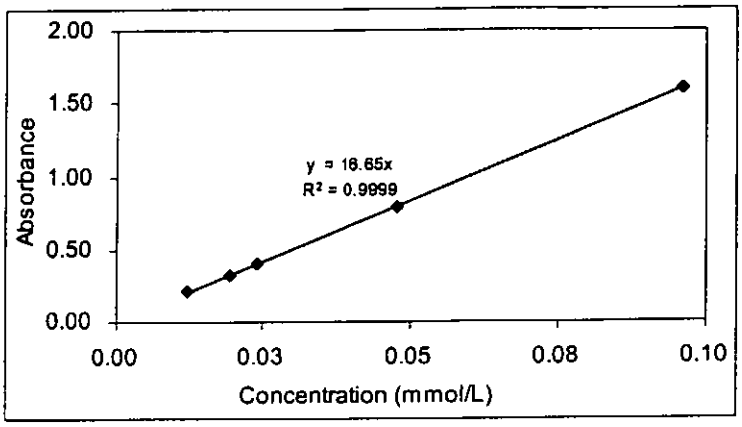

Figure 3.2: Calibration Curve for Acid Green 25 at λ_{max} = 642nm

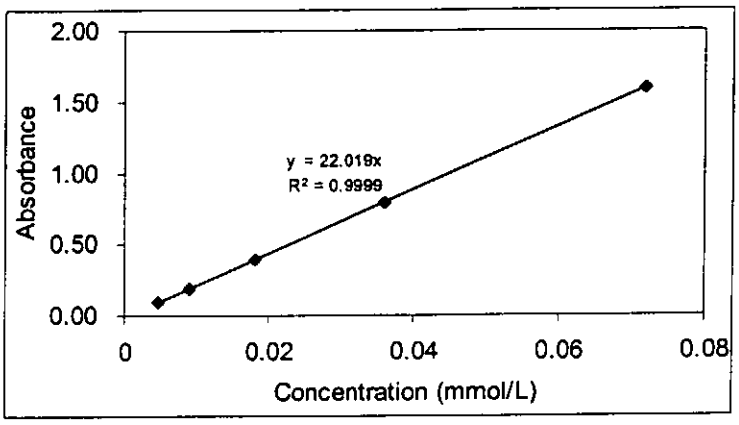

Figure 3.3: Calibration Curve for Acid Orange 10 at λ_{max} = 475nm

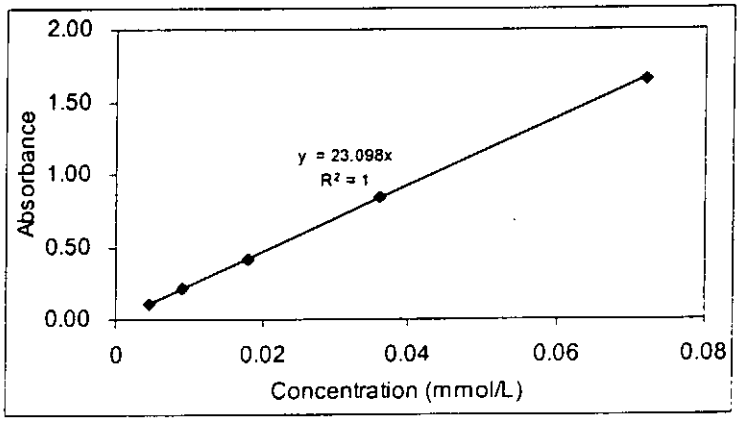

Figure 3.4: Calibration Curve for Acid Orange 12 at λ_{max} = 482nm

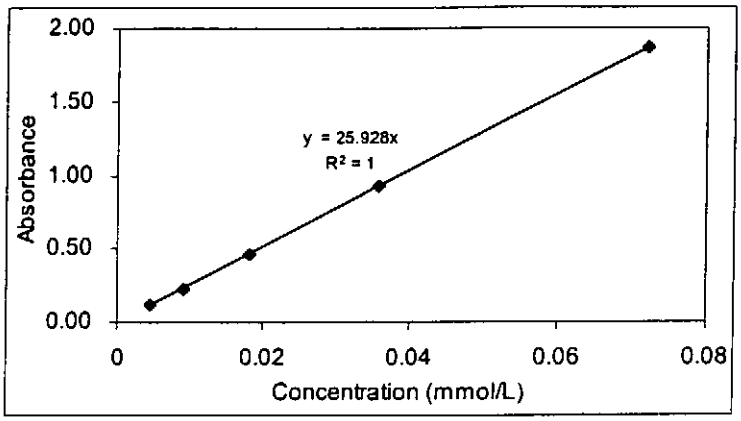

Figure 3.5: Calibration Curve for Acid Red 18 at λ_{max} = 506nm

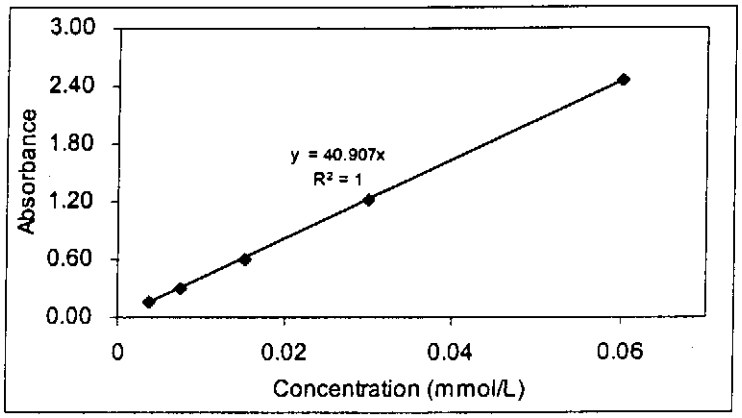

Figure 3.6: Calibration Curve for Acid Red 73 at λ_{max} = 510nm

3.2.3 Equilibrium Sorption Studies

A fixed mass of chitosan (DD=53%, 0.2000g) was weighed into 120 ml conical flasks and brought into contact with 100ml of dye solutions with predetermined initial dye concentrations. The initial pH of the solutions was adjusted to 4.00 ± 0.1 by the addition of 20% in volume of citric acid buffer, made up of citric acid and sodium hydroxide. The flasks were sealed and agitated for 24 hours at 200 rpm in the

thermostatic shaker bath and maintained at a temperature of 25 °C ± 1 °C until equilibrium was reached. At time $t = 0$ and equilibrium, the dye concentrations of the solutions were measured by UV-VIS Spectrometer. These data were used to calculate the adsorption capacity, q_e, of the adsorbent. Finally, adsorption capacity, q_e, against equilibrium concentration, C_e, was plotted.

The same procedure was employed for the equilibrium sorption studies of chitosan with different degree of deacetylation (DD=72% and 95%) and various system temperatures (40°C, 60°C and 80°C)

3.2.3.1 Calculation of Dye Concentration of Isotherm Studies

The dye concentration at equilibrium, q_e, was calculated from:

$$q_e = \frac{(C_0 - C_e)V}{m} \tag{3.6}$$

where q_e = Dye concentration in sorbent at equilibrium

C_o = Initial dye concentration in liquid phase

Ce = Liquid phase dye concentration at equilibrium

V = Total volume of dye solution used

M = Mass of sorbent used

3.2.4 Batch Contact Time Studies

These sets of experiments were used to investigate the influence of sorbent mass, initial concentration and particle size of the adsorbent on the adsorption rate. An adsorber vessel in a standard batch stirred tank configuration was used in all of the experiments.

3.2.4.1 Construction of the Adsorption Vessel

The standard tank configuration was used to derive the relative dimensions of the vessel and its components (Furusawa and Smith, 1973). The relationships with respect to the vessel inside diameter, D_i, are shown in Figure 3.7.

A 2 dm^3 plastic beaker of internal diameter = 0.13 m holding 1.7dm^3 of dye solution was used as the adsorber vessel. Mixing was provided by a six bladed, flat plastic impeller of 0.065 m in diameter and blade height equal to 0.013 m. A Heidolph variable motor was used to drive the impeller using a 0.005 m diameter plastic shaft. Six plastic baffles were evenly spaced around the circumference of the vessel, positioned at 60° intervals and held securely in place on top of the vessel. The baffles were to prevent the formation of a vortex and the consequential reduction in relative motion, between liquid and solid particles, and power losses due to air entrainment at the impeller. Polystyrene baffles were 0.2 m long and 0.01 m wide. They were secured in a position slightly away from the vessel wall and bottom of the tank in

order to prevent particle accumulation. The power number for a vessel with this standard configuration may be calculated as predicted by Furusawa and Smith (1973).

$$P = \rho_l \cdot N_p \cdot N_i^3 \cdot D_i^5 \tag{3.7}$$

Where N_p = Power number*

N_i = Impeller rotation speed (rps)

ρ_l = Particle-free liquid density (kg/m3)

D_i = Impeller diameter (m)

P = Power consumption of the slurry due to agitation (W)

These arrangements and construction enable several experiments to be performed in parallel, thus ensuring the consistency of experimental conditions.

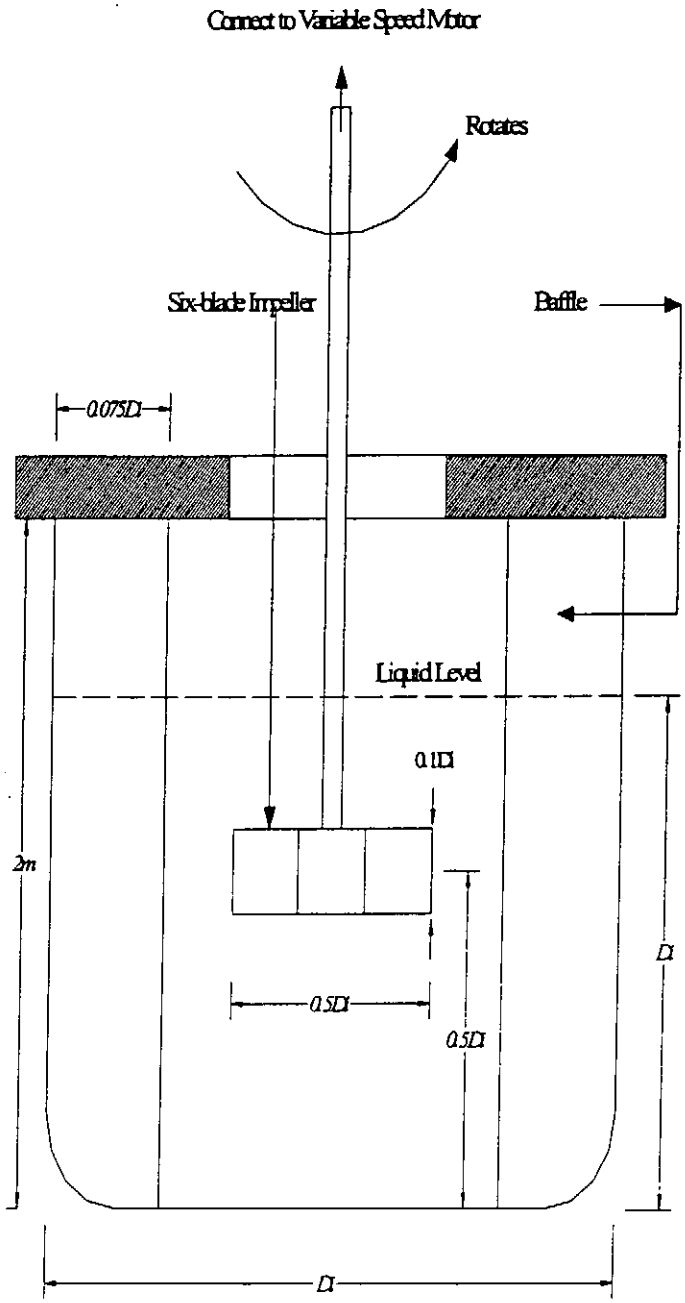

Figure 3.7: Standard Tank Configuration for Batch Contact Time Studies

3.2.4.2 Kinetic Experiments on Various Dyes

The adsorption vessel was used to obtain kinetic data, and the following variable parameters were studied:

i. Effect of initial dye concentration

The effect of initial dye concentration on the adsorption rate was studied by contacting a fixed mass of chitosan (1.7000g) at a fixed particle size (355-500 μm) with fixed temperature (room temperature) and pH (4.00) using a range of initial concentrations of dye solution (from a minimum of 0.25 mmol/L up to a maximum of 2.125 mmol/L, depending on the dye being studied). At time = 0 and at selected time intervals (up to a maximum of 6 hours), adequate volume of samples were extracted using a Hamiton 2.50 ml syringe. The sample concentration was determined by UV/VIS spectrophotometer.

ii. Effect of sorbent mass

The effect of chitosan mass on the adsorption rate was studied using the same conditions as in (i) except the initial concentration of solution which was set at 1.00 mmol/L or 2.00 mmol/L (depending on the type of dye) and a range of sorbent masses (0.4250, 0.8500, 1.275, 1.7000 and 2.1250 g) were used. Sampling, analysis and treatment of results were as previously described in (i).

iii. Effect of Particle Size of Sorbent

The effect of sorbent particle size on the adsorption rate was studied using the same conditions as in (i and ii) except different particle size ranges of chitosan (125-250, 250-355 and 355-500 μm) were used. Sampling, analysis and treatment of results were as previously described in (i).

3.2.4.2.1 Calculation of Dye Concentration

The concentration of dye adsorbed at time t, q_t, was calculated as follows:

$$q_t = \frac{(C_0 - C_t)V}{m} \tag{3.8}$$

at equilibrium, $q_t = q_e$.

CHAPTER 4: EQUILIBRIUM & KINETIC MODELING

4.1 Equilibrium Model

In order to optimize the design of a sorption system to remove the dyes, it is important to establish the most appropriate correlation for the equilibrium curves. The equilibrium sorption capacity can be obtained by testing the sorption isotherm of the Acid Dyes to the chitosan. The experimental data of the amount of sorbate on the sorbent are substituted into an equilibrium isotherm model to determine the best-fit model for the sorption system, in which case any variation in the concentration of dye on the chitosan with the concentration of dye in solution is correlated.

4.1.1 Langmuir Isotherm

Langmuir (1918) proposed a theory to describe the adsorption of gas molecules onto metal surfaces. The Langmuir adsorption isotherm has found successful application to many other real sorption processes of monolayer adsorption. Langmuir's model of adsorption depends on the assumption that intermolecular forces decrease rapidly with distance and consequently predicts the existence of monolayer coverage of the adsorbate at the outer surface of the adsorbent. The isotherm equation further assumes that adsorption takes place at specific homogeneous sites within the adsorbent. It is then assumed that once a dye molecule occupies a site, no further adsorption can take place at that site. Moreover, the Langmuir equation is based on the assumption of a structurally homogeneous adsorbent where all sorption sites are

identical and energetically equivalent. Theoretically, the sorbent has a finite capacity for the sorbate. Therefore, a saturation value is reached beyond which no further sorption can take place. The saturated or monolayer (as $C_t \rightarrow \infty$) capacity can be represented by the expression:

$$q_e = \frac{K_L C_e}{1 + a_L C_e} \tag{4.1}$$

where q_e is solid phase sorbate concentration at equilibrium (mg/g), C_e is aqueous phase sorbate concentration at equilibrium (mg/dm^3), K_L is Langmuir isotherm constant (dm^3/g), a_L is Langmuir isotherm constant (dm3/mg).

Therefore, a plot of C_e/q_e versus C_e gives a straight line of slope a_L/K_L and intercept $1/K_L$. Where K_L/a_L gives the theoretical monolayer saturation capacity, Q_0. The Langmuir equation is applicable to homogeneous sorption where the sorption of each sorbate molecule onto the surface has equal sorption activation energy. The Langmuir equation obeys Henry's Law at low concentration; when the concentration is very low, $a_L C_e$ is far smaller than unity, it implies $q_e = K_L C_e$, hence, it is analogous to Henry's Law. Therefore, a linear expression of Langmuir equation is:

$$\frac{C_e}{q_e} = \frac{1}{K_L} + \frac{a_L}{K_L} C_e \tag{4.2}$$

4.1.2 Freundlich Isotherm

The Freundlich (1906) equation is an empirical equation employed to describe heterogeneous systems, in which it is characterized by the heterogeneity factor 1/n. Hence, the empirical equation can be written:

$$q_e = K_F C_e^{\frac{1}{n}} \tag{4.3}$$

where q_e is solid phase sorbate concentration in equilibrium (mg/g), C_e is liquid phase sorbate concentration in equilibrium (mg/dm^3), K_F is Freundlich constant (dm^3/g) and $1/n$ is the heterogeneity factor. A linear form of the Freundlich expression can be obtained by taking logarithms of Equation (4.3).

$$\ln q_e = \ln K_F + \frac{1}{n} \ln C_e \tag{4.4}$$

Therefore, a plot of ln q_e versus ln C_e enables the constant K_F and exponent $1/n$ to be determined. This isotherm is another form of the Langmuir approach for adsorption on an "amorphous" surface. The amount adsorbed material is the summation of adsorption on all sites. The Freundlich isotherm is derived by assuming an exponential decay energy distribution function inserted in to the Langmuir equation. It describes reversible adsorption and is not restricted to the formation of the monolayer.

4.1.3 Redlich-Peterson Isotherm

Redlich and Peterson (1959), incorporate three parameters into an empirical isotherm. The Redlich-Peterson isotherm model combines elements from both the Langmuir and Freundlich equation and the mechanism of adsorption is a hybrid one and does not follow ideal monolayer adsorption.

$$q_e = \frac{K_R C_e}{1 + a_R C_e^{\beta}} \tag{4.5}$$

where q_e is solid phase sorbate concentration in equilibrium (mg/g), C_e is liquid phase sorbate concentration in equilibrium (mg/dm^3), K_R is Redlich-Peterson isotherm constant (dm^3/g), a_R is Redlich-Peterson isotherm constant (dm^3/mg) and β is the exponent which lies between 1 and 0. The application of this equation has been discussed elsewhere and its limiting behavior is summarized here:

where β = 1

$$q_e = \frac{K_R C_e}{1 + a_R C_e} \tag{4.6}$$

It becomes a Langmuir equation.

where β = 0

$$q_e = \frac{K_R C_e}{1 + a_R} \tag{4.7}$$

i.e. the Henry's Law equation

Equation (4.5) can be rearranged as follows:

$$K_R \frac{C_e}{q_e} - 1 = a_R C_e^{\beta} \tag{4.8}$$

This equation can be converted to a linear form by taking logarithms:

$$\ln\left(K_R \frac{C_e}{q_e} - 1 \right) = \ln a_R + \beta \ln C_e \tag{4.9}$$

Plotting the left-hand side of equation (4.9) against ln C_e to obtain the isotherm constants is not applicable because of the three unknowns, a_R, K_R and β. Therefore, a minimization procedure is adopted to solve equation (4.9) by maximizing the correlation coefficient between the theoretical data for q_e predicted from equation (4.9) and experimental data.

4.2 Kinetic Model

The use of kinetic equations in acid dye sorption has been studied for many years. The mechanism of acid dye sorption onto various sorbents has been subjected to extensive research, debate and controversy for decades. Numerous researches are based on a reaction kinetic sorption process in which reaction rate constants are determined as key parameters describing the process. The most appropriate kinetic model will determine the reaction order of the sorption process of acid dyes onto chitosan.

4.2.1 The Pseudo-First Order Equation

Lagergren (1898) suggested a pseudo-first order equation for the sorption of liquid/solid system based on solid capacity. The Lagergren equation is the most widely used rate equation in liquid phase sorption process and can be represented as follows:

$$\frac{dq_t}{d_t} = k_1 \left(q_e - q_t \right) \tag{4.10}$$

where q_t is solid phase sorbate concentration at time t (mmol/g), q_e is solid phase sorbate concentration at equilibrium (mmol/g) and k_1 is rate constant (hr^{-1}).

Integrating this for the boundary conditions $t = 0$ to $t = t$ and $q_t = 0$ to $q_t = q_t$,

$$q_t = q_e \left(1 - e^{-k_1 t} \right) \tag{4.11}$$

Equation (4.11) can be linearized by taking logarithms as shown by equation (4.12):

$$\log(q_e - q_t) = \log(q_e) - \frac{k_1}{2.303}t \tag{4.12}$$

or

$$\ln(q_e - q_t) = \ln(q_e) - k_1 t \tag{4.13}$$

The pseudo-first order rate constants, k_1, can be correlated by equations of the form:

$$k_1 = A_1[C_0]^{\beta_1} \tag{4.14}$$

where C_0 is the initial liquid phase solute concentration (mmol/dm^3) A_1 and β_1 are pseudo-first order constants.

4.2.2 The Elovich Equation

The Elovich equation has general application to chemisorption kinetics. The equation has been proved satisfactorily applicable to most chemisorption data and will cover a large range of slow adsorption. A detailed report to interpret the use of this equation in the kinetics of chemisorption of gases on solids was demonstrated by Low (1960). The Elovich equation is formulated as:

$$\frac{dq_t}{d_t} = a\exp(-bq_t) \tag{4.15}$$

where q_t is solid phase sorbate concentration at time t (mmol/g), a and b are kinetic rate constants. Intergration of equation (4.15) with boundary conditions $q = 0$ at $t = 0$ and $q = q_t$ at $t = t$.

$$q_t = \frac{1}{b}\ln(1 + abt) \tag{4.16}$$

Assume $$t_0 = \frac{1}{ab} \tag{4.17}$$

By substituting, equation (4.17) into equation (4.16):

$$q_t = \frac{1}{b}\ln\left(1+\frac{t}{t_0}\right) \tag{4.18}$$

Then, rearrange equation (4.18) to form a linear transformation of the Elovich kinetic equation:

$$q_t = \frac{1}{b}\ln\left[ab\left(t+t_0\right)\right] \tag{4.19}$$

or

$$q_t = \frac{1}{b}\ln ab + \frac{1}{b}\ln\left(t+t_0\right) \tag{4.20}$$

Thus, a linear plot of equation (4.20) q_t versus $\ln\left(t+t_0\right)$, yields both constants a and b from the intercept and the slope. Determination of constant t_0 is based on the trial and error method, and then backs the correlation with equation (4.17).

4.2.3 The Ritchie and Modified Second Order Equation

Ritchie (1977) found that the Elovich plot gives curved lines or sharp changes in the gradient in some cases. The sharp changes in gradient are sometimes interpreted as indicating a change in adsorption mechanism. As a result, an alternative method for the kinetic study was proposed by assuming that the rate of adsorption depends solely on the fraction of sites, which are not occupied at time t:

$$\frac{d\theta}{dt} = k_2'\left(1-\theta\right)^n \tag{4.21}$$

where θ is surface coverage of sorbent, q_t / q_e (dimensionless), k_2'is kinetic rate constant.

Integration of Equation (4.21) to,

For $n \neq 1$

$$\frac{1}{(1-\theta)^{n-1}} = (n-1)k_2't + 1 \tag{4.22}$$

For $n = 1$,

$$\theta = 1 - e^{-k_2't} \tag{4.23}$$

It is assumed that no site is occupied at $t = 0$, and the amount of adsorption, q_t, occurs at time t.

Then, equation (4.22) becomes:

$$\frac{q_e^{n-1}}{(q_e - q_t)^{n-1}} = (n-1)k_2't + 1 \tag{4.24}$$

Similarly, equation (4.23) becomes:

$$q_t = q_e\left(1 - e^{-k_2't}\right) \tag{4.25}$$

For $n = 2$, equation (4.24) becomes:

$$\frac{q_e}{(q_e - q_t)} = k_2't + 1 \tag{4.26}$$

Rearranging equation (4.26) yields the linear forms of Ritchie equation (4.27 or 4.28)

$$\frac{1}{q_t} = \frac{1}{k_2'q_e t} + \frac{1}{q_e} \tag{4.27}$$

or

$$\frac{t}{q_t} = \frac{1}{k_2' q_e} + \frac{t}{q_e} \tag{4.28}$$

A plot of $\frac{t}{q_t}$ versus t yields the constants q_e and k_2' from the slope and intercept. If the results were plotted with equation (4.26), a reasonablely straight line is obtained. The intercept, however, at t = 0 may not equal to 1.0, which indicates that some adsorption was shown at time t = 0. A possible solution to the situation can be attributed to the redefinition of the boundary conditions of equation (4.21), in which at t = 0, and at $q = q_0 \neq 0$. Then, it is assumed that the pre-second order reaction occurs very rapidly at $t \approx 0$:

$$\frac{d\theta}{dt} = k_2'(1-\theta)^n \tag{4.21}$$

$$\int_{\theta_0}^{\theta} \frac{d\theta}{(1-\theta)^n} = k_2' \int_0^t dt \tag{4.29}$$

where $\theta_0 = q_0 / q_e$, at $t = 0$,

$$\frac{1}{(1-\theta)^{n-1}}\Big|_{\theta_0}^{\theta} = (n-1)k_2' t \tag{4.30}$$

$$\frac{1}{(1-\theta)^{n-1}} = (n-1)k_2' t + \frac{1}{(1-\theta_0)^{n-1}} \tag{4.31}$$

For $n = 2$ and $\theta = q_t / q_e$, equation (4.31) becomes:

$$\frac{q_e}{(q_e - q_t)} = k_2' t + \frac{1}{1-\theta_0} \tag{4.32}$$

Assume $\beta = \frac{1}{1-\theta_0}$,

$$\frac{q_e}{(q_e - q_t)} = k_2' t + \beta \tag{4.33}$$

Rearranging equation (4.33) gives the non-linear form:

$$q_t = q_e \left[\frac{(\beta - 1) + k_2' t}{\beta + k_2' t} \right] \tag{4.34}$$

or

$$q_t = q_e \left[1 - \frac{1}{\beta + k_2' t} \right] \tag{4.35}$$

The linear form becomes:

$$\frac{1}{q_t} = \frac{1}{q_e \left[(\beta - 1) + k_2' t \right]} + \frac{1}{q_e} \tag{4.36}$$

When $\theta_0 = 0$, i.e. no surface coverage at t = 0, then, $\beta = 1$, equation (4.34) becomes equation (4.27). Since, equation (4.34) contains three unknown parameters, which cannot be solved by the linear plot of the equation. Therefore, the trial and error method is used to minimize the sum of error squares.

4.3 Error Analysis

For single component isotherm studies, the fitness of the isotherms to the experimental equilibrium data is optimized by error function. In this study, five different error functions were employed and the isotherm parameters were determined

by minimizing the respective error function across the entire concentration range of studies using the solver add-in with Microsoft's spreadsheet, Excel.

4.3.1 The Sum of the Squares of the Errors (SSE)

Equation of the sum of the squares of the errors:

$$\sum_{i=1}^{p}\left(q_{e,calc}-q_{e,meas}\right)_i^2 \tag{4.37}$$

This is the most common error function in use, it has, however, a major drawback in which isotherm parameters derived using this error function will provide a better fit as the magnitude of the errors and thus sum of the squares of the errors increases – biasing the fit towards data obtained at the high end of the concentration range.

4.3.2 The Hybrid Fractional Error Function (HYBRID)

This error function was developed by the authors in an attempt to improve the fit of the sum of the squares of the errors at low concentrations by dividing by the measured value. It also includes the number of degrees of freedom of the system – the number of data points n minus the number of parameter p of the isotherm equation – as a divisor.

$$\frac{100}{n-p}\sum_{i=1}^{n}\left[\frac{\left(q_{e,meas}-q_{e,calc}\right)}{q_{e,meas}}\right]_i \tag{4.38}$$

4.3.3 Marquardt's Percent Standard Deviation (MPSD) (Marquardt, 1963)

$$100\sqrt{\frac{1}{n-p}\sum_{i=1}^{p}\left(\frac{\left(q_{e,meas}-q_{e,calc}\right)}{q_{e,meas}}\right)_i^2} \tag{4.39}$$

This error function is similar in some respects to a geometric mean error distribution modified according to the number of degrees of freedom of the system.

4.3.4 The Average Relative Error (ARE) (Kapoor *et al*, 1989)

$$\frac{100}{n}\sum_{i=1}^{p}\left|\frac{\left(q_{e,calc}-q_{e,meas}\right)}{q_{e,meas}}\right|_i \tag{4.40}$$

This error function attempts to minimize the fractional error distribution across the entire concentration range.

4.3.5 The Sum of the Absolute Errors (EABS)

$$\sum_{i=1}^{p}\left|q_{e,calc}-q_{e,meas}\right|_i \tag{4.41}$$

This approach is similar to the sum of the squares of the errors to some extent. Isotherm parameters determined using this error function would provide a better fit as the magnitude of the error increases, biasing the fit towards the high concentration data.

As all the experiments were carried out at the almost exactly the m/V ratios of 1g/dm^3, therefore, according to the formulation of the problem, both C_e and q_e contribute equally to weighting the error criterion for the model solution procedure. Hence, the

difference in the sorbed phase concentration reflects the differences in the predicted concentration for both phases.

4.4 Determination of Isotherm Model

The traditional approach of determining the isotherm parameters by linear regression of isotherm equations appears to give very good fits to the experimental data as most of their respective regression correlation coefficients are close to unity. However, the correlation coefficient R^2 yields the best-fit isotherm constants based on the linearised isotherm plots which has the disadvantage that it may not provide the best isotherm constants to correlate the original isotherm equation with experimental data points. Besides, for the three-parameter isotherm the constants cannot be determined by best fitting a linear plot because there are three unknowns. In addition, since the R^2 factor is based on the square of the difference between theoretical and experimental data points, it will result in higher weighting to the higher C_e value data points. Consequently, it will give a better fit correlation to the higher C_e value data points. Therefore, due to the inherent bias resulting from linearisation, alternative single component parameters will be determined by non-linear regression with the solver add-in facility for Microsoft Excel 1997.

As each of the error functions produce a different set of isotherm parameters, an overall optimum parameter set is difficult to identify directly. Thus, a normalization of each parameter is employed in order to have a better comparison between the

parameter sets for the single isotherm model. The normalization processes are as follows:

- Choosing each error function in turn and determining the results for each parameter set;
- Dividing the errors determined for a given error function by the maximum to obtain the normalized errors for each parameter set; and
- Summing the normalized errors for each parameter set.

4.4 Determination of the Kinetic Model

Four kinetic models will be used to determine the best fitting equation, which correlates the theoretically predicted data with the experimental data. The best fitting kinetic model will be determined by choosing the equation resulting in the lowest sum of error squares (SSE). If the differences between the correlation coefficients among the three kinetic models are too close to determine the true kinetic reaction: Ungarish *et al.* (1981) reported that the applicability of the Elovichian kinetics could be compared directly by plotting the reciprocal of the rate $Z=(d_q/d_t)^{-1}$ against t. Therefore, a sensitivity analysis-plotting $Z=(d_q/d_t)^{-1}$ against t will used to identify a true kinetic model.

For the Pseudo-first Order Equation

$$\frac{dq_t}{dt} = k_1(q_e - q_t) \tag{4.10}$$

Rearranging equation (4.10) gives:

$$Z_p = \frac{1}{k_1(q_e - q_t)} \tag{4.42}$$

Equation (4.42) is the definition of pseudo-first order equation, which is in term of k_1, q_e and q_t. Differentiating the pseudo-first order equation (4.11), it becomes equation (4.43):

$$q_t = q_e\left(1 - e^{-k_1 t}\right) \tag{4.11}$$

$$Z_L = \left(\frac{1}{q_e k_1 e^{-k_1 t}}\right) \tag{4.43}$$

From equation (4.43), Z_L is expressed in terms of k_1, q_e and t.

Since q_t was the sorption capacity at time t, if the pseudo-first order equation is the true kinetic model for the sorption system, the value Z obtained from equation (4.42) and (4.43) should be identical at time t.

For the Elovich Equation

$$\frac{dq_t}{dt} = a\exp(-bq_t) \tag{4.15}$$

By rearranging equation (4.15), then:

$$Z_p = \frac{1}{a\exp(-bq_t)} \tag{4.44}$$

Differentiating equation (4.20) gives::

$$q_t = \frac{1}{b}\ln ab + \frac{1}{b}\ln(t+t_0) \tag{4.20}$$

$$Z_L = b(t+t_0) \tag{4.45}$$

For the Modified Second Order Equation

From equation (4.21), the equation is rearranged in terms of q_t and q_e..

$$\frac{d\theta}{dt} = k_2'(1-\theta)^n \tag{4.21}$$

$$\frac{dq_t}{dt} = \left(\frac{k_2'}{q_e}\right)(q_e - q_t)^2 \tag{4.46}$$

Rearrange:

$$Z_p = \left(\frac{q_e}{k_2'(q_e - q_t)^2}\right) \tag{4.47}$$

Differentiating equation (4.35) gives equation (4.48)

$$q_t = q_e\left[1-\frac{1}{\beta+k_2 t}\right] \tag{4.35}$$

$$Z_L = \frac{\left(\beta+k_2 t\right)^2}{q_e k_2} \tag{4.48}$$

Equations (4.42), (4.44) and (4.47) are expressed in terms of parameters and q_t. Therefore, the Z versus t plot can be obtained and used for a visual sensitivity analysis. Identical results of the differential form of the kinetic model, in terms of parameters and t, will be obtained for the fitted kinetic model.

CHAPTER 5: RESULTS AND DISCUSSION

5.1 Equilibrium Isotherms

Adsorption isotherms describe how adsorbates interact with adsorbents and so are critical in optimizing the use of adsorbents. Therefore, the correlation of equilibrium data by either theoretical or empirical equations is essential to the practical design and operation of adsorption systems. In order to optimize the design of a sorption system to remove dyes from effluents, it is important to establish the most appropriate correlation for the equilibrium curves. In the present studies, the experimental data of five dye-chitosan equilibrium isotherms, which were the sorption of Acid Green 25 (AG25), Acid Orange 10 AO10), Acid Orange (AO12), Acid Red 18 (AR18) and Acid Red 73 (AR73) as shown in Figure 5.1 were compared using three isotherm equations namely, Langmuir, Freundlich and Redlich-Peterson (R-P).

5.1.1 Langmuir Isotherm

The Langmuir adsorption isotherm assumes that the adsorbed layer is one molecule in thickness. The strength of the inter-molecular attractive forces is believed to fall off rapidly with distance. The sorption data were analyzed according to the linear form equation (4-2) of the Langmuir isotherm. The plots of specific sorption Ce/qe against the equilibrium concentration, Ce for five dyes, Acid Green 25 (AG25), Acid Orange 10 (AO10), Acid Orange 12 (AO12), Acid Red 18 (AR18) and Acid Red 73 (AR73), are shown in Figure 5.2 (a) to Figure 5.2 (c). The isotherms of AO10, AO12, AG25,

AR18 and AR73 were found to be linear over the whole concentration range studies and the correlation coefficients were extremely high as shown in Table 5.1. These values of the correlation coefficients strongly support the fact that the dyes-chitosan sorption data closely follow the Langmuir model of sorption. The isotherm constants, a_L, K_L and equilibrium monolayer capacities, Q_o are presented in Table 5.1. The Langmuir monolayer capacity Q_o represents the saturation capacity of acid dyes of AO10, AO12, AG25, AR18 and AR73 and these values are 929.9, 1006.3, 645.1, 693.2 and 728.2 mg/g respectively. The plots in Figure 5.2 (a) and (c) demonstrate that the Langmuir equation provides an accurate description of the experimental data, which is further confirmed by the extremely high values of the correlation coefficient.

The saturation capacities of acid dyes in each of the systems are demonstrated on Figure 5.1. The saturation capacities of AG25, AO10, AO12, AR18 and AR73 are 1.03, 1.54, 2.66, 1.11 and 1.25 mmol/g respectively.

The possible mechanisms of the adsorption process of chitosan and acid dye are discussed: In aqueous solution, the acid dye is first dissolved and the sulphonate groups of acid dye (D-SO_3Na) is dissociated and converted to anionic dye ions.

$$D\text{-}SO_3Na \xrightarrow{H_2O} D\text{-}SO_3^- + Na^+ \qquad (5\text{-}1)$$

Also, in the presence of H^+, the amino groups of chitosan (R-NH_2) were protonated.

$$R\text{-}NH_2 + H^+ \rightleftharpoons R\text{-}NH_3^+ \qquad (5\text{-}2)$$

The adsorption process then proceeds due to the electrostatic attraction between these two counter ions,

$$R\text{-}NH_3^+ + D\text{-}SO_3^- \rightleftharpoons R\text{-}NH_3^+\text{-}O_3S\text{-}D \qquad (5\text{-}3)$$

Therefore, the difference in the degree of adsorption may mainly be attributed to the chemical structure of each dye. Both Figure 3.1 and Table 3.1 indicate Acid Orange 12 (AO12) has only one sulphonate acid group (monovalent) and has the smallest molecular size which not only increases the dye/chitosan ratio in the system, but also enables a deeper penetration of dye molecules to the internal pore structure of chitosan. In the case of divalent Acid Orange 10 (AO10) and Acid Red 73, a slightly higher adsorption capacity is observed for AO10 than the capacity of AR73, suggesting that the larger dye ions do not completely penetrate the particle, and that the dyes preferentially adsorb near the outer surface of the particle and a similar phenomenon was reported previously by Mckay *et al* (1982), for the adsorption of certain dyes on chitin. Moreover, lower capacities in case of Acid Green 25 (AG25) and Acid Red 18 (AR18) similarly show that large dye molecules and trivalent dye ions result in a lower adsorption capacity values.

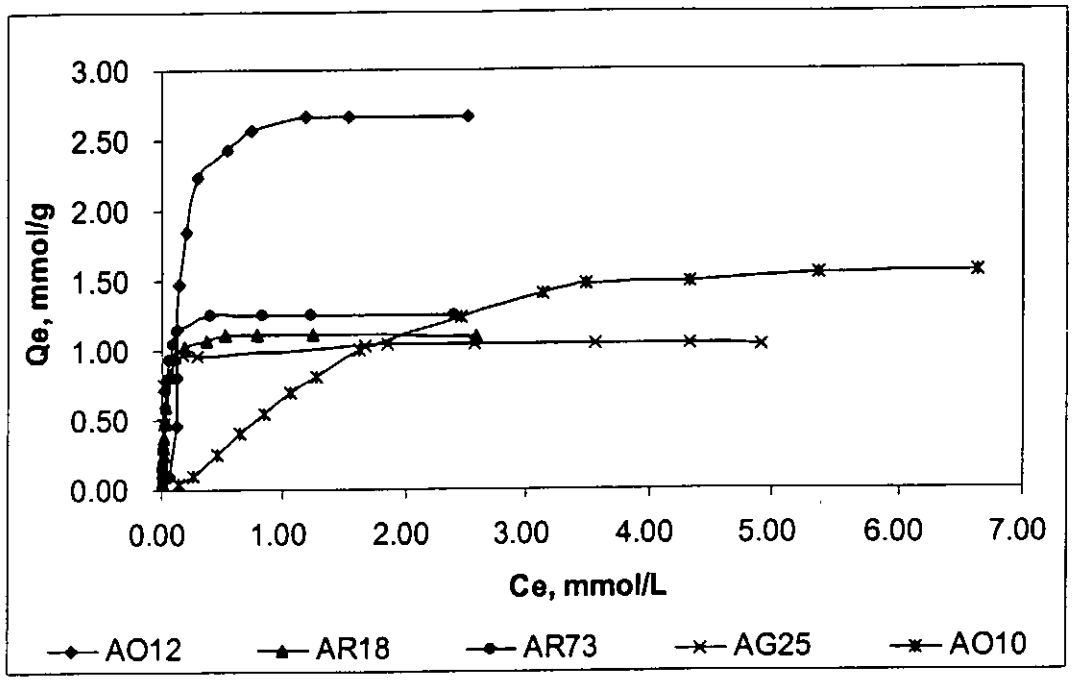

Figure 5.1 Sorption of Acid Dyes onto Chitosan at Temp. = 25 °C, Degree of Deacetylation (DD) = 53%, pH = 4.00, dp = 355-500 μm.

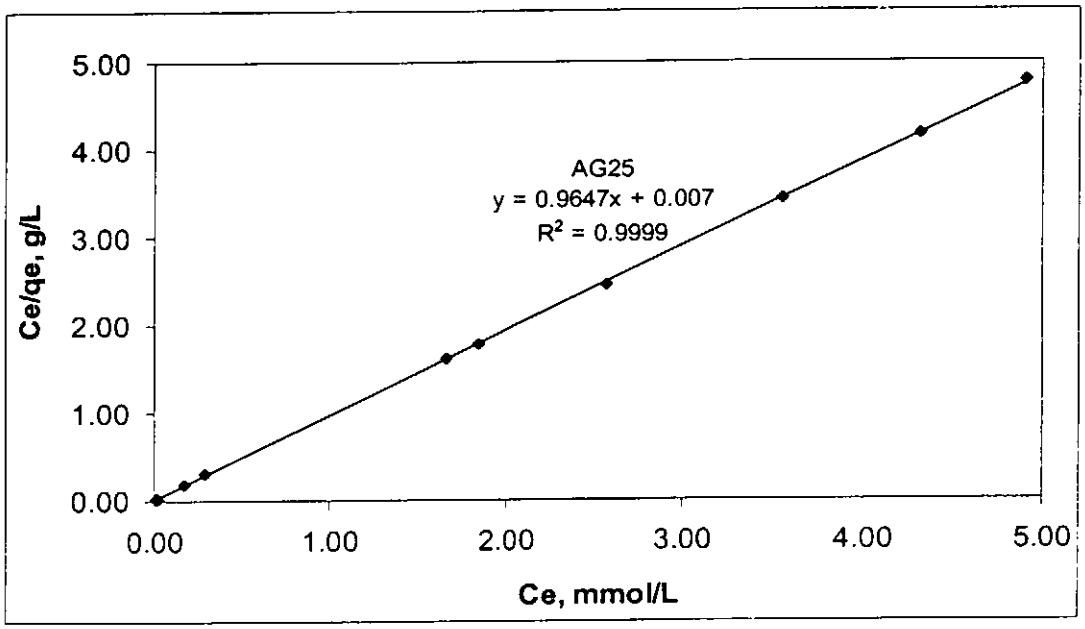

Figure 5.2 (a) Langmuir Isotherm Linear Plots for the Sorption of Acid Green 25 onto Chitosan at Temp. = 25 °C, Degree of Deacetylation (DD) = 53%, pH = 4.00, dp = 355-500 μm

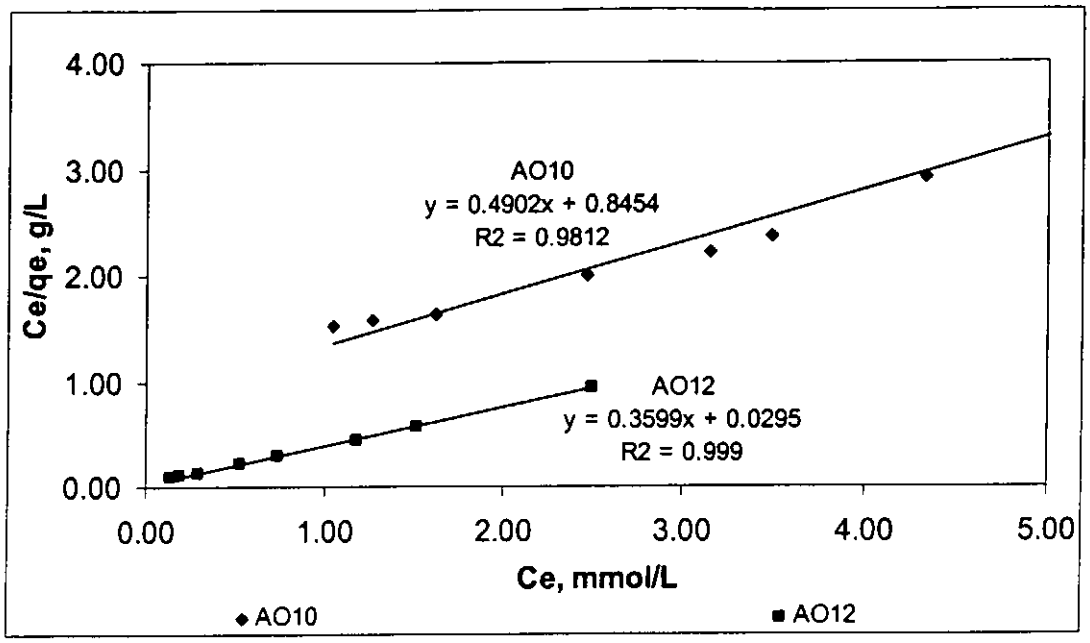

Figure 5.2 (b) Langmuir Isotherm Linear Plots for the Sorption of Acid Orange 10 & Acid Orange 12 onto Chitosan at Temp. = 25 °C, Degree of Deacetylation (DD) = 53%, pH = 4.00, dp = 355-500 μm

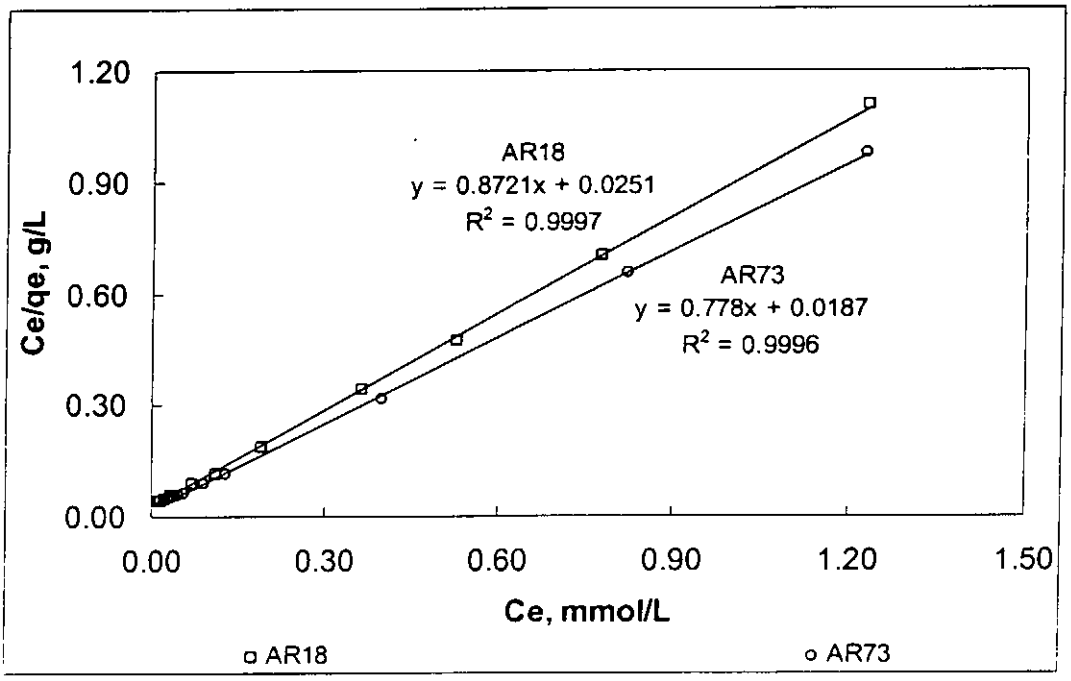

Figure 5.2 (c) Langmuir Isotherm Linear Plots for the Sorption of Acid Red 18 & Acid Red 73 onto Chitosan at Temp. = 25 °C, Degree of Deacetylation (DD) = 53%, pH = 4.00, dp = 355-500 μm.

	K_L (dm^3/g)	a_L ($dm^3/mmol$)	Q_o (mg/g)	R^2
AG25	175.4390	169.316	645.1	0.9999
AO10	1.1829	6.5798	81.3	0.9812
AO12	33.8983	12.200	973.3	0.999
AR18	39.8406	34.745	693.2	0.9997
AR73	53.4759	41.6043	728.2	0.9996

Table 5.1 Langmuir Sorption Isotherm Constants for AG25, AO10, AO12, AR18 and AR73

5.1.2 Freundlich Isotherm

The Freundlich equation predicts that the dye concentrations on the adsorbent will increase so long as there is an increased in the dye concentration in the liquid. The experimental data in the present systems indicate that there is a limiting value of the solid phase concentration. By plotting the linear transformation of the Freundlich equation, Figure 5.3 (a) to (e) show the logarithmic plots of the Freundlich expression for the selected acid dyes. The Figures exhibit deviation from linearity on the Freundlich linear plot for the whole concentration range. However, if the whole concentration range is divided into regions, i.e. region 1, region 2, and region3, excellent fits to the experimental data can be observed., especially at the lower concentration region 1 and 2. Region 3 does not fit the Freundlich equation well. Table 5.2 shows the Freundlich sorption isotherm constants, b_F and K_F, and the correlation coefficients, R^2 for the different concentration regions.

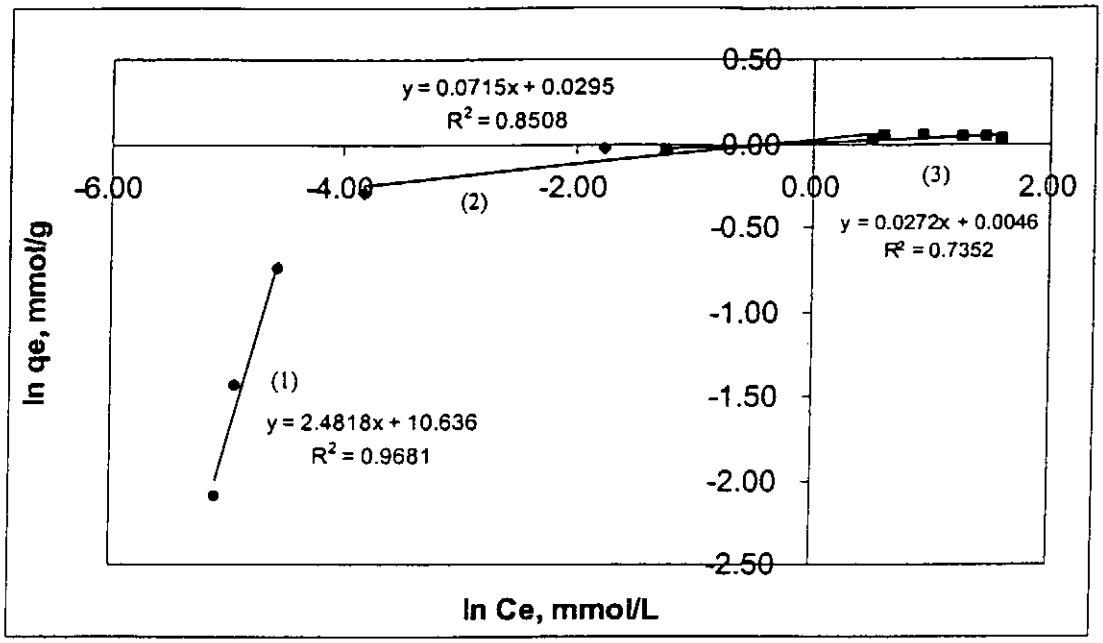

Figure 5.3(a) Freundlich Isotherm Linear Plots for the Sorption of Acid Green 25 onto Chitosan at Temperature = 25 °C, Degree of Deacetylation (DD) = 53%, pH = 4.00, dp = 355-500 μm

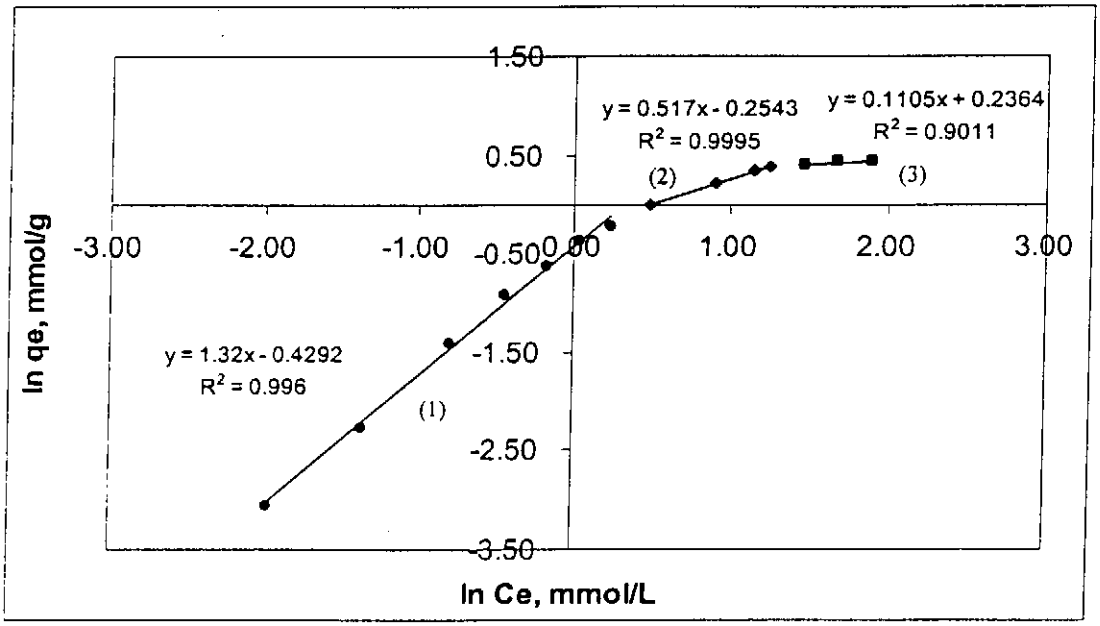

Figure 5.3(b) Freundlich Isotherm Linear Plots for the Sorption of Acid Orange 10 onto Chitosan at Temperature = 25 °C, Degree of Deacetylation (DD) = 53%, pH = 4.00, dp = 355-500 μm

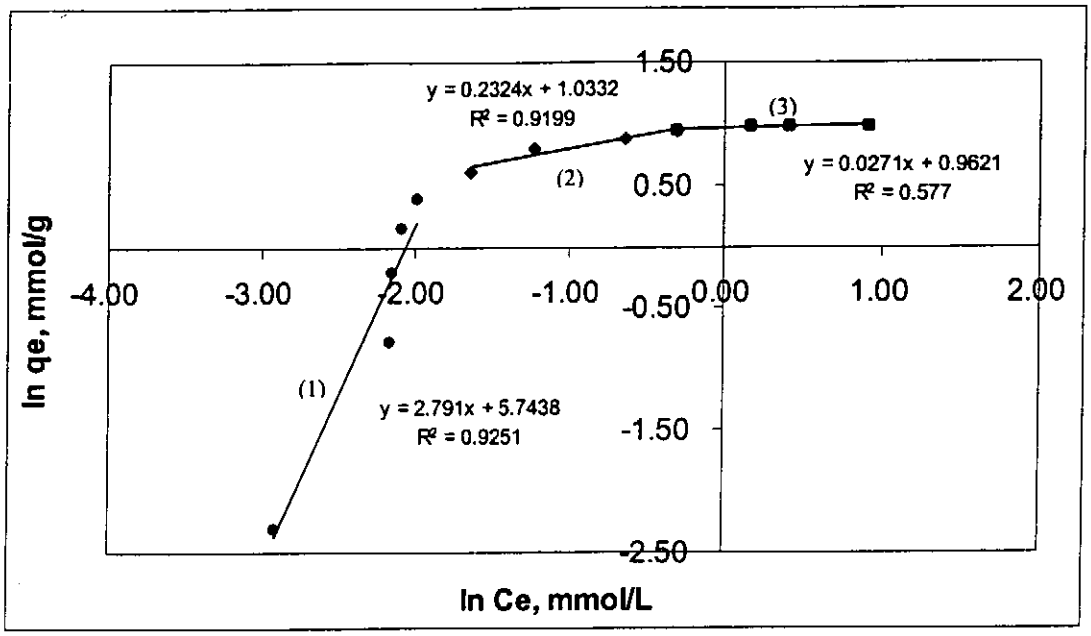

Figure 5.3(c) Freundlich Isotherm Linear Plots for the Sorption of Acid Orange 12 onto Chitosan at Temperature = 25 °C, Degree of Deacetylation (DD) = 53%, pH = 4.00, dp = 355-500 μm

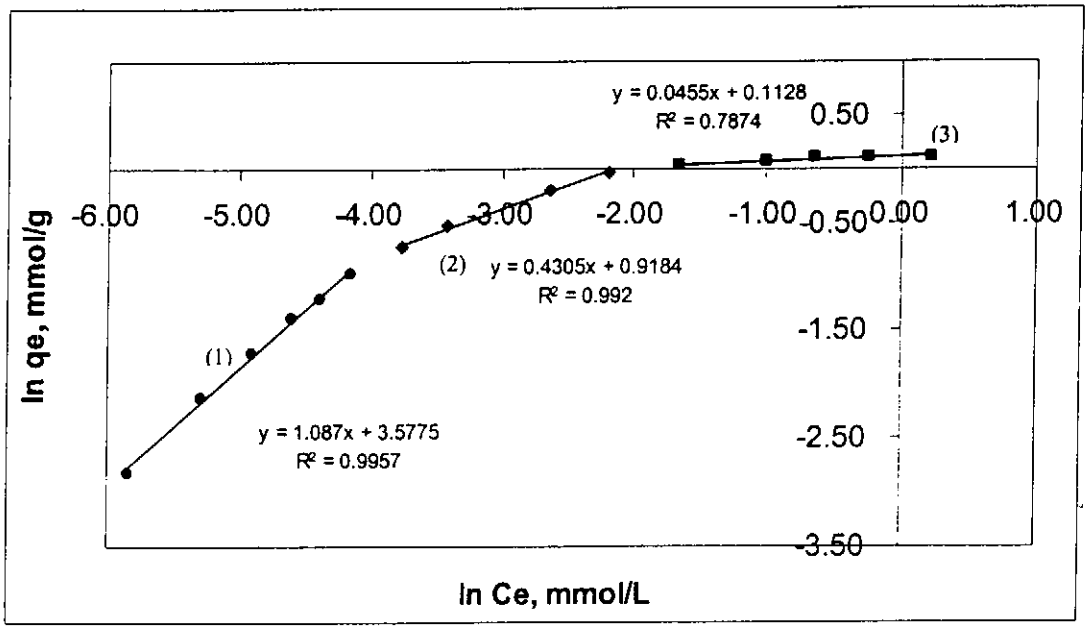

Figure 5.3(d) Freundlich Isotherm Linear Plots for the Sorption of Acid Red 18 onto Chitosan at Temperature = 25 °C, Degree of Deacetylation (DD) = 53%, pH = 4.00, dp = 355-500 μm

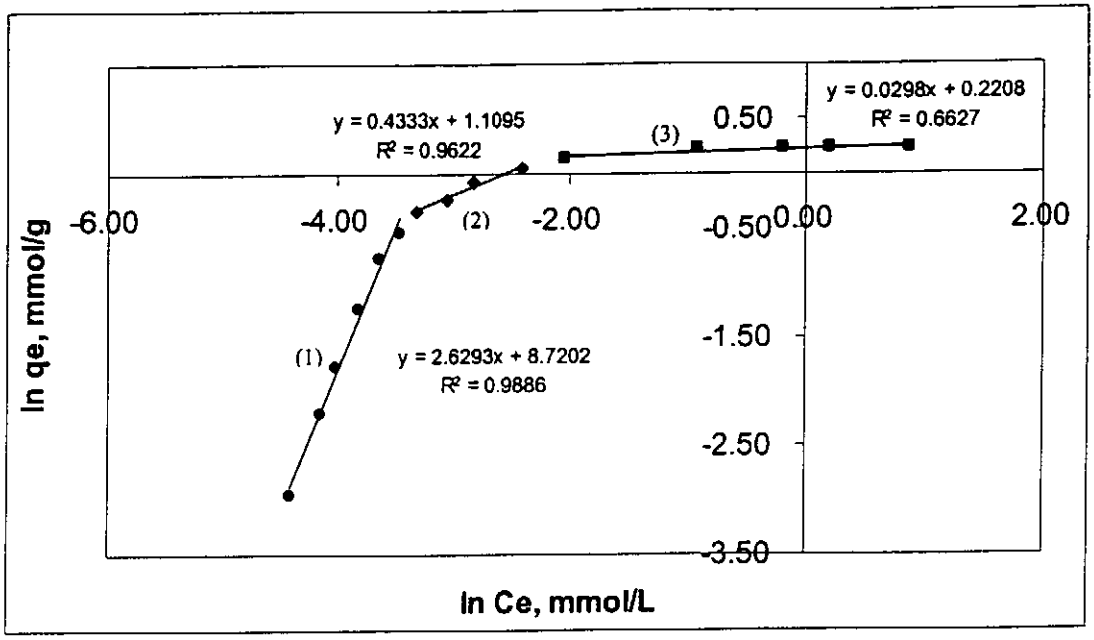

Figure 5.3(e) Freundlich Isotherm Linear Plots for the Sorption of Acid Red 73 onto Chitosan at Temperature = 25 °C, Degree of Deacetylation (DD) = 53%, pH = 4.00, dp = 355-500 μm

Dye	Region	b_F	K_F (mg^3/g)	R^2
AG25	(1)	2.4818	41606	0.9681
	(2)	0.0715	1.0299	0.8508
	(3)	0.0272	1.0046	0.7352
AO10	(1)	1.32	0.651	0.996
	(2)	0.517	0.7755	0.9995
	(3)	0.1105	1.2667	0.9011
AO12	(1)	0.2791	312.249	0.9251
	(2)	0.2324	2.81	0.9199
	(3)	0.027	2.6172	0.577
AR18	(1)	1.087	35.784	0.9957
	(2)	0.4305	2.5053	0.992
	(3)	0.0455	1.1194	0.7874
AR73	(1)	2.6293	6125.4	0.9886
	(2)	0.4333	3.0328	0.9622
	(3)	0.0298	1.2471	0.6627

Table 5.2 Freundlich Sorption Isotherm Constants for AG25, AO10, AO12, AR18 and AR73 at Different Concentration Ranges

5.1.3 Redlich-Peterson Isotherm

The Redlich-Peterson isotherm contains three parameters and the isotherm equation includes features of the Langmuir and the Freundlich isotherm equations. The parameters of the Langmuir and Freundlich models can be determined using the linear forms of the equations. However, the parameters of the Redlich-Peterson isotherms cannot be determined by linearisation because these three parameter model equations cannot be solved from the linear equation. Therefore, the parameters of the equations

were determined by minimizing the distance between the experimental data points and the theoretical model predictions with the solver add-in function of the Microsoft Excel.

The sorption behavior of AO10, AO12, AG25, AR18 and AR73 onto chitosan can be described by the Redlich-Peterson isotherm equation. The linearized form of the Redlich-Peterson isotherm plots for the sorption of the five dyes onto chitosan are presented in Figure 5.4 (a) and (b). Examination of the data shows that the Redlich-Peterson model describes the sorption of AG25, AR18 and AR73 on chitosan extremely well over the concentration ranges studied and gives moderate fits for AO10 and AO12. The Redlich-Peterson isotherm constants a_R, K_R and β and the correlation coefficients, R^2, for the Redlich-Peterson isotherm are listed in Table 5.3. .

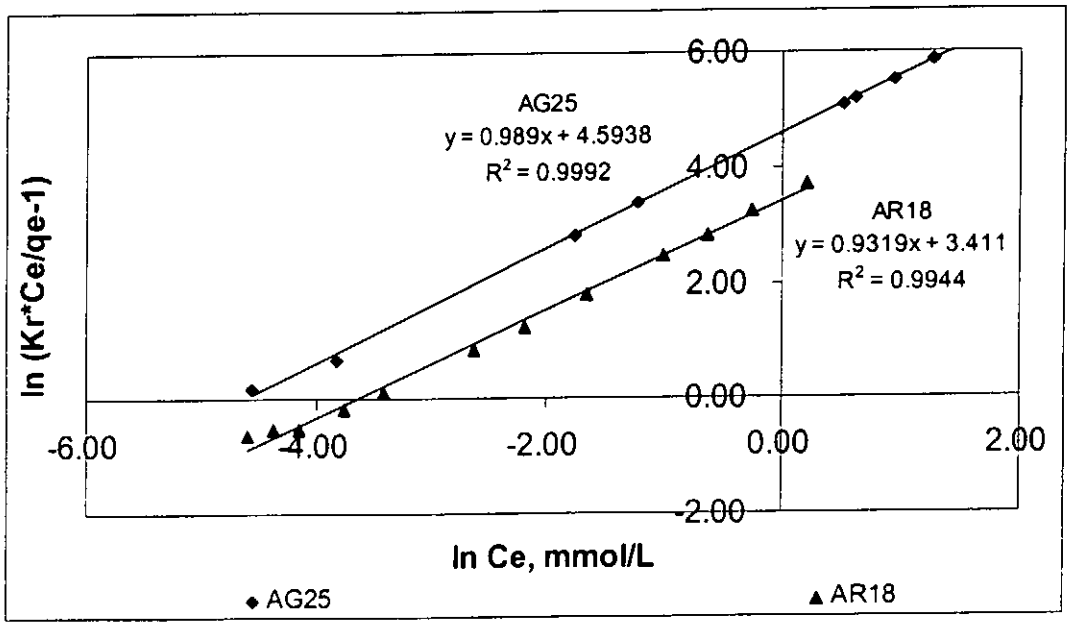

Figure 5.4(a) Redlich-Peterson Isotherm Linear Plots for the Sorption of AG25 and AR18 onto Chitosan at Temperature = 25 °C, Degree of Deacetylation (DD) = 53%, pH = 4.00, dp = 355-500 μm

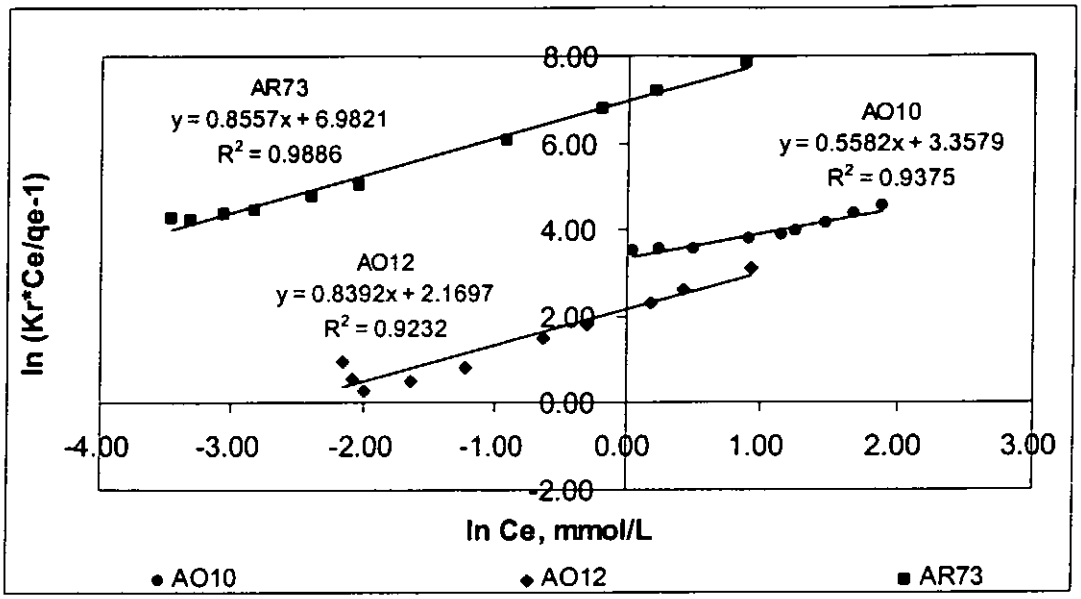

Figure 5.4(b) Redlich-Peterson Isotherm Linear Plots for the Sorption of AO10, AO12 and AR73 onto Chitosan at Temperature = 25 °C, Degree of Deacetylation (DD) = 53%, pH = 4.00, dp = 355-500 μm

	β	K_R (dm^3/g)	a_R (dm^3/mg)	R^2
AG25	0.9963	101.824	98.5366	0.9992
AO10	0.6081	22.435	26.4819	0.9375
AO12	0.9108	25.2658	8.2203	0.9232
AR18	0.9816	38.0287	32.0983	0.9944
AR73	0.9074	1377.996	1119.255	0.9886

Table 5.3 Redlich-Peterson Sorption Isotherm Constants for AG25, AO10, AO12, AR18 and AR73

By comparing the results presented in Tables 5.1 to 5.3, it is shown that the Langmuir sorption isotherm can accurately describe the sorption of Acid Green 25 (AG25),

Acid Red 18 (AR18) and Acid Red 73 (AR73) onto chitosan in this study and that the experimental sorption data of Acid Orange 10 can fit the composite Freundlich isotherm model. Figure 5.5 (a) to (e) show plots comparing the theoretical Langmuir, Freundlich and Redlich-Peterson isotherm equations with experimental data.

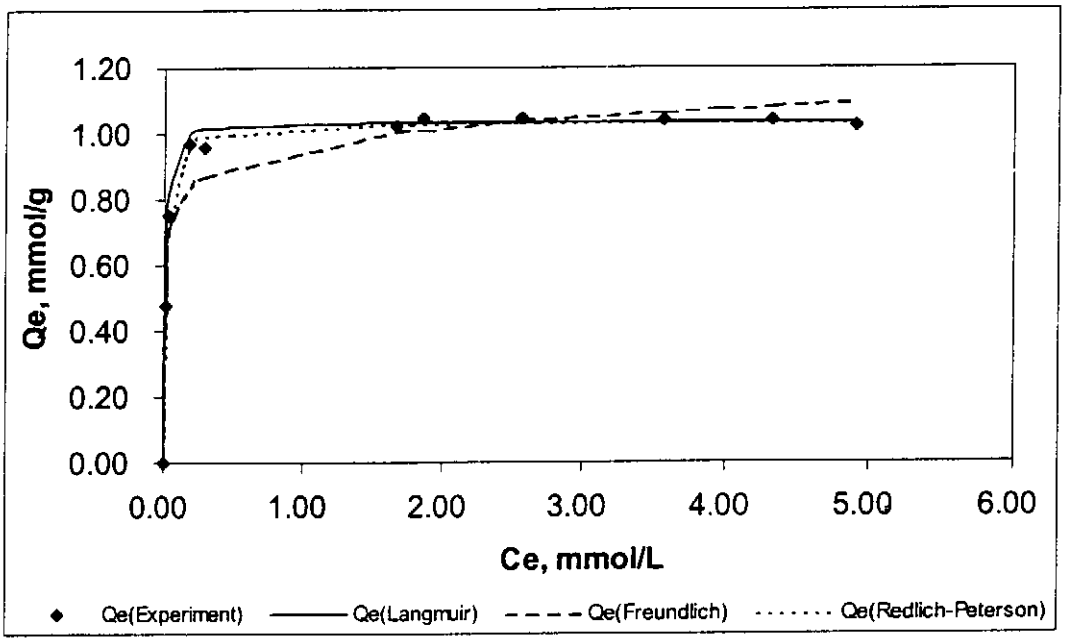

Figure 5.5 (a) Different Isotherm Equation Plots for the Sorption of Acid Green 25 onto Chitosan at Temperature = 25 °C, Degree of Deacetylation (DD) = 53%, pH = 4.00, dp = 355-500 μm

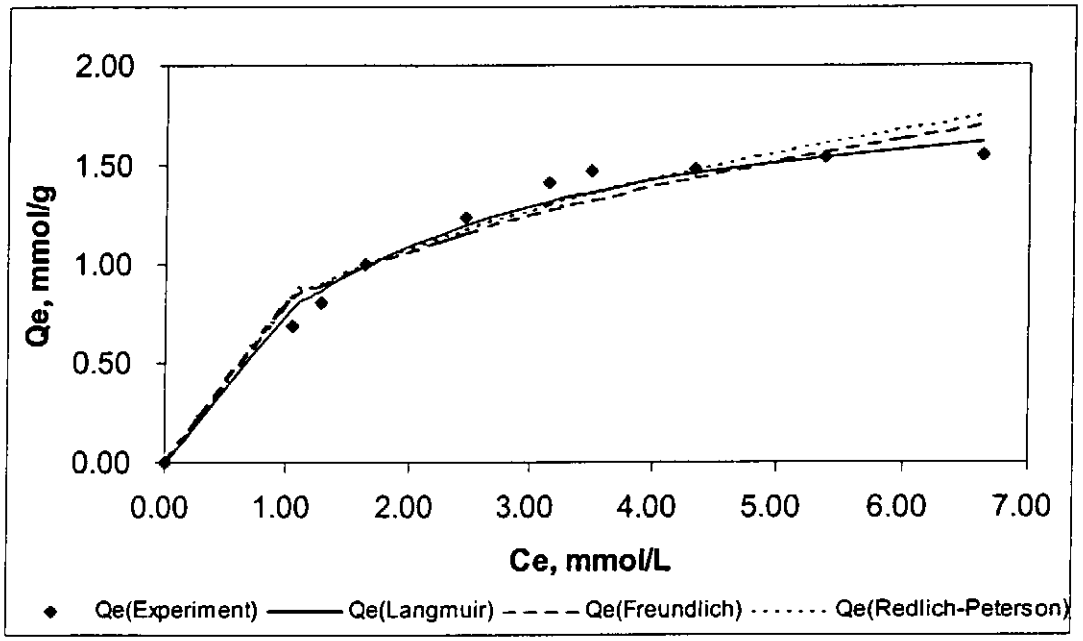

Figure 5.5 (b) Different Isotherm Equation Plots for the Sorption of Acid Orange 10 onto Chitosan at Temperature = 25 °C, Degree of Deacetylation (DD) = 53%, pH = 4.00, dp = 355-500 μm

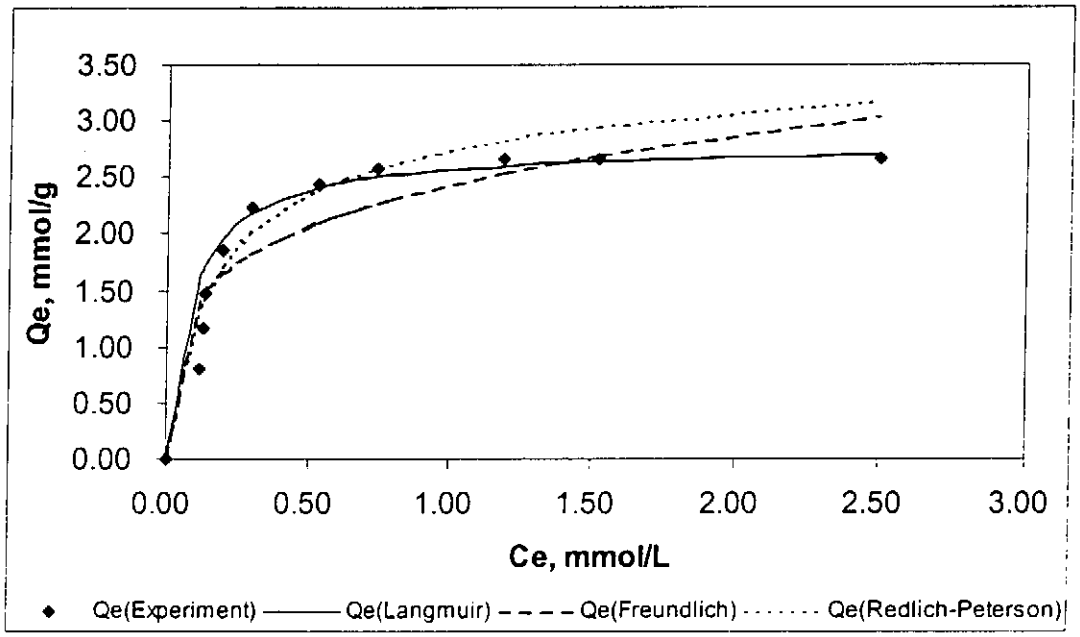

Figure 5.5 (c) Different Isotherm Equation Plots for the Sorption of Acid Orange 12 onto Chitosan at Temperature = 25 °C, Degree of Deacetylation (DD) = 53%, pH = 4.00, dp = 355-500 μm

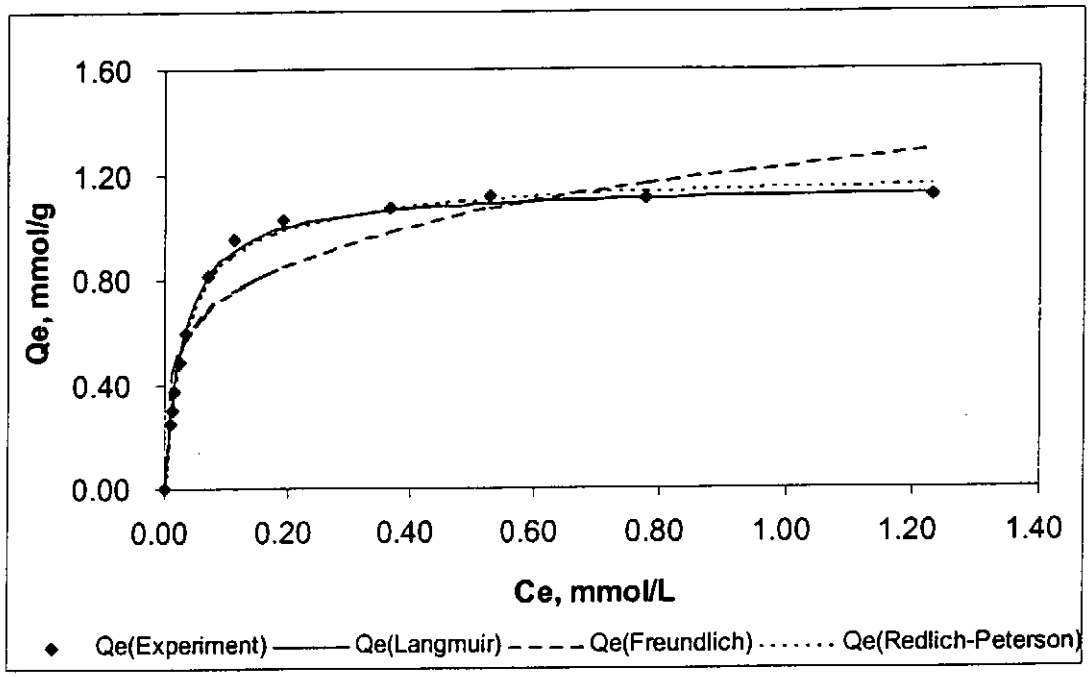

Figure 5.5 (d) Different Isotherm Equation Plots for the Sorption of Acid Red 18 onto Chitosan at Temperature = 25 °C, Degree of Deacetylation (DD) = 53%, pH = 4.00, dp = 355-500 μm

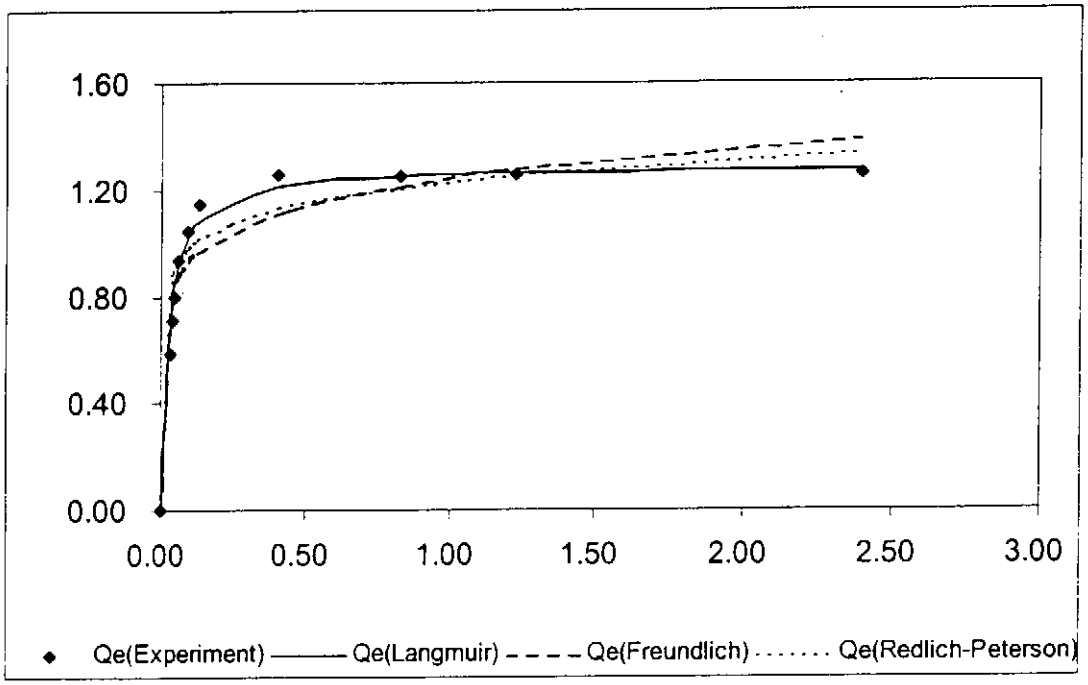

Figure 5.5 (e) Different Isotherm Equation Plots for the Sorption of Acid Red 73 onto Chitosan at Temperature = 25 °C, Degree of Deacetylation (DD) = 53%, pH = 4.00, dp = 355-500 μm

5.2 Modeling Selection by Error Analysis

The use of R^2 is limited to solving linear forms of isotherm equation, which measure the difference between experimental data and theoretical data in linear plots only, but not the errors in isotherm curves. Besides, the parameters of the Redlich-Peterson isotherm cannot be solved from the linear equation. Purely from a comparison of the correlation coefficients (R^2 values) for the linearised models, will result in higher weighting to the higher C_e value data points, thus giving a better fit correlation to the higher C_e value date points. Due to the inherent bias resulting from linearisation, different error functions of non-linear regression basin were employed in this study. The five error functions used were:

- The Sum of the Squares of the Errors (SSE)
- A Hybrid Fractional Error Function (HYBRID)
- Marquardt's Percent Standard Deviation (MPSD)
- The Average Relative Error (ARE)
- The Sum of the Absolute Errors (EABS)

These error methods and equation were described in Chapter 4, Section 4.3.1 to 4.3.5. The values of all five error measurements were presented in Tables 5.4 to 5.8 and the sorption of Acid Green 25 on chitosan with different error analysis methods are shown in Figure 5.6 (a) to (c). By comparing the results of the values for the error function, contradicting 'best-fit' results from linearization were obtained, in which, the Redlich-Peterson isotherm results in the lowest values for the error function and thus fit the data better than the previous prediction analysis using R^2, i.e the Langmuir

isotherm was the best fit model for AG25, AR18, AR73 and Freundlich isotherm was the best fit model for AO10 and AO12 on chitosan.

The Redlich-Peterson equation is a combination of the Langmuir and Freundlich models. It approaches the Freundlich model at high concentration and is in accord with the low concentration limit of the Langmuir equation (Suen, 1996). Furthermore, the Redlich-Peterson equation incorporates three parameters into an empirical isotherm, and therefore can be applied either in homogenous or heterogeneous systems due to the high versatility of the equation. In fact, by considering the adsorption of acid dyes onto the surface of chitosan, different mechanisms may be involved such as ionic attraction between anionic sulphonate group(s) of dissolved dye molecules and the cationic amino groups of protonated chitosan, hydrophobic attraction of the alkyl groups.

	SSE	HYBRID	MPSD	ARE	EABS
Freundlich	0.3304	7.7950	39.1717	27.5162	1.5550
Langmuir	0.0066	0.1000	3.7219	7.3517	0.1770
Redlich-Peterson	0.0065	0.1130	0.1546	1.9052	0.2120

Table 5.4 The Values of Five Different Error Analyses of Isotherm Models of AG25 on Chitosan

	SSE	HYBRID	MPSD	ARE	EABS
Freundlich	0.3316	5.4590	32.6093	27.3966	1.8610
Langmuir	0.0352	0.3570	5.3605	4.0174	0.5590
Redlich-Peterson	0.0036	0.0390	0.9764	23.0837	0.7980

Table 5.5 The Values of Five Different Error Analyses of Isotherm Models of AO10 on Chitosan

	SSE	HYBRID	MPSD	ARE	EABS
Freundlich	2.7527	38.1300	61.8326	50.5622	4.8520
Langmuir	0.4233	3.6710	16.7511	10.6549	1.6310
Redlich-Peterson	0.0149	0.1200	1.1376	2.6486	0.2520

Table 5.6 The Values of Five Different Error Analyses of Isotherm Models of AO12 on Chitosan

	SSE	HYBRID	MPSD	ARE	EABS
Freundlich	0.3513	6.3070	40.2105	31.6543	1.9880
Langmuir	0.0059	0.0840	3.6278	2.7272	0.2150
Redlich-Peterson	0.0104	0.0200	0.0366	1.4128	0.1210

Table 5.7 The Values of Five Different Error Analyses of Isotherm Models of AR18 on Chitosan

	SSE	HYBRID	MPSD	ARE	EABS
Freundlich	0.9710	19.7920	63.2987	52.3622	3.2910
Langmuir	0.0218	0.3200	6.1530	4.1126	0.3750
Redlich-Peterson	0.0085	0.1290	0.1588	3.9739	1.0380

Table 5.8 The Values of Five Different Error Analyses of Isotherm Models of AR73 on Chitosan

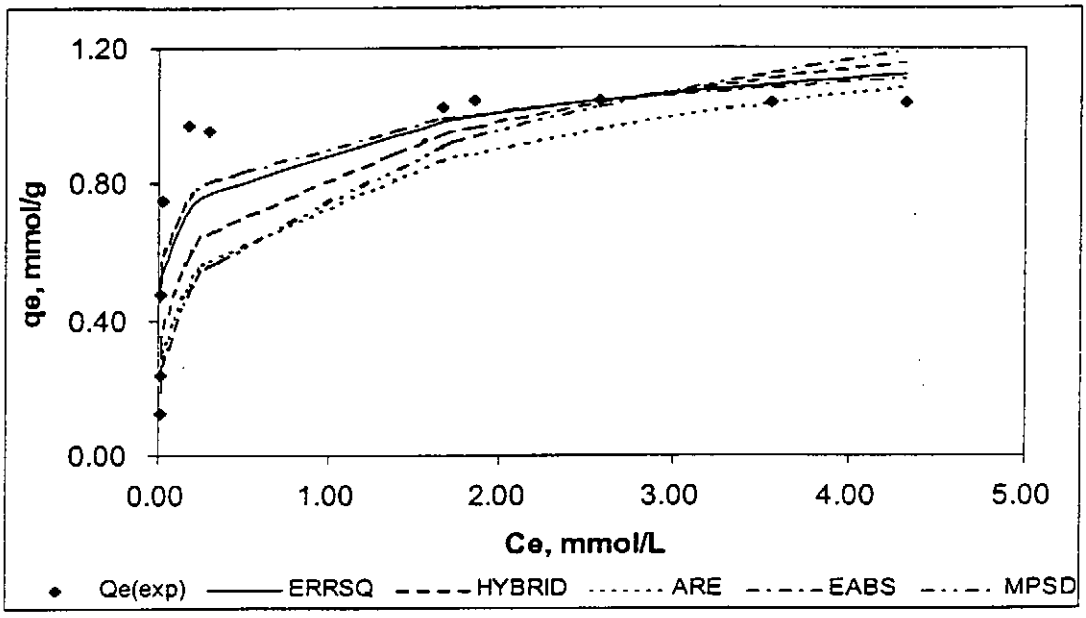

Figure 5.6 (a) Freundlich Isotherm Plots for the Sorption of Acid Green 25 onto Chitosan at 25 °C, Degree of Deacetylation (DD) = 53%, pH = 4.00, dp = 355-500 μm using Different Error Analysis Methods

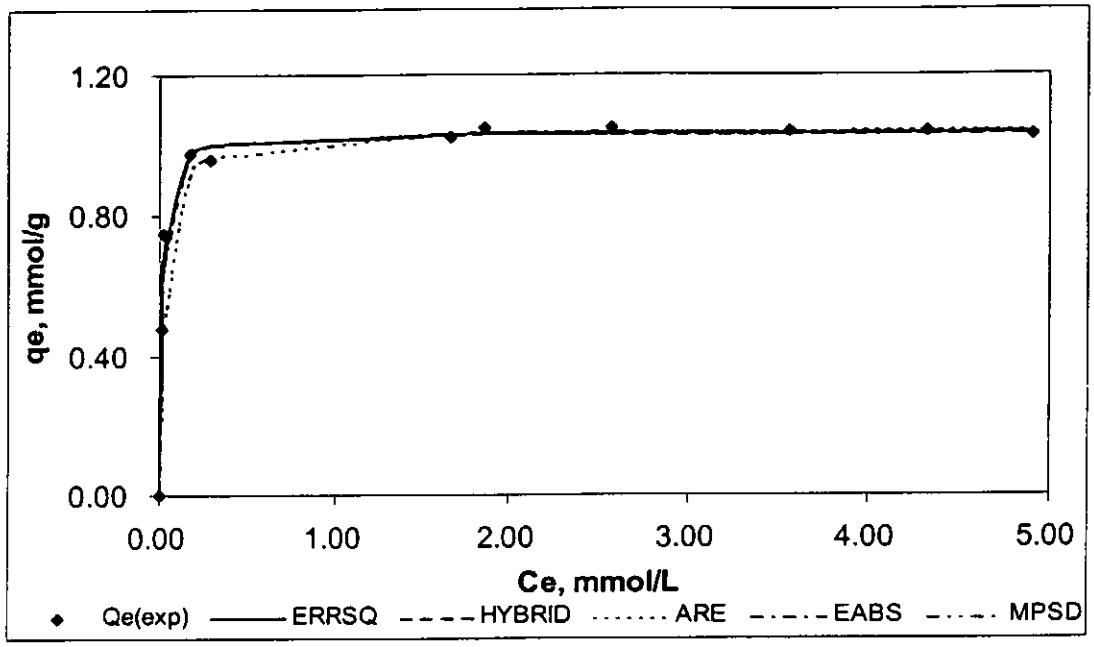

Figure 5.6 (b) Langmuir Isotherm Plots for the Sorption of Acid Green 25 onto Chitosan at 25 °C, Degree of Deacetylation (DD) = 53%, pH = 4.00, dp = 355-500 μm using Different Error Analysis Methods

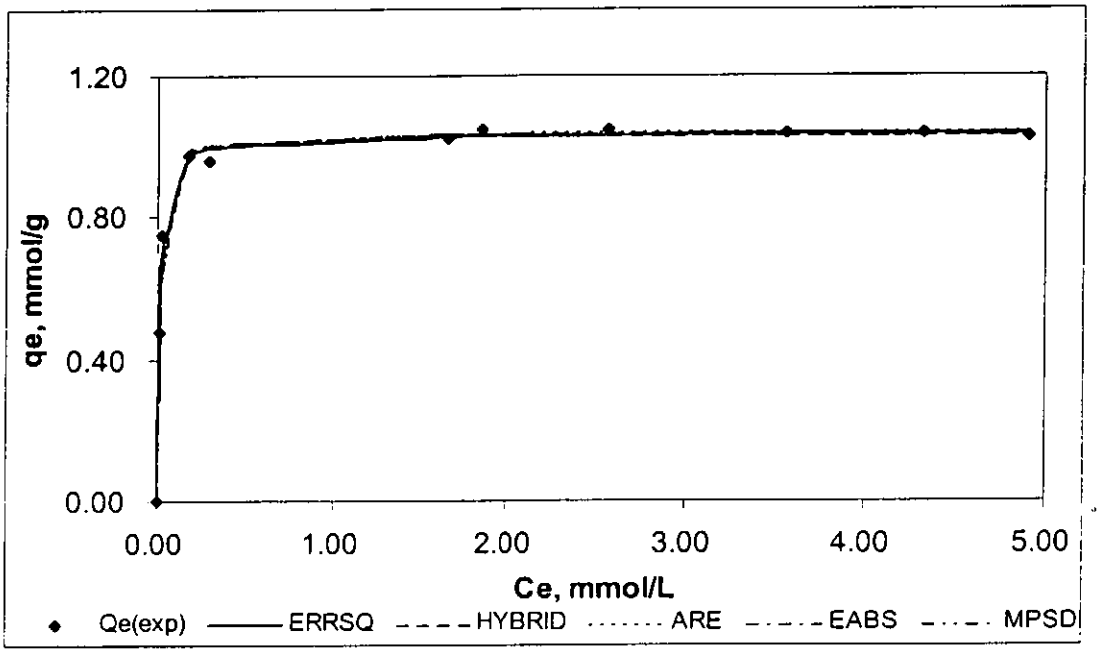

Figure 5.6 (c) Redlich-Peterson Isotherm Plots for the Sorption of Acid Green 25 onto Chitosan at 25 °C, Degree of Deacetylation (DD) = 53%, pH = 4.00, dp = 355-500 μm using Different Error Analysis Methods

5.3 Effect of Temperature

The effect of temperature on the adsorption of Acid Orange 10, Acid Red 18, and Acid Red 73 is shown in Figure 5.7 (a) to (c) respectively. The results show that the adsorption capacities increase with increasing temperature from 25 °C to 60 °C. This phenomenon is quite common and is due to the fact that increasing temperature not only increases the mobility of the large dye ions, but may also produce a swelling effect within the internal structure of the chitosan. Besides, higher temperature enables the large dye molecules to penetrate further and a similar result was reported previously by McKay *et al.* (1982), for the adsorption of dyes on chitin. Further increase in the temperature from 60 °C to 80°C has little or no influence on its ability to adsorb Acid Red 73, but the adsorption capacity of Acid Red 18 increases its maximum at 80°C. However, a completely different effect is observed for the adsorption of Acid Orange 10, the capacity decreases with increasing temperature, such an effect is probably due to the enhanced magnitude of the reverse step (or desorption) in the mechanism as the temperature increases (McKay *et al.*, 1982). Furthermore, Figures 5.7 (a) to (c) also indicate that the amount of adsorbed dyes on chitosan decreases with an increase in temperature at lower initial concentration levels and a similar finding was reported previously by Yoshida *et al* (1991).

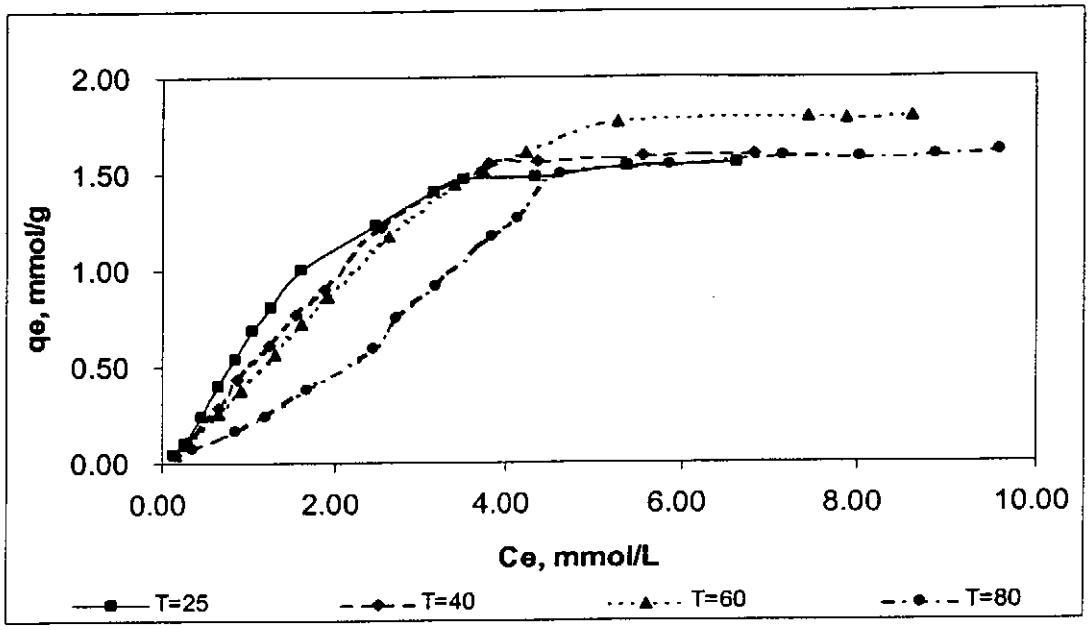

Figure 5.7 (a) Sorption of Acid Orange 10 onto Chitosan at Different Temperature, Degree of Deacetylation (DD) = 53%, pH=4.00, dp = 355-500μm

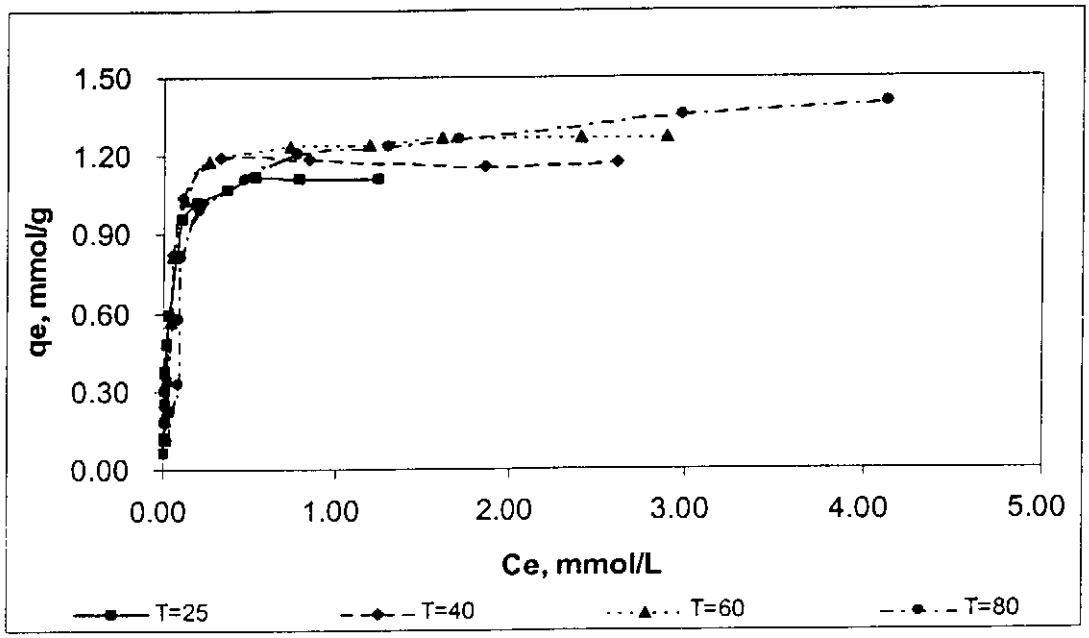

Figure 5.7 (b) Sorption of Acid Red 18 onto Chitosan at Different Temperature, Degree of Deacetylation (DD) = 53%, pH=4.00, dp = 355-500μm

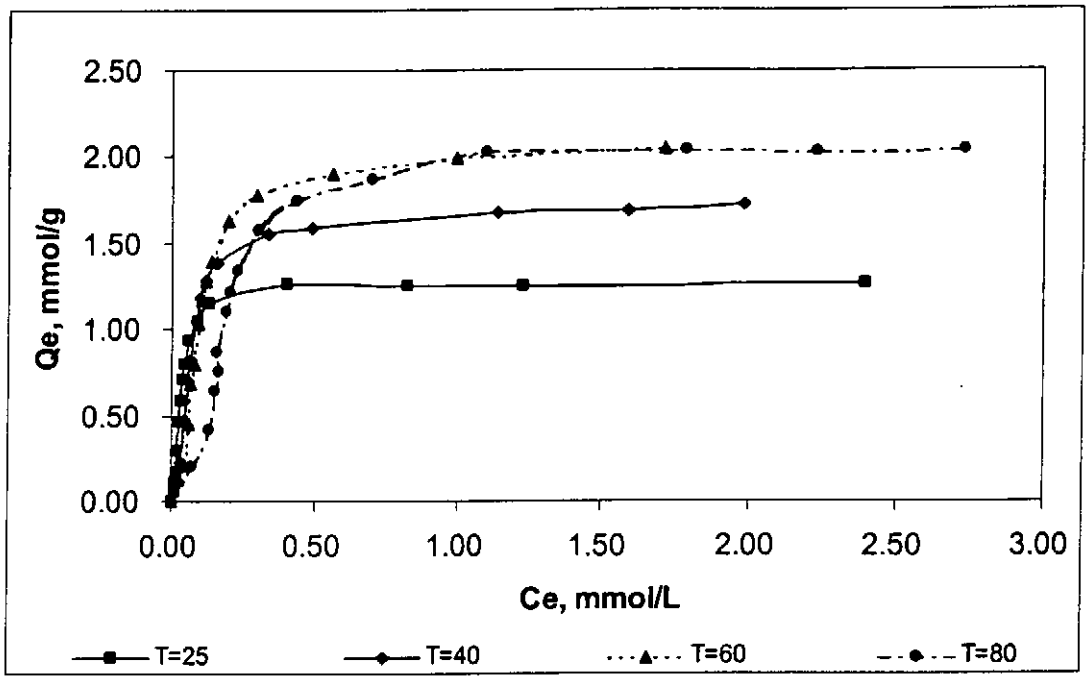

Figure 5.7 (c) Sorption of Acid Red 73 onto Chitosan at Different Temperature, Degree of Deacetylation (DD) = 53%, pH=4.00, dp = 355-500μm

5.4 Effect of Particle Size (dp)

The influence of adsorbent particle size is shown in Figure 5.8 (a) and (b) indicating that chitosan particle size strongly affected the amount of acid dye being absorbed. The amount of dye adsorbed increased with decreasing particle size due to the inability of the large dye molecules to penetrate into the internal pore structure of chitosan and a similar phenomenon was reported previously Shimizu *et. al.* (1995) and Annadurai *et. al.* (1997). Annadurai and Krishnan (1997) also showed that the specific dye uptake at equilibrium increased owing to the increase in total surface area made available for adsorption that was proved by the increase in the specific BET surface areas in the smaller particle sizes. More recent studies published by Carlough

et al. (1991) indicated that decreasing particle size would increase the driving force of a reactive dye from the bulk phase onto and into the solid chitosan, thus increasing the initial adsorption rate and the final equilibrium capacity.

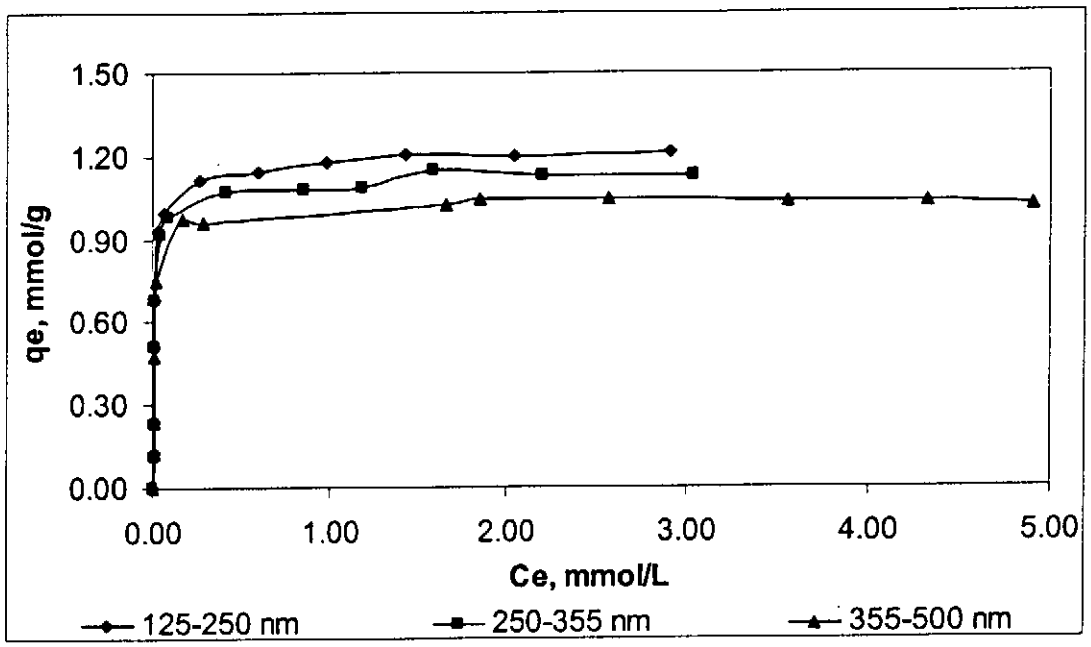

Figure 5.8 (a) Sorption of Acid Green 25 onto Chitosan with Different Particle Size (dp) at 25 °C, Degree of Deacetylation (DD) = 53%, pH=4.00.

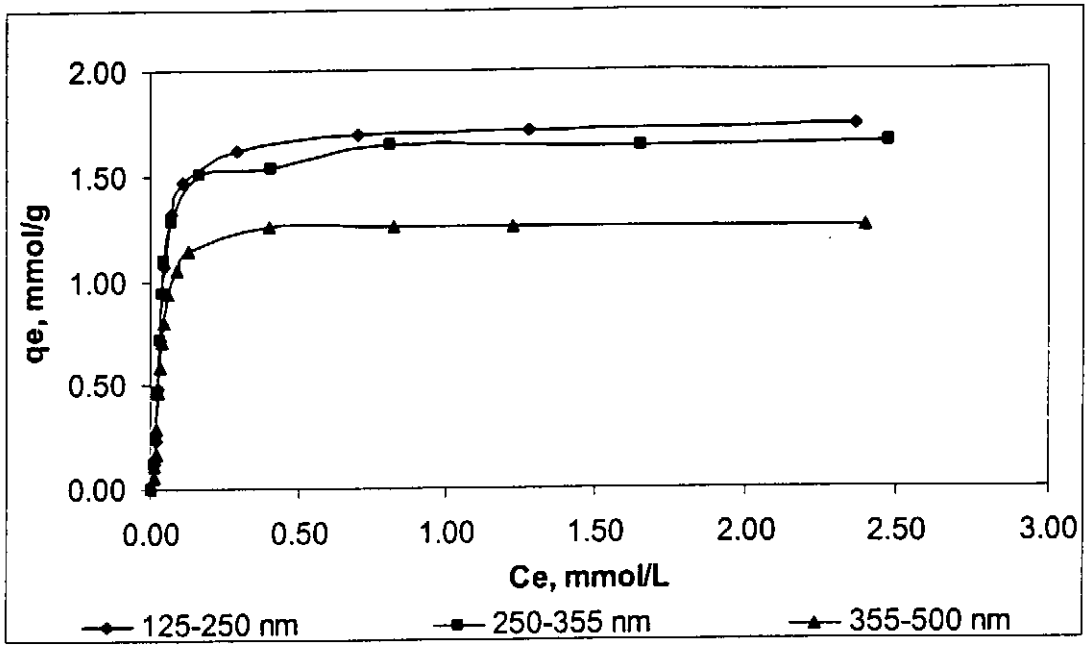

Figure 5.8 (b) Sorption of Acid Red 73 onto Chitosan with Different Particle Size (dp) at 25 °C, Degree of Deacetylation (DD) = 53%, pH=4.00.

5.5 Effect of Degree of Deacetylation (DD%)

The effect of degree of deacetylation (DD) on the adsorption of acid dyes onto chitin and chitosan was presented at Figure 5.9 (a) and (b). Mckay *et al.* (1982) reported that sorption of dye anions on chitin and chitosan could be attributed to many different interactions between the sorbate and sorbent molecules, namely, ionic bonding ability, hydrophobic interaction due to planarity and other geometric configurations of the dye molecules, chelating ability of the chitin-dye and chitosan-dye system through coordinating bonding in premetallized dyes and hydrogen bonding. The significant increases in sorption capacities of three chitosans were mainly due to an increase in amino groups of the sorbent and low pH of the system, which facilitate ionic bonding between the protonated amino groups of chitosan and

dye anions. However, the adsorption process of dyes onto chitosan mainly take place at the amorphous region within chitosan, and therefore explaining that a further increase in the DD % of chitosan leads to a decrease in the specific capacities. The homogeneity of the internal structure of chitosan with higher DD % facilitates the formation of a crystalline region within the sorbent. Besides, Kim *et al.* (1997) also suggested that a higher DD % leads to a reduction in the hydrophobicity of the chitosan. This may become substantial, resulting in low capacities. Similar results were published by Coughlin *et al.* (1990) for the adsorption of nickel ions onto chitosan.

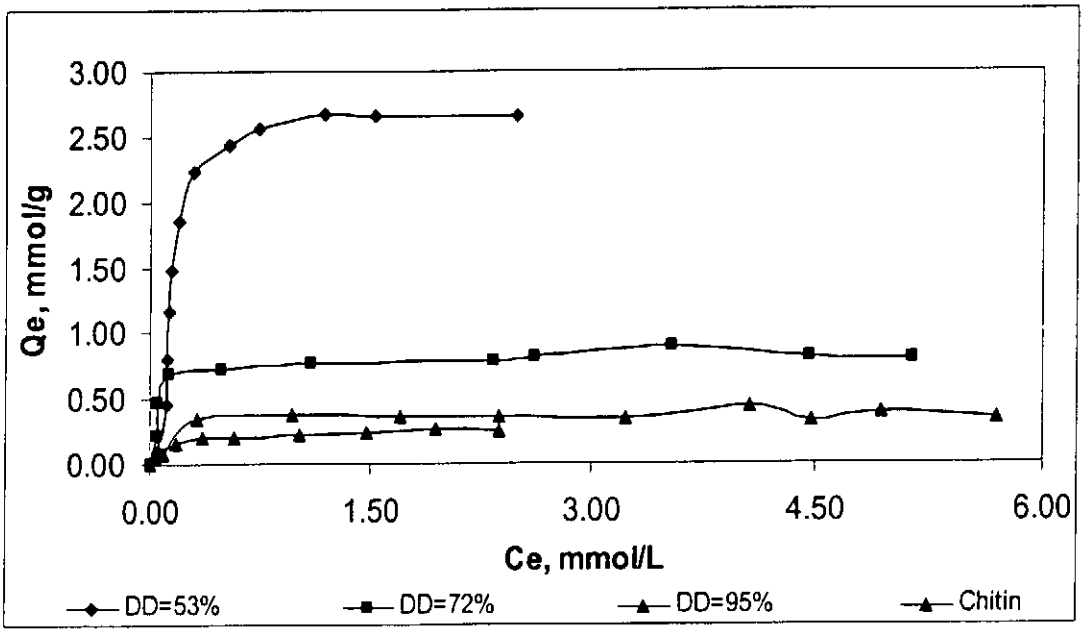

Figure 5.9 (a) Sorption of Acid Orange 12 onto Chitosan with Different Degree of Deacetylation (DD) at 25 °C, pH=4.00, dp = 355-500μm.

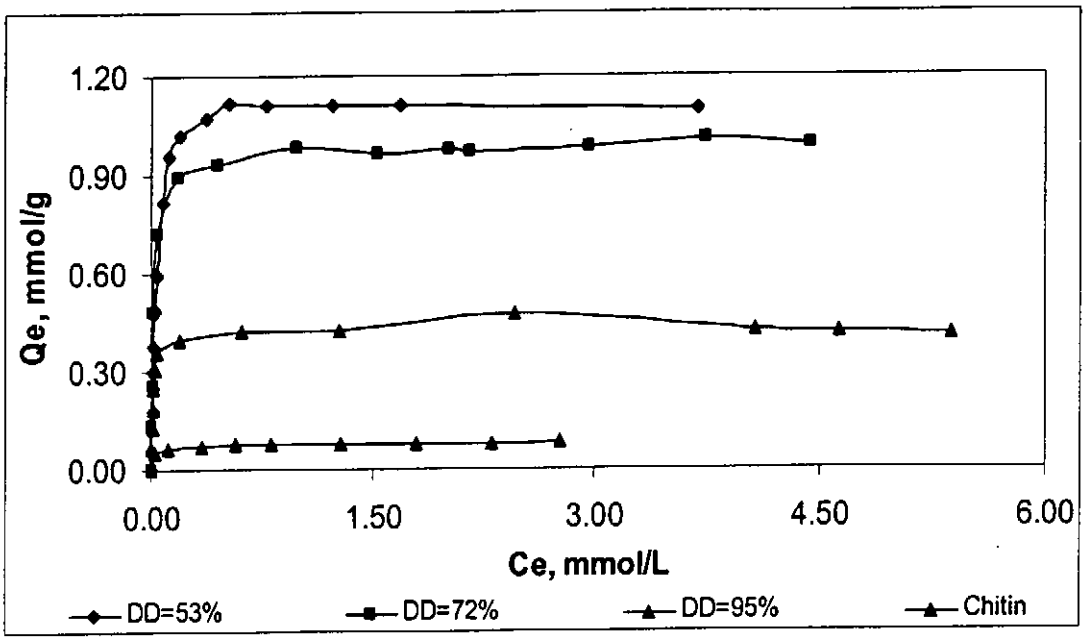

Figure 5.9 (b) Sorption of Acid Red 18 onto Chitosan with Different Degree of Deacetylation (DD) at 25 °C, pH=4.00, dp = 355-500μm.

5.6 Batch Kinetic Systems

Sorption systems have been investigated to assess the applicability of chitosan as a suitable sorbent for the removal of acid dyes in dye wastewater. An equilibrium analysis is the most important fundamental information required for evaluating the affinity or capacity of a sorbent. However, an ideal sorbent for wastewater pollution control must not only have a large sorbate capacity, but also the sorption rate must be fast. Therefore, the sorption rate is the other important factor for the selection of the sorbent and sorption kinetics which must be taken into account.

In this research, there are totally four kinetic models applied to the sorption of acid dyes to chitosan. The kinetic models are the pseudo-first order equation, the pseudo-second order equation, the modified second order equation and the Elovich equation. The parameters of the modified second order equation were determined by Solver to minimize the sum of error squares. However, the parameters of the pseudo-first order equation, pseudo-second order equation and the Elovich equation were determined by the linear plots of those equations to obtain the highest value of the correlation coefficient (R^2).

5.6.1 The Pseudo-first Order Equation

Linear form of Pseudo-first order equation is:

$$\log(q_e - q_t) = \log(q_e) - \frac{k_1}{2.303}t \qquad (4.14)$$

Where k_1 is the rate constant of adsorption and q_e is the equilibrium capacity of sorbent. The rate constant, k_1, is calculated from the slope of equation (4.14). The equilibrium capacity q_e is calculated by use a trial and error method in conjunction with an optimization routine to maximize the correlation coefficient for equation (4.14) by Solver. The correlation coefficients (R^2) were calculated by equation (5.4):

$$R^2 = 1 - \frac{SSE}{SST} \qquad (5.4)$$

Where, $SSE = \sum (q_{exp} - q_{cal})^2$ = Sum of Error Square

$$SST = \sum (q_{exp})^2 - \frac{(\sum q_{exp})^2}{n} \text{ = Sum of Total Error Square}$$

Figure 5.10 (a) to (e) and Figure 5.10 (f) to (i) are the linear plots of pseudo-first order equation with different initial concentrations of various acid dyes and different mass of chitosan respectively during the first 3 hours of the sorption period. The rate constant, k_1, and equilibrium capacity, q_e, of each kinetic system were determined by an iterative procedure to obtain the highest value of correlation coefficient. Table 5.9 listed the rate constant, k_1, equilibrium capacity, q_e, Sum of Error Square, SSE, and correlation coefficient, R^2, for the first order equation. However, the equilibrium capacities of various acid dyes obtained by Solver could not be applied to the later stages of the sorption process, i.e. after 3 hours, of the sorption period, it was apparent that the sorption kinetics at the later stages may involve diffusion kinetics, other reaction kinetics and/or their combinations, which could not correlated well with the Pseudo-1st Order Equation.

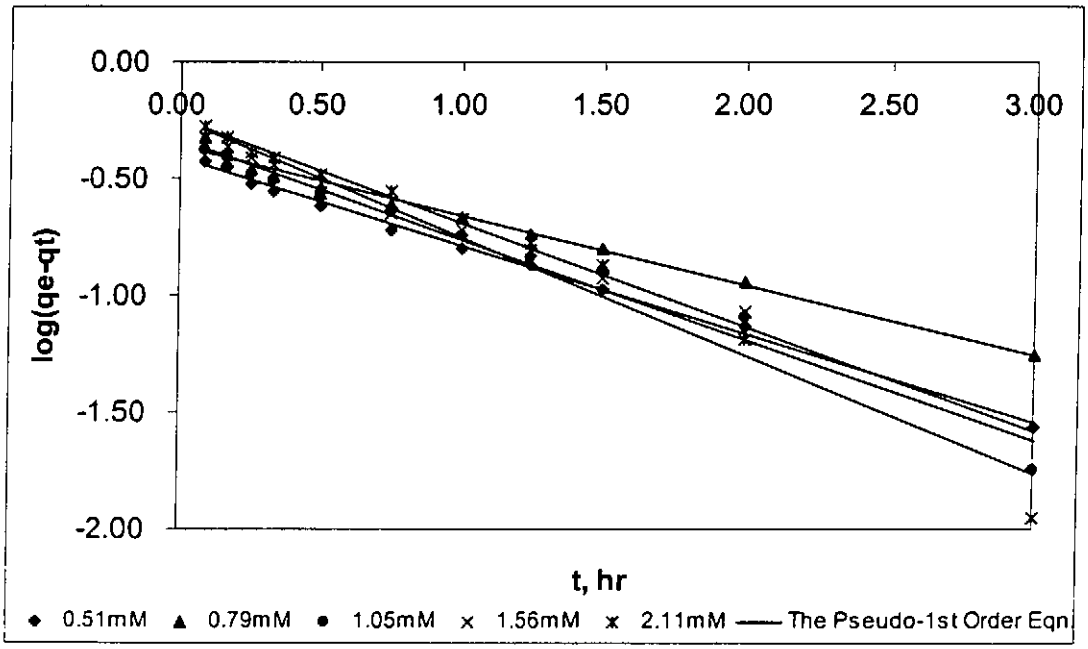

Figure 5.10 (a) Linear Plot of The Pseudo-1st Order Equation of the Sorption of Acid Green 25 onto Chitosan with Different Initial Concentrations at Room Temperature, Mass=1.7000g, Degree of Deacetylation (DD=53%), pH=4.00, dp=355-500 μm

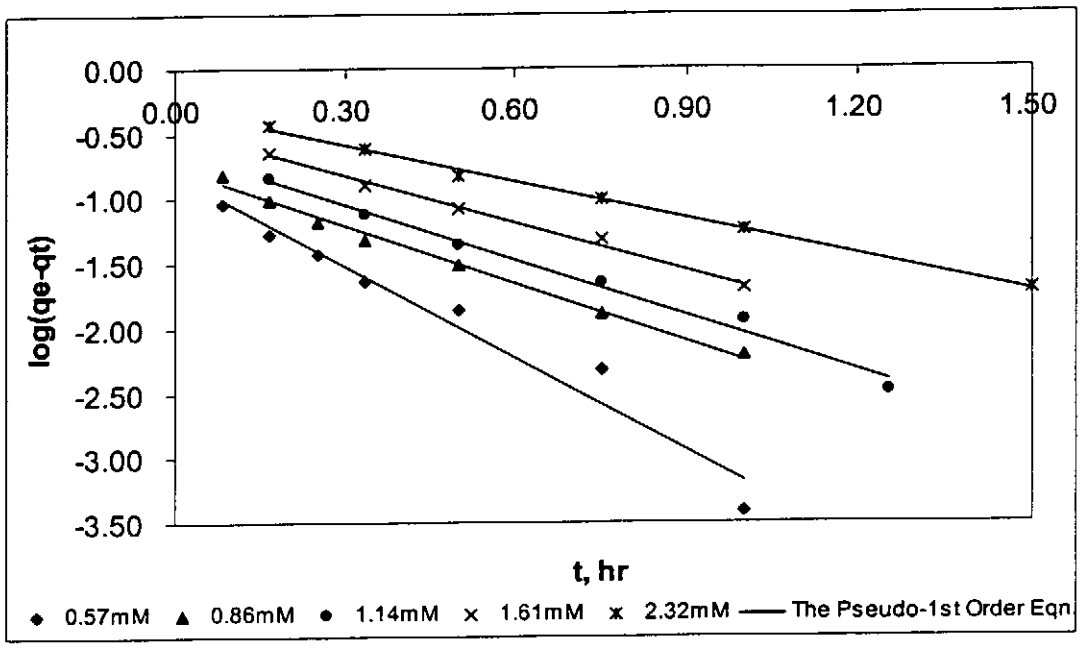

Figure 5.10 (b) Linear Plot of The Pseudo-1st Order Equation of the Sorption of Acid Orange 10 onto Chitosan with Different Initial Concentrations at Room Temperature, Mass=1.7000g, Degree of Deacetylation (DD=53%), pH=4.00, dp=355-500 μm

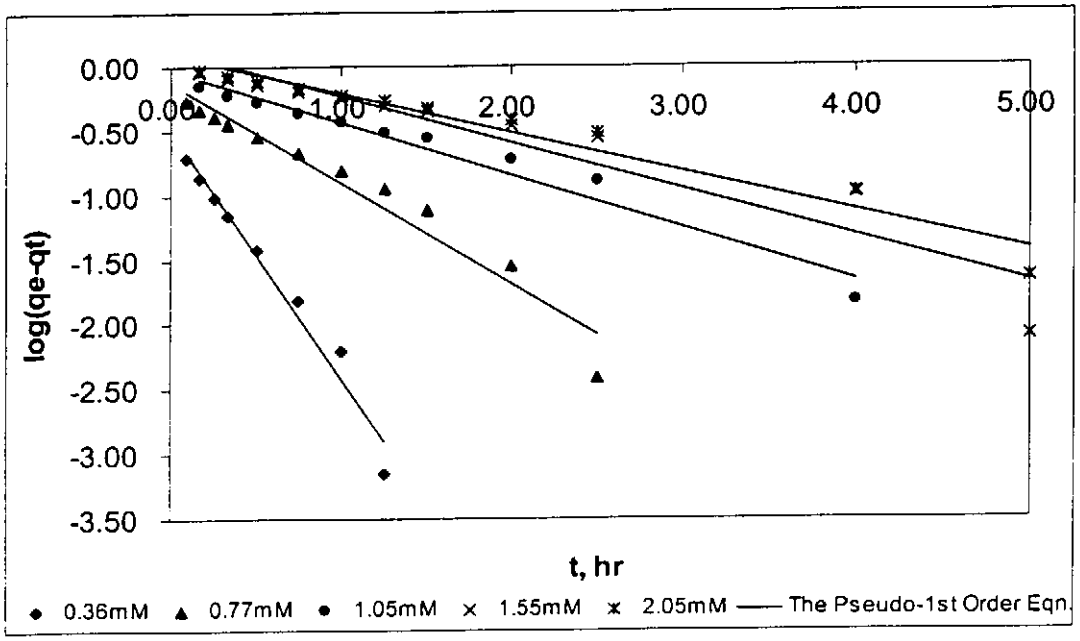

Figure 5.10 (c) Linear Plot of The Pseudo-1st Order Equation of the Sorption of Acid Orange 12 onto Chitosan with Different Initial Concentrations at Room Temperature, Mass=1.7000g Degree of Deacetylation (DD=53%), pH=4.00, dp=355-500 μm

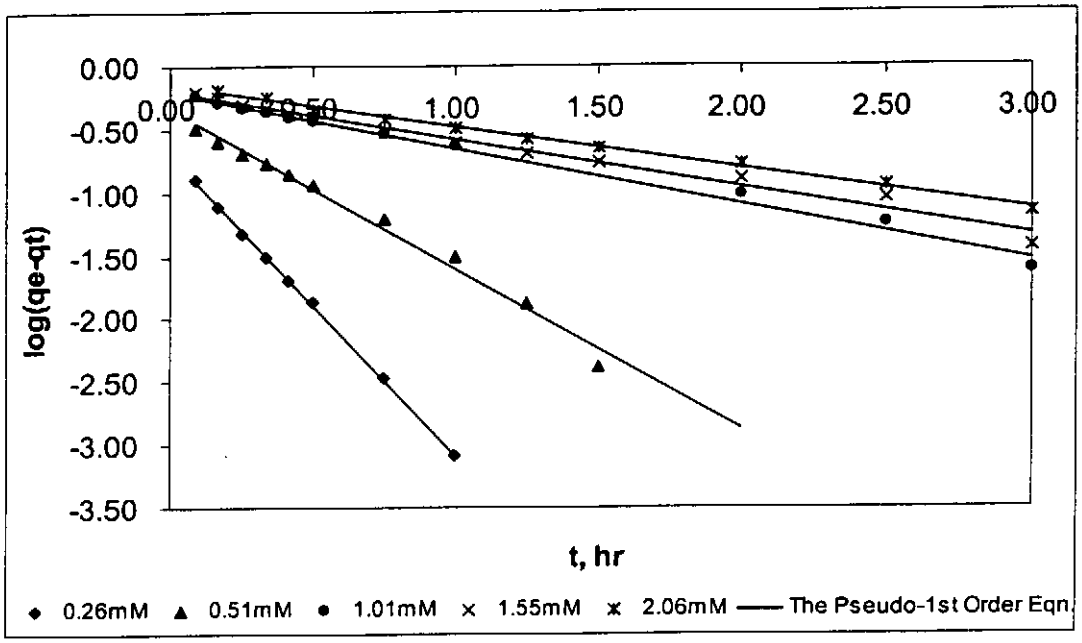

Figure 5.10 (d) Linear Plot of The Pseudo-1st Order Equation of the Sorption of Acid Red 18 onto Chitosan with Different Initial Concentrations at Room Temperature, Mass=1.7000g, Degree of Deacetylation (DD=53%), pH=4.00, dp=355-500 μm

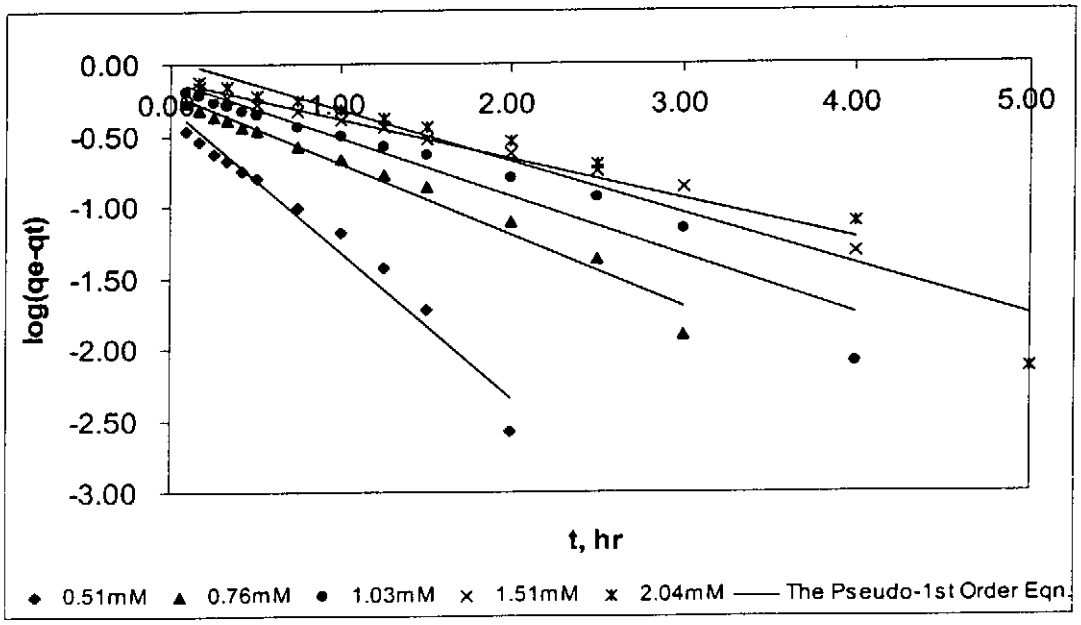

Figure 5.10 (e) Linear Plot of The Pseudo-1st Order Equation of the Sorption of Acid Red 73 onto Chitosan with Different Initial Concentrations at Room Temperature, Mass=1.7000g, Degree of Deacetylation (DD=53%), pH=4.00, dp=355-500 μm

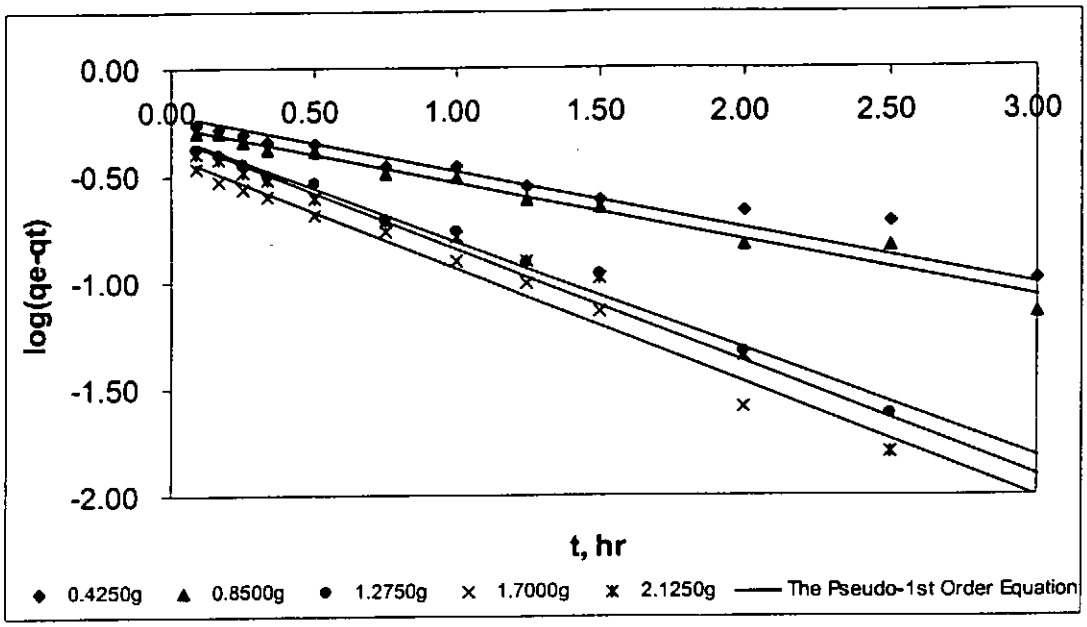

Figure 5.10 (f) Linear Plot of The Pseudo-1st Order Equation of the Sorption of Acid Green 25 onto Chitosan with Different Masses at Room Temperature, C_o=1.00mM, Degree of Deacetylation (DD=53%) pH=4.00, dp=355-500 μm

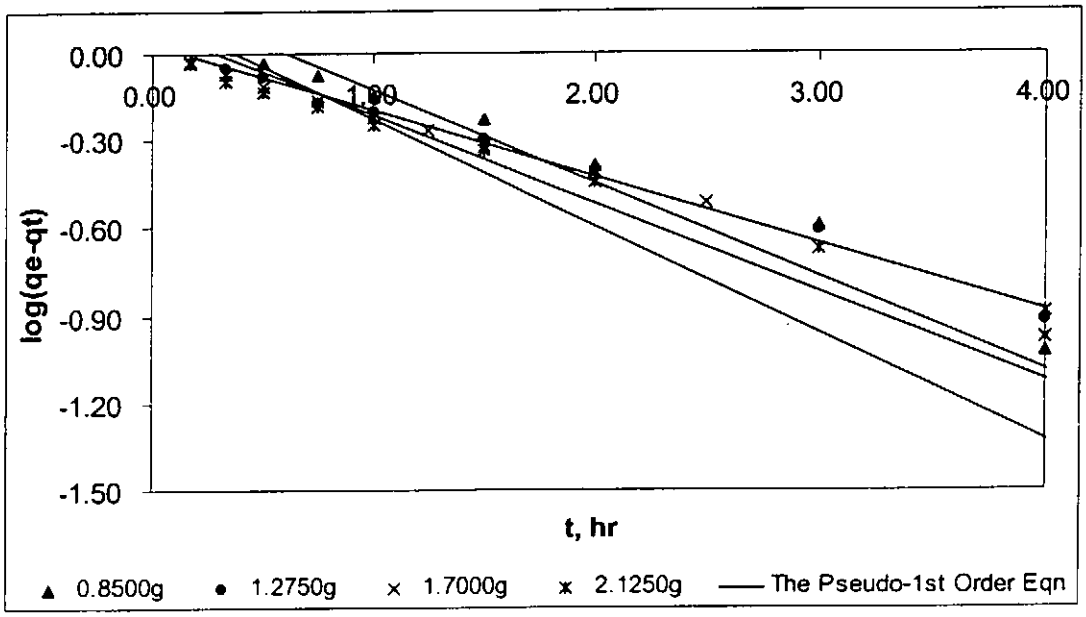

Figure 5.10 (g) Linear Plot of The Pseudo-1st Order Equation of the Sorption of Acid Orange 12 onto Chitosan with Different Masses at Room Temperature, C_o=2.00mM, Degree of Deacetylation (DD=53%) pH=4.00, dp=355-500 μm

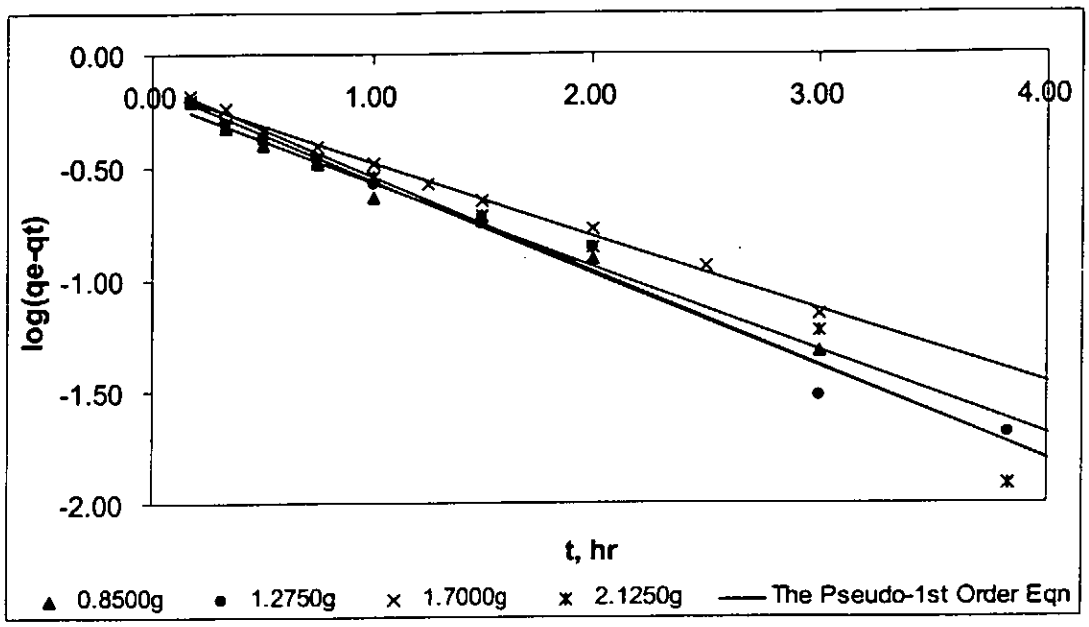

Figure 5.10 (h) Linear Plot of The Pseudo-1st Order Equation of the Sorption of Acid Red 18 onto Chitosan with Different Masses at Room Temperature, C_o=2.00mM, Degree of Deacetylation (DD=53%) pH=4.00, dp=355-500 μm

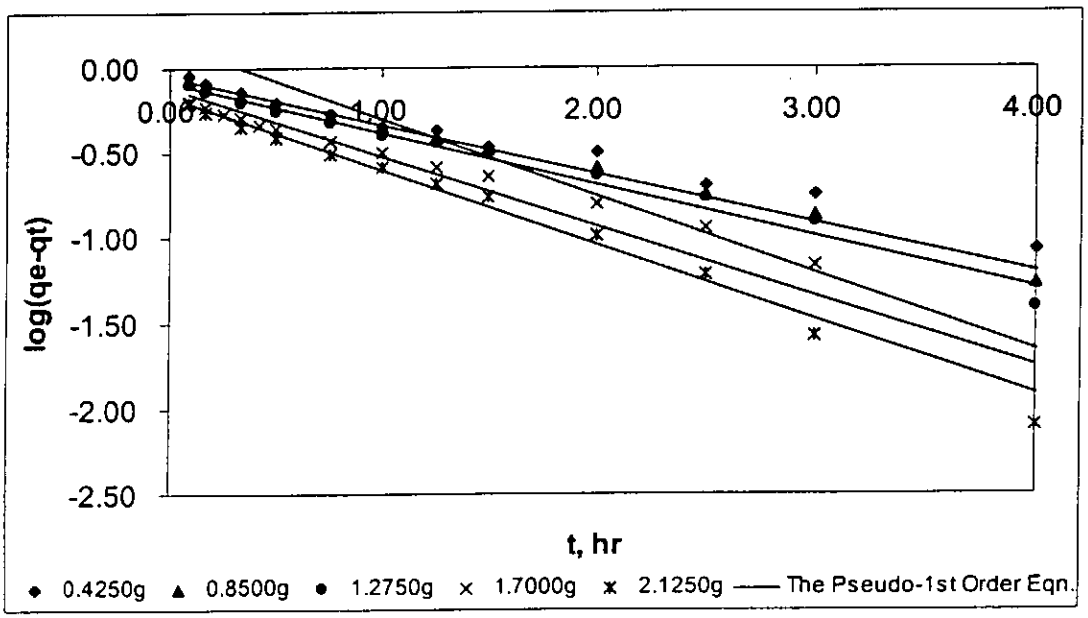

Figure 5.10 (i) Linear Plot of The Pseudo-1st Order Equation of the Sorption of Acid Red 73 onto Chitosan with Different Masses at Room Temperature, C_o=1.00mM, Degree of Deacetylation (DD=53%), pH=4.00, dp=355-500 μm

Concentration Effect					
AG25	Concentration (mM)	k_1	q_e	SSE	R^2
	0.51	1.1310	0.4470	0.0079	0.9635
	1.05	1.1738	0.5065	0.0186	0.9432
	1.56	1.2071	0.5623	0.0100	0.9758
	2.11	1.3218	0.6622	0.0226	0.9555
AO10	Concentration (mM)	k_1	q_e	SSE	R^2
	0.57	7.9765	0.2034	0.0006	0.9423
	0.86	7.2933	0.3361	0.0023	0.9293
	1.14	6.1393	0.4619	0.0023	0.9052
	1.61	5.3418	0.6562	0.0060	0.9038
	2.32	4.2312	0.9127	0.0181	0.8974
A012	Concentration (mM)	k_1	q_e	SSE	R^2
	0.36	4.7935	0.3105	0.0005	0.9902
	0.77	1.7583	0.6861	0.0142	0.9711
	1.05	0.9542	0.9328	0.0271	0.9600
	1.55	0.6992	1.1486	0.05070	0.9534
	2.05	0.6760	1.2011	0.0594	0.9496
AR18	Concentration (mM)	k_1	q_e	SSE	R^2
	0.26	6.9969	0.2544	0.0003	0.9857
	0.51	3.2743	0.4906	0.0049	0.9728
	1.01	1.5337	0.7742	0.0380	0.9443
	1.55	1.3530	0.8113	0.0623	0.9226
	2.06	1.1148	0.9269	0.0487	0.9259
AR73	Concentration (mM)	k_1	q_e	SSE	R^2
	0.51	2.4393	0.4717	0.0051	0.9629
	0.76	1.3548	0.6778	0.0235	0.9555
	1.03	0.9939	0.7765	0.0414	0.9766
	1.51	0.7716	0.8686	0.0325	0.9848
	2.04	0.7246	0.9697	0.0327	0.9707

Table 5.9 Parameters of Pseudo-1st Order Equation for the sorption of AG25, AO10, AO12, AR18 and AR73 onto chitosan with Different Initial Concentration at Room Temperature, Mass=1.7000g, Degree of Deacetylation (DD=53%), pH=4.00, dp=355-500 μm

Mass Effect					
	Mass of Sorbent (g)	**k_1**	**q_e**	**SSE**	**R^2**
AG25	0.4250	0.6607	0.6408	0.0237	0.9539
	0.8500	0.7858	0.6270	0.0258	0.9474
	1.2750	1.2406	0.5161	0.0062	0.9875
	1.7000	1.5390	0.4512	0.0127	0.9680
	2.1250	1.2336	0.4825	0.0055	0.9869
	Mass of Sorbent (g)	**k_1**	**q_e**	**SSE**	**R^2**
A012	---	---	---	---	---
	0.8500	0.6809	1.4478	0.0305	0.9848
	1.2750	0..7036	1.2694	0.0671	0.9516
	1.7000	0.6760	1.2011	0.0594	0.8995
	2.1250	0.6811	1.1389	0.0468	0.9586
	Mass of Sorbent (g)	**k_1**	**q_e**	**SSE**	**R^2**
AR18	---	---	---	---	---
	0.8500	1.4546	0.8919	0.0376	0.9274
	1.2750	1.2868	0.8687	0.0307	0.9418
	1.7000	1.1148	0.9269	0.0487	0.9258
	2.1250	1.2532	0.8671	0.0343	0.9355
	Mass of Sorbent (g)	**k_1**	**q_e**	**SSE**	**R^2**
AR73	0.4250	0.7122	0.9816	0.0346	0.9800
	0.8500	0.7733	0.9765	0.0291	0.9770
	1.2750	0.8291	0.9261	0.0402	0.9936
	1.7000	0.9939	0.7765	0.0414	0.9840
	2.1250	1.1954	0.7613	0.0227	0.9911

Table 5.10 Parameters of Pseudo-1st Order Equation for the Sorption of AG25, AO10, AO12, AR18 and AR73 onto Chitosan with Different Masses at Room Temperature, Degree of Deacetylation (DD=53%), pH=4.00, dp=355-500 μm

The parameters of rate constant and the equilibrium capacity for the sorption of acid dyes onto chitosan in the pseudo-1st order equation were established. The relationship of rate constants and equilibrium capacities against initial concentration of solutions were shown in Figure 10 (j) to (m).

The rate constants against the change of initial concentration of solutions were best fitted to the equation of power function:

$$k_1 = A_1[C_o]^{B_1} \tag{5.5}$$

Linear equations were used to fit the equilibrium capacities against the change of initial concentration.

$$q_e = D_1 \ln[C_o] + E_1 \tag{5.6}$$

The correlations of the parameters were shown in Table 5.10.

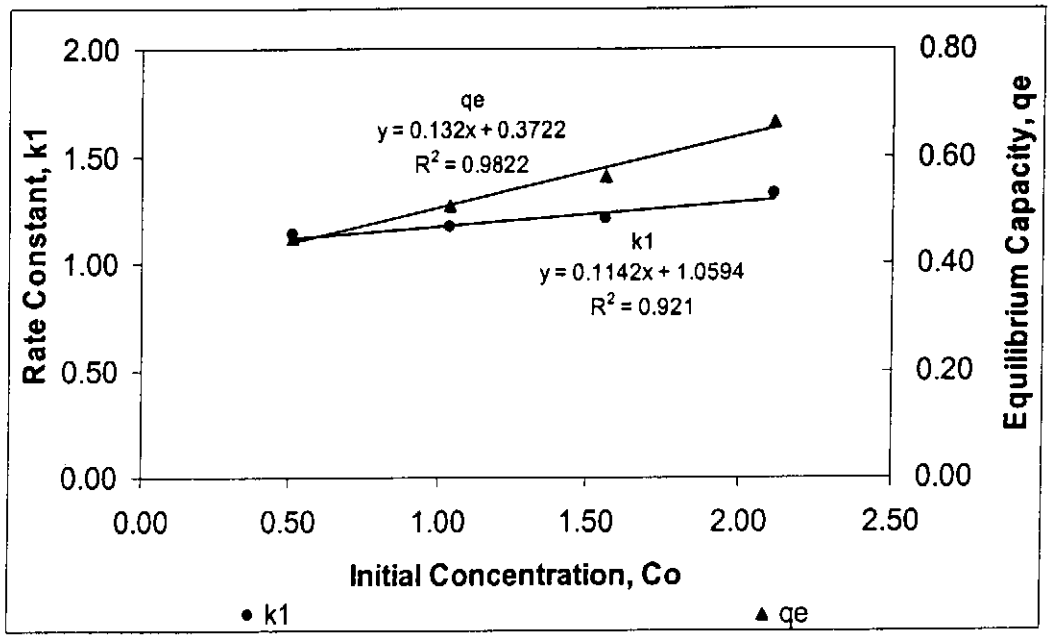

Figure 5.10 (j) The Relationship of Rate Constants and Equilibrium Capacities against Initial Concentration of Acid Green 25

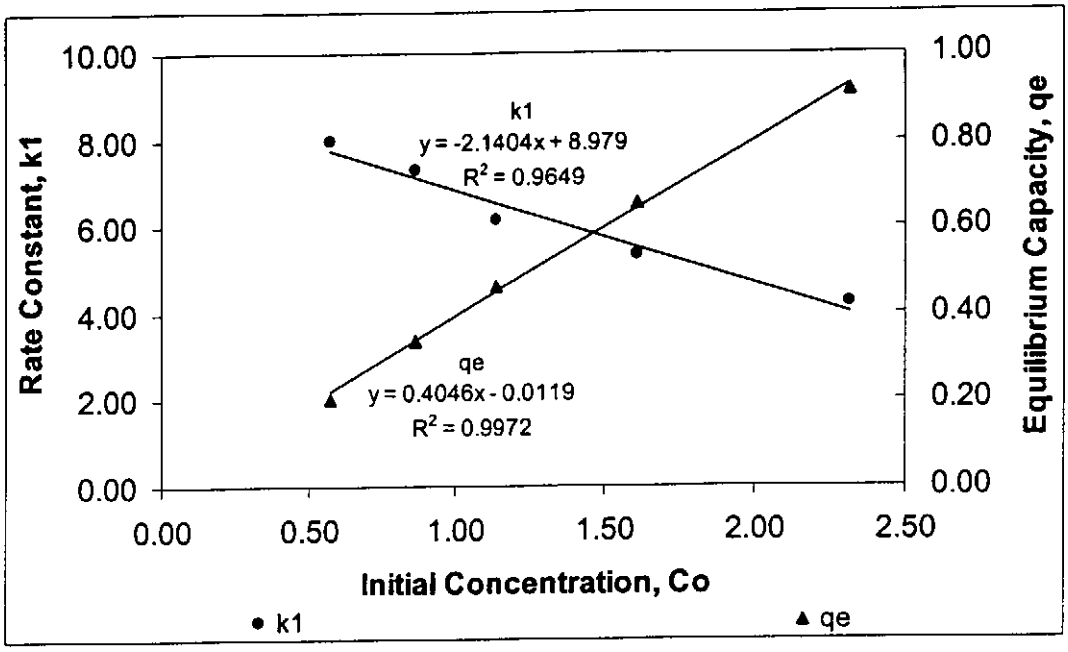

Figure 5.10 (k) The Relationship of Rate Constants and Equilibrium Capacities against Initial Concentration of Acid Orange 10

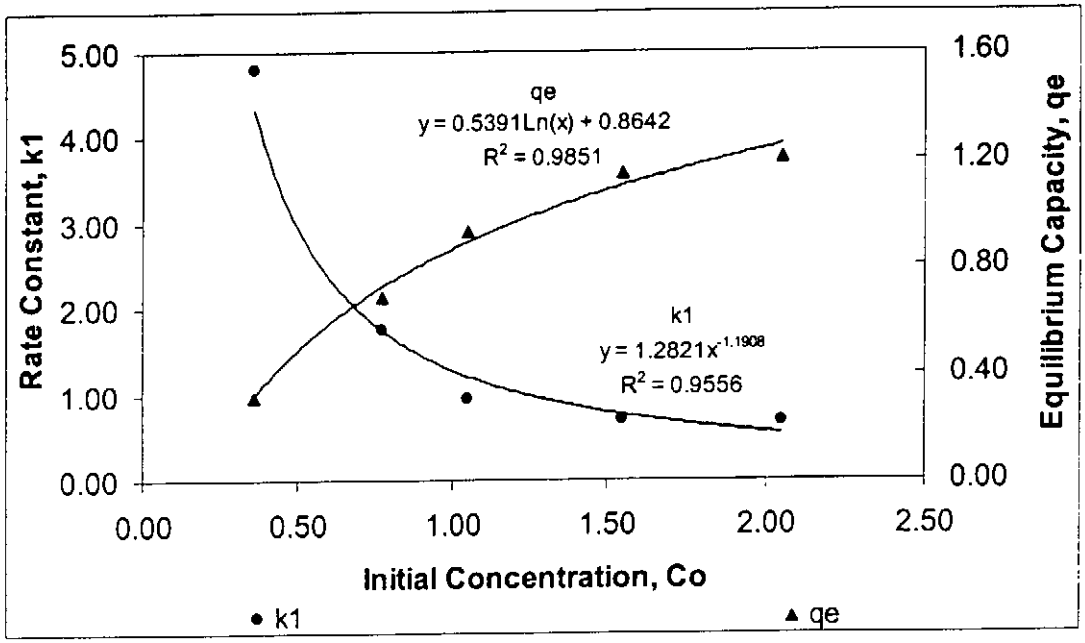

Figure 5.10 (l) The Relationship of Rate Constants and Equilibrium Capacities against Initial Concentration of Acid Orange 12

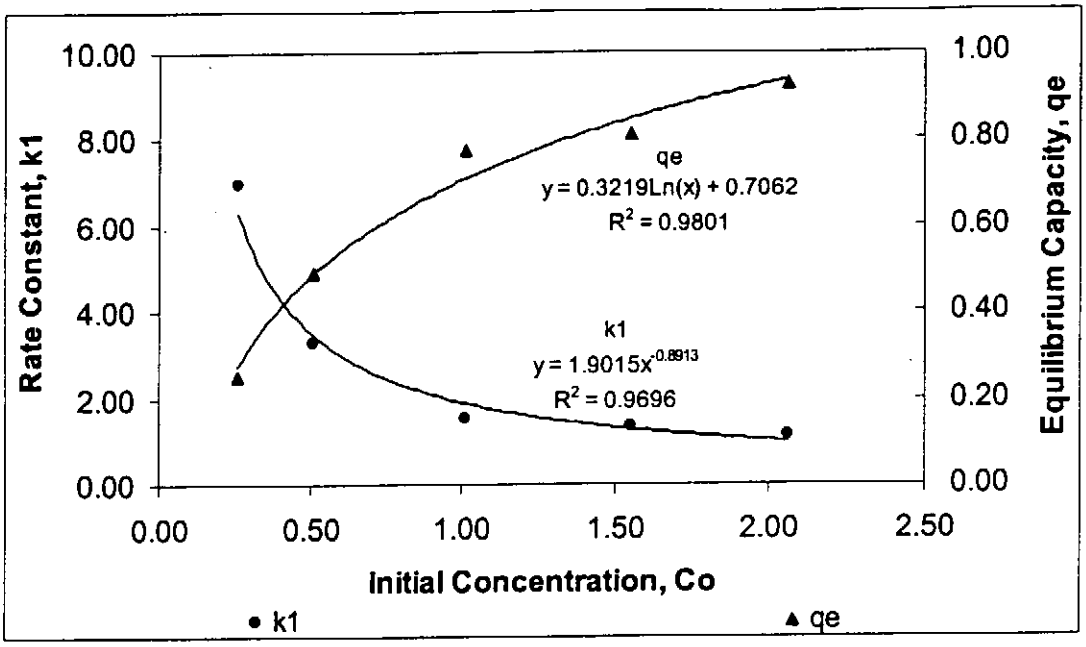

Figure 5.10 (m) The Relationship of Rate Constants and Equilibrium Capacities against Initial Concentration of Acid Red 18

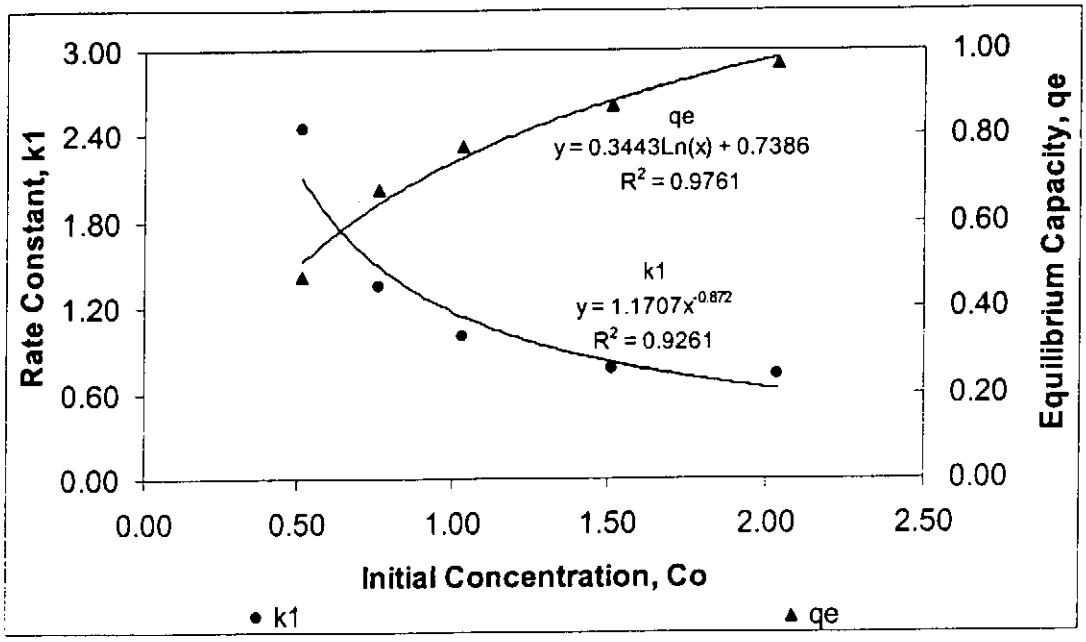

Figure 5.10 (n) The Relationship of Rate Constants and Equilibrium Capacities against Initial Concentration of Acid Red 73

5.6.2 The Elovich Equation

Linear form of Elovich equation is:

$$q_t = \frac{1}{b}\ln ab + \frac{1}{b}\ln(t + t_0) \tag{4.20}$$

Figure 5.11 (a) to (e) show the linear plots of Elovich equation for the sorption of AG25, AO10, AO12, AR18 and AR73 onto chitosan with the change of initial concentrations respectively. The values of t_0 were estimated by an iterative procedure from a linear plot of q_t against $\ln(t+t_0)$. The parameters a and b are calculated from the intercept and the slopes of the lines. The correlation coefficients are very high in these five systems. The experimental data points could also be plotted as q_t versus t graphs such as Figure 5.11 (f), the curves for different concentrations of Acid Orange 12 were completely separated and similar results, which were obtained for other acid dyes were not shown. The Elovich constants, a, b and t_o, the Sum of Error Square, SSE and the correlation coefficient, R^2, were reported in Table 5.11. The values demonstrated that increase the concentration of acid dyes will lead to decrease in both constant a and b. In this study, the Elovich constant b was plotted against initial concentration, Co, and the best correlating equation is the power equation data are shown in Figure 5.11 (g)

$$b = A[C_o]^B \tag{5.7}$$

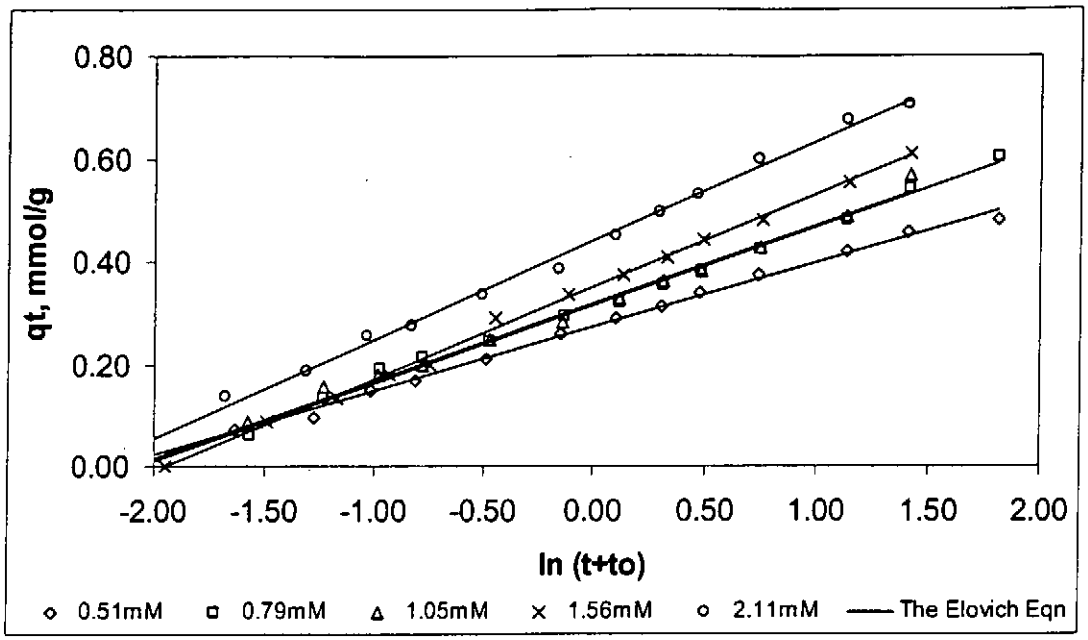

Figure 5.11 (a) Linear Plot for the Elovich Equation for the Sorption of Acid Green 25 onto Chitosan with Different Initial Concentrations at Room Temperature, Mass=1.7000g, Degree of Deacetylation (DD=53%), pH=4.00, dp=355-500 μm

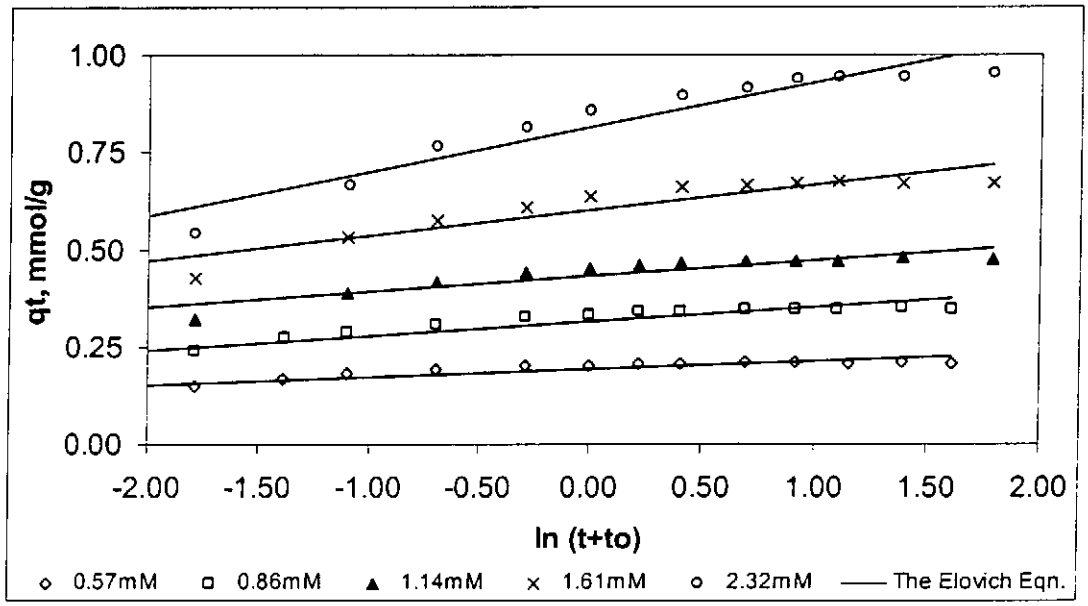

Figure 5.11 (b) Linear Plot for the Elovich Equation for the Sorption of Acid Orange 10 onto Chitosan with Different Initial Concentrations at Room Temperature, Mass=1.7000g, Degree of Deacetylation (DD=53%), pH=4.00, dp=355-500 μm

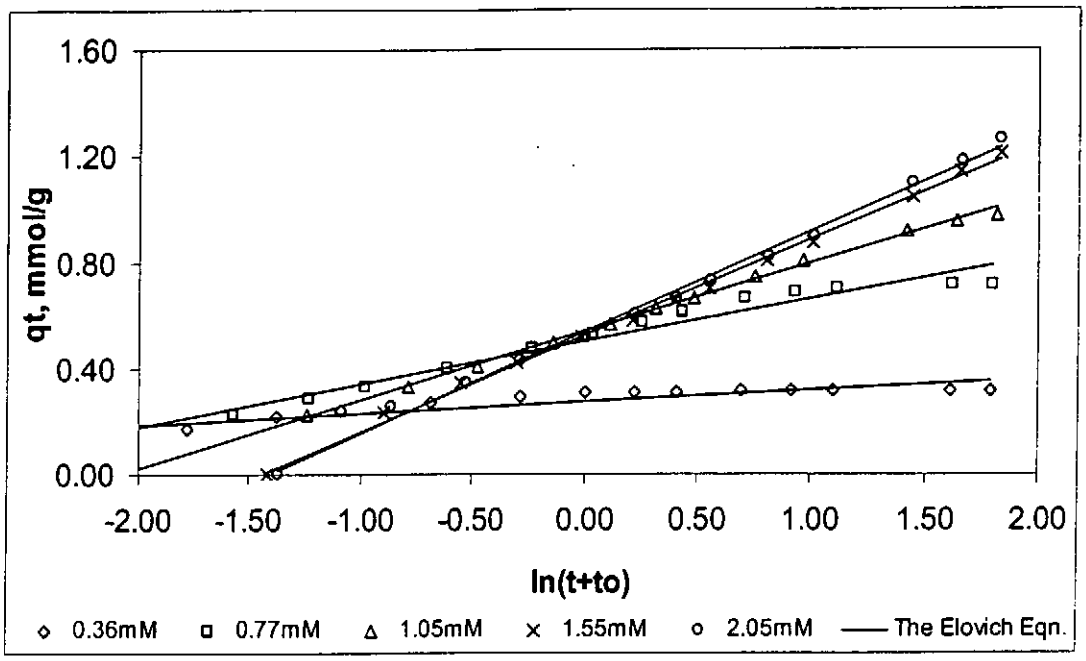

Figure 5.11 (c) Linear Plot for the Elovich Equation for the Sorption of Acid Orange 12 onto Chitosan with Different Initial Concentrations at Room Temperature, Mass=1.7000g, Degree of Deacetylation (DD=53%), pH=4.00, dp=355-500 μm

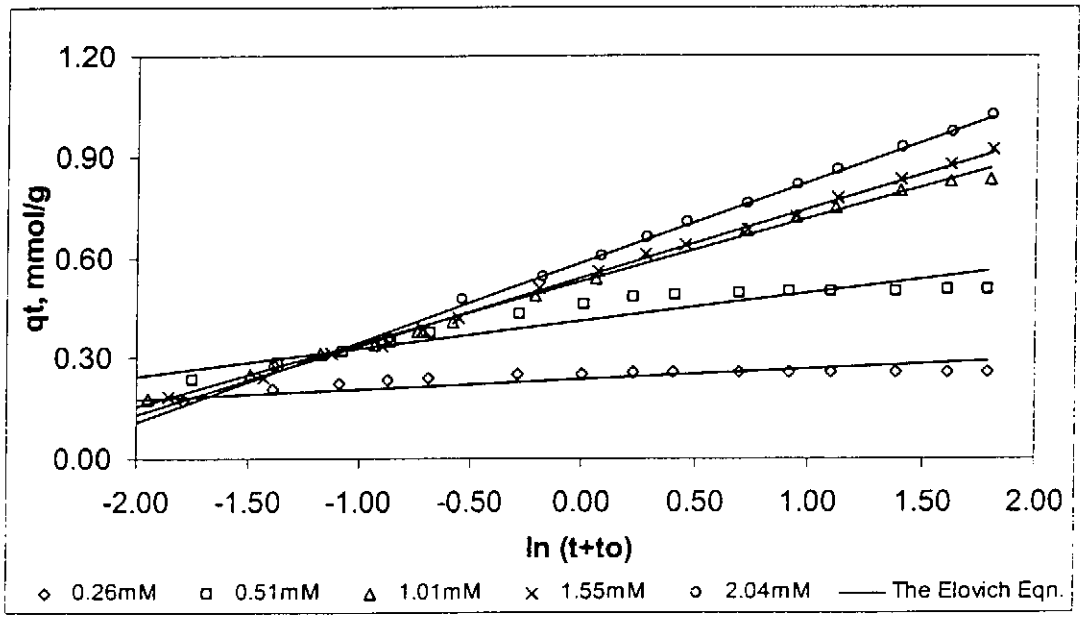

Figure 5.11 (d) Linear Plot for the Elovich Equation for the Sorption of Acid Red 18 onto Chitosan with Different Initial Concentrations at Room Temperature, Mass=1.7000g, Degree of Deacetylation (DD=53%), pH=4.00, dp=355-500 μm

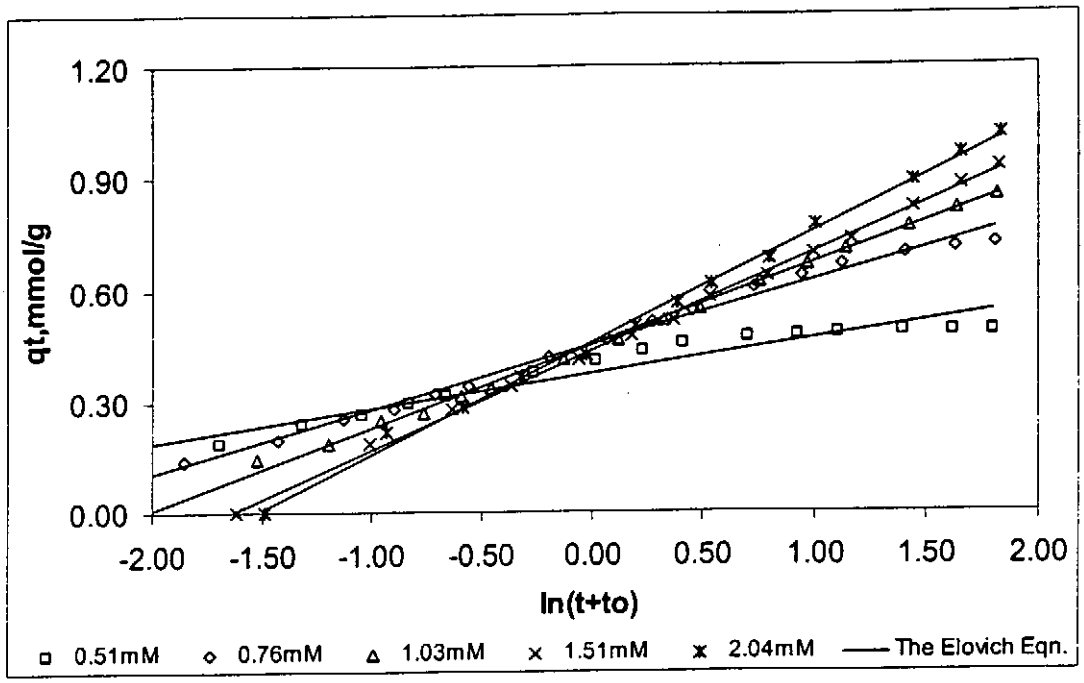

Figure 5.11 (e) Linear Plot for the Elovich Equation for the Sorption of Acid Red 73 onto Chitosan with Different Initial Concentrations at Room Temperature, Mass=1.7000g, Degree of Deacetylation (DD=53%), pH=4.00, dp=355-500 μm

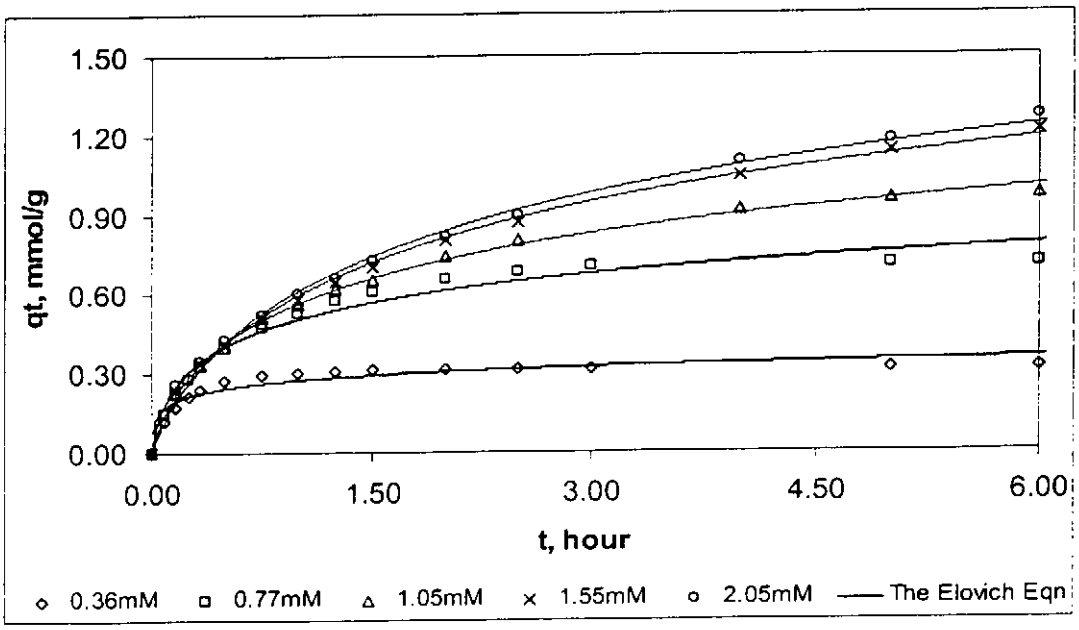

Figure 5.11 (f) The Elovich Equation for the Sorption of Acid Orange 12 onto Chitosan with Different Initial Concentrations at Room Temperature, Mass=1.7000g, Degree of Deacetylation (DD=53%), pH=4.00, dp=355-500 μm

Concentration Effect						
AG25	Concentration (mM)	a	b	1/ab	SSE	R^2
	0.51	1.1171	8.0045	0.11	0.0008	0.9963
	0.79	1.2090	6.5846	0.13	0.0018	0.9941
	1.05	1.2233	6.5196	0.13	0.0026	0.9921
	1.56	1.2509	5.5663	0.14	0.0008	0.9981
	2.11	1.8718	5.1569	0.10	0.0019	0.9963
AO10	Concentration (mM)	a	b	1/ab	SSE	R^2
	0.57	244.20	49.1355	0.00	0.0020	0.8078
	0.86	175.86	26.9885	0.00	0.0048	0.8525
	1.14	1842.93	24.8209	0.00	0.0043	0.8227
	1.61	642.25	15.2484	0.00	0.0095	0.8476
	2.32	140.96	8.7454	0.00	0.0159	0.9097
A012	Concentration (mM)	a	b	1/ab	SSE	R^2
	0.36	23.8932	22.9020	0.00	0.0095	0.8131
	0.77	3.7558	6.3169	0.04	0.0165	0.9665
	1.05	2.6849	3.8954	0.12	0.0021	0.9969
	1.55	1.5162	2.7384	0.24	0.0045	0.9959
	2.05	1.5246	2.5911	0.26	0.0080	0.9932
AR18	Concentration (mM)	a	b	1/ab	SSE	R^2
	0.26	329.73	40.2352	0.00	0.0060	0.7142
	0.51	12.5735	12.2351	0.01	0.0187	0.8962
	1.01	3.1459	5.3617	0.06	0.0026	0.9962
	1.55	2.8420	4.8481	0.07	0.0018	0.9978
	2.06	2.7846	4.1852	0.09	0.0012	0.9982
AR73	Concentration (mM)	a	b	1/ab	SSE	R^2
	0.51	5.2409	10.8277	0.02	0.0136	0.9362
	0.76	6.3592	5.8087	0.07	0.0045	0.9922
	1.03	1.6610	4.5004	0.13	0.0019	0.9976
	1.51	1.3495	3.7489	0.20	0.0017	0.9974
	2.04	1.3504	3.2913	0.23	0.0039	0.9949

Table 5.11 Parameters of the Elovich Equation for the sorption of AG25, AO10, AO12, AR18 and AR73 onto chitosan with Different Initial Concentration at Room Temperature, Mass=1.7000g, Degree of Deacetylation (DD=53%), pH=4.00, dp=355-500 μm

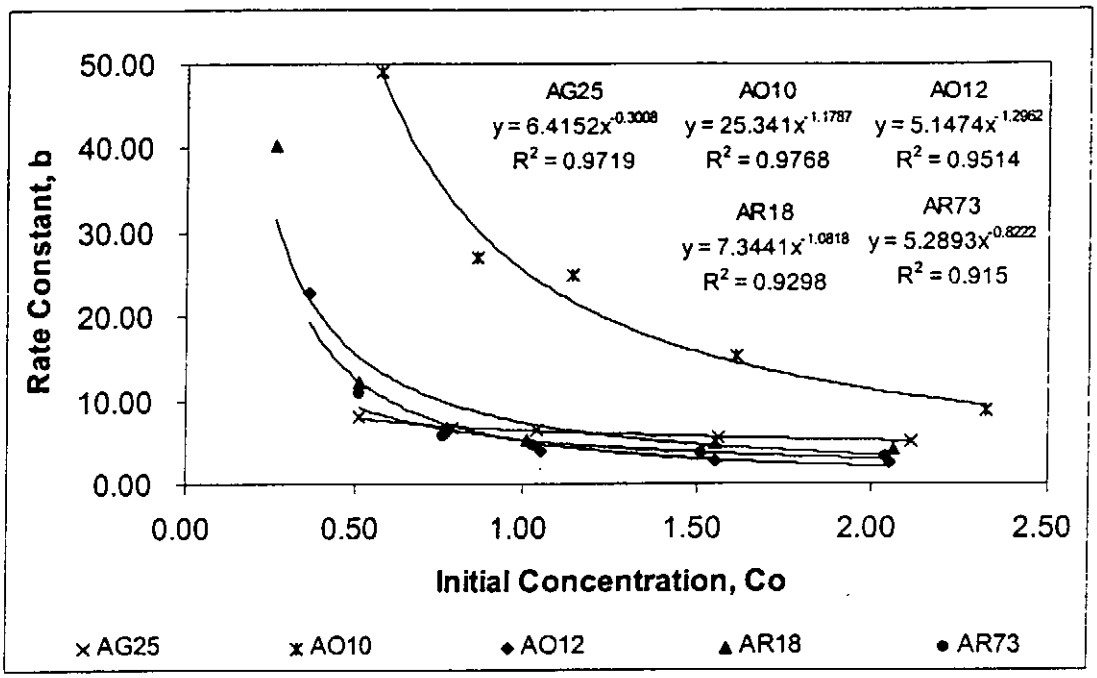

Figure 5.11 (g) The relationship of the Elovich Rate Constant, b against Initial Concentration, Co, for AG25, AO10, AO12, AR18 and AR73

5.6.3 The Pseudo-second Order Equation

The experimental results were substituted into the linear form of the pseudo-second order equation to evaluate the fitness of the model on the sorption of acid dyes to chitosan for different initial concentrations. The results Figures 5.12 (a) to (e) show that the distance between each line is clearly separated and the experimental data were almost perfectly fitted with an extremely high correlation coefficient.

Equation (4.28) is the linear form of the equation:

$$\frac{t}{q_t} = \frac{1}{k_2 q_e^2} + \frac{1}{q_e} t \qquad (4.28)$$

The equilibrium capacity can be determined from the slope of the linear plot and the rate constant k_2 can be calculated from the intercepting point of the line.

Alternatively, in this research, the pseudo second order equation constants were obtained by the trial and error method to optimize the SSE. Figure 5.12 (f) shows the effect of initial concentration of Acid Red 73 on the rate constant, k_2, and the equilibrium capacity, q_e. Similar results obtained for AG 25, AO10, AO12 and AR18 are not presented. The parameters of the pseudo second order equation for the effect of different initial concentration and the effect of change of sorbent mass are listed in Table 5.12. The parameters were best fitted to the equations.

$$k_2 = A_3 [C_o]^{B_3} \tag{5.8}$$

$$q_e = A_4 \ln[C_o] + B_4 \tag{5.9}$$

The parameters qt against t can be plotted to show the effect of change of sorbent mass on the sorption of acid dyes by the pseudo-second order equation. However, the results show that the theoretical lines are very close together and some lines overlap. This suggests that the sorption rate of the dyes onto chitosan is fairly independent of mass and the rate parameter, k_2, is reasonably constant for the range of chitosan masses used in the experiments. Furthermore, the plots of change of chitosan mass are similar for the other dyes and are not shown in here. The parameters of the pseudo second order equation for the effect of change of sorbent mass are given in Table 5.13.

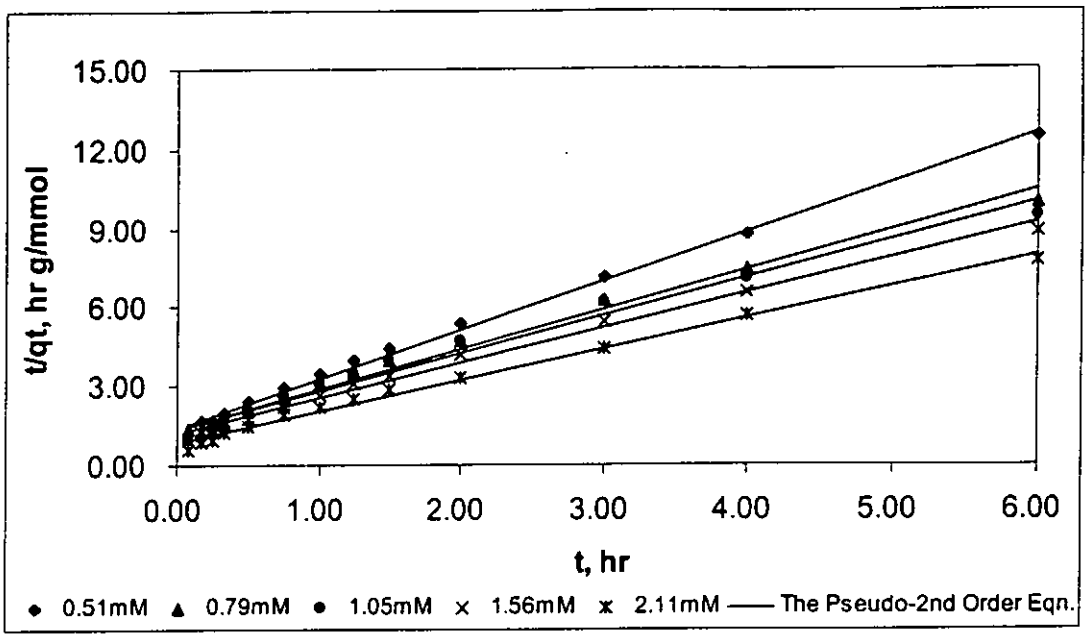

Figure 5.12 (a) Linear Plot of The Pseudo-second Equation of the Sorption of Acid Green 25 onto Chitosan with Different Initial Concentrations at Room Temperature, Mass=1.7000g, Degree of Deacetylation (DD=53%), pH=4.00, dp=355-500 μm

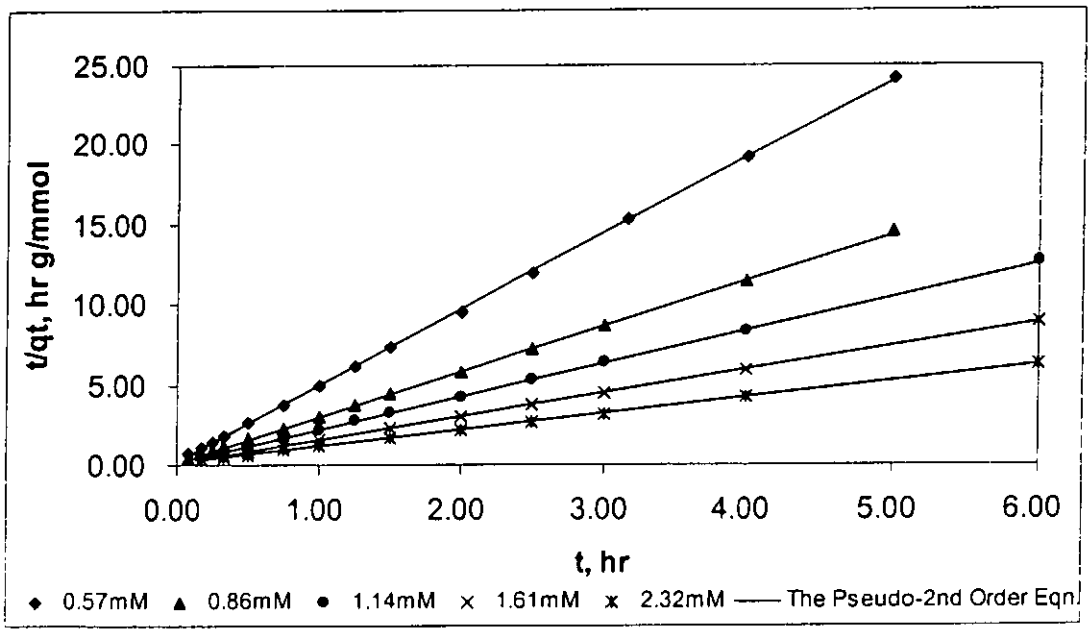

Figure 5.12 (b) Linear Plot of The Pseudo-second Equation of the Sorption of Acid Orange 10 onto Chitosan with Different Initial Concentrations at Room Temperature, Mass=1.7000g, Degree of Deacetylation (DD=53%), pH=4.00, dp=355-500 μm

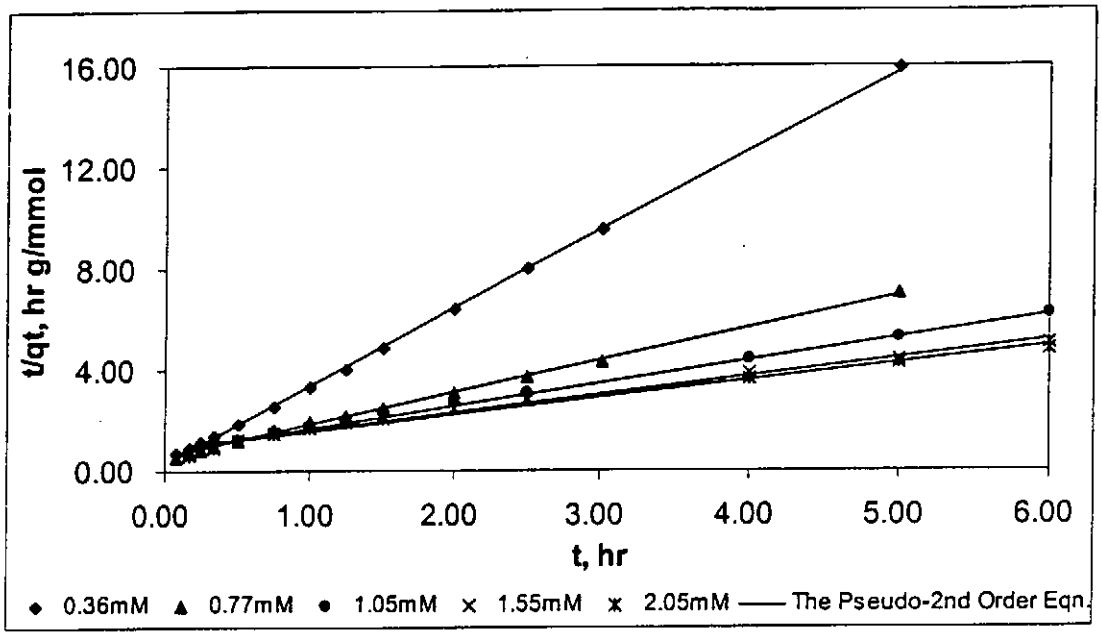

Figure 5.12 (c) Linear Plot of The Pseudo-second Equation of the Sorption of Acid Orange 12 onto Chitosan with Different Initial Concentrations at Room Temperature, Mass=1.7000g, Degree of Deacetylation (DD=53%), pH=4.00, dp=355-500 μm

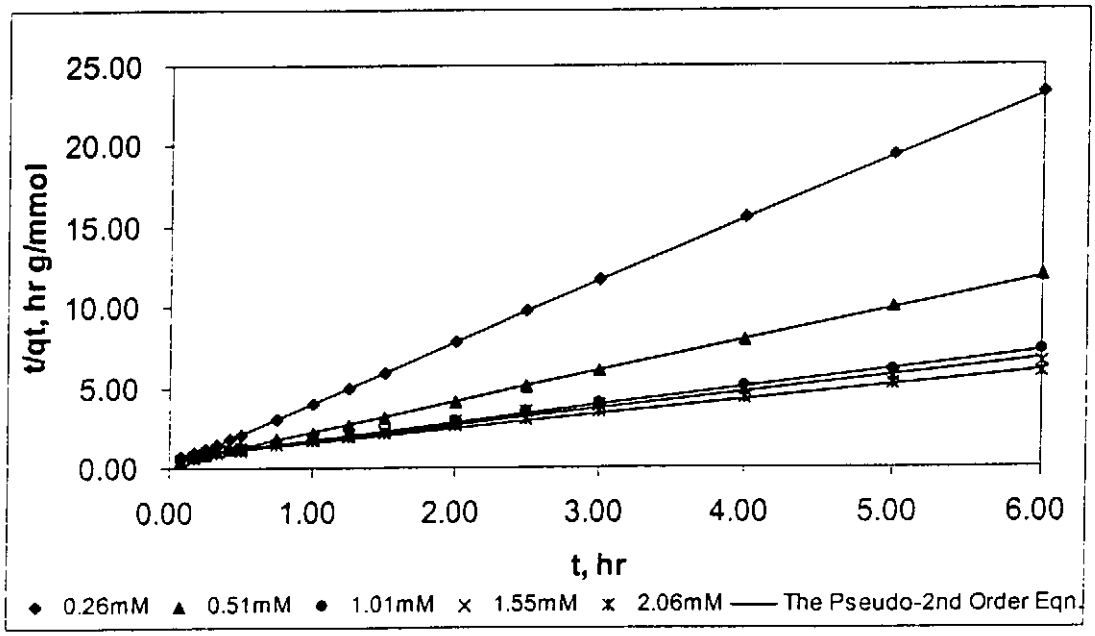

Figure 5.12 (d) Linear Plot of The Pseudo-second Equation of the Sorption of Acid Red 18 onto Chitosan with Different Initial Concentrations at Room Temperature, Mass=1.7000g, Degree of Deacetylation (DD=53%), pH=4.00, dp=355-500 μm

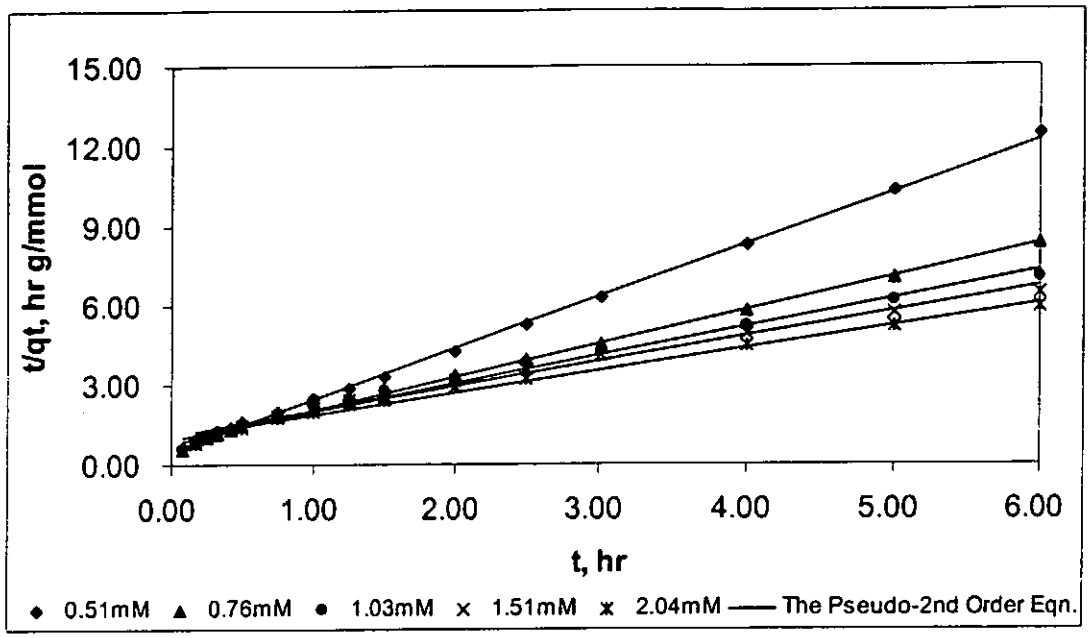

Figure 5.12 (e) Linear Plot of The Pseudo-second Equation of the Sorption of Acid Red 73 onto Chitosan with Different Initial Concentrations at Room Temperature, Mass=1.7000g, Degree of Deacetylation (DD=53%), pH=4.00, dp=355-500 μm

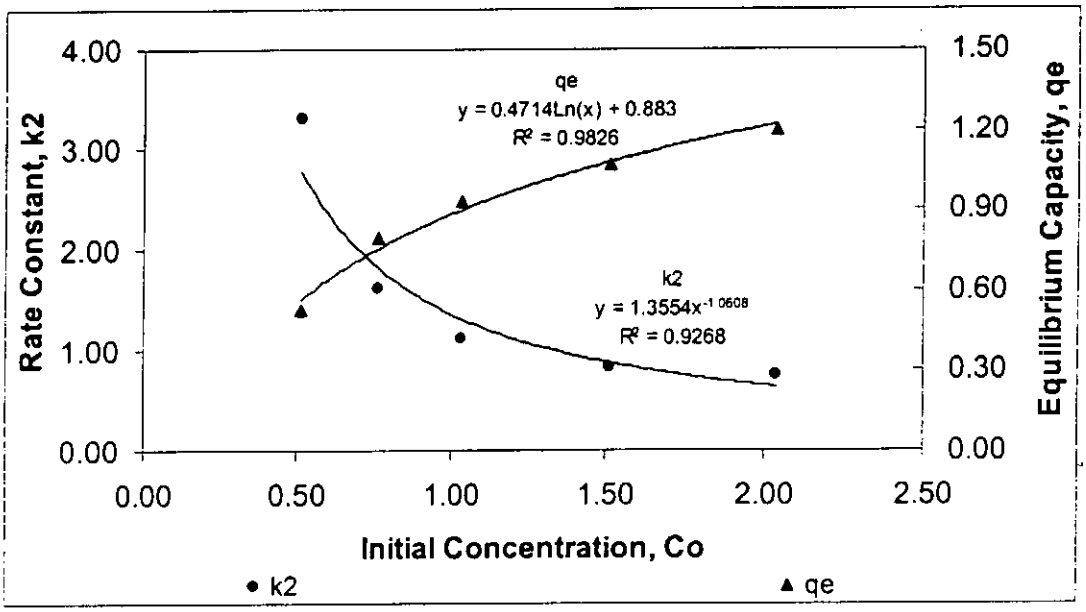

Figure 5.12 (f) The relationship of Rate Constants and Equilibrium Capacities against Initial Concentration of Acid Red 73

Concentration Effect					
	Concentration (mM)	**k_2**	**q_e**	**SSE**	**R^2**
AG25	0.51	1.2878	0.5315	0.0018	0.9917
	0.79	1.1709	0.6382	0.0090	0.9707
	1.05	1.2920	0.6158	0.0089	0.9780
	1.56	1.2576	0.6947	0.0029	0.9924
	2.11	1.4791	0.7983	0.0087	0.9829
	Concentration (mM)	**k_2**	**q_e**	**SSE**	**R^2**
AO10	0.57	14.1810	0.2143	0.0001	0.9904
	0.86	12.4622	0.3558	0.0001	0.9969
	1.14	11.6667	0.4870	0.0001	0.9959
	1.61	9.6484	0.6953	0.0004	0.9936
	2.32	6.9925	0.9797	0.0008	0.9955
	Concentration (mM)	**k_2**	**q_e**	**SSE**	**R^2**
A012	0.36	7.4127	0.3340	0.0009	0.9823
	0.77	2.2265	0.7848	0.0028	0.9943
	1.05	1.0953	1.1097	0.0051	0.9925
	1.55	0.7212	1.4249	0.0145	0.9867
	2.05	0.6910	1.4962	0.0179	0.9848
	Concentration (mM)	**k_2**	**q_e**	**SSE**	**R^2**
AR18	0.26	12.6330	0.2682	0.0007	0.9667
	0.51	4.8418	0.5346	0.0021	0.9883
	1.01	1.8233	0.8900	0.0077	0.9887
	1.55	1.6030	0.9484	0.0133	0.9835
	2.06	1.3398	1.0897	0.0114	0.9826
	Concentration (mM)	**k_2**	**q_e**	**SSE**	**R^2**
AR73	0.51	3.3144	0.5246	0.0017	0.9920
	0.76	1.6130	0.7902	0.0034	0.9941
	1.03	1.1104	0.9314	0.0079	0.9900
	1.51	0.8220	1.0679	0.0088	0.9866
	2.04	0.7528	1.1985	0.0093	0.9879

Table 5.12 Parameters of Pseudo-second Order Equation for the sorption of AG25, AO10, AO12, AR18 and AR73 onto chitosan with the Effect of different Initial Concentration at Room Temperature, Mass=1.7000g, Degree of Deacetylation (DD=53%), pH=4.00, dp=355-500 μm

Mass Effect					
AG25	**Mass of Sorbent (g)**	**k_2**	**q_e**	**SSE**	**R^2**
	0.4250	0.6677	0.8047	0.0137	0.9733
	0.8500	0.8427	0.7681	0.0137	0.9720
	1.2750	1.1897	0.6622	0.0029	0.9941
	1.7000	1.6809	0.5510	0.0059	0.9851
	2.1250	1.1889	0.6182	0.0021	0.9950
A012	**Mass of Sorbent (g)**	**k_2**	**q_e**	**SSE**	**R^2**
	---	---	---	---	---
	0.8500	0.6615	1.8346	0.0106	0.9947
	1.2750	0.7218	1.5792	0.0300	0.9784
	1.7000	0.6910	1.4962	0.0286	0.757
	2.1250	0.6859	1.4271	0.0205	0.9818
AR18	**Mass of Sorbent (g)**	**k_2**	**q_e**	**SSE**	**R^2**
	---	---	---	---	---
	0.8500	1.8303	1.0215	0.0078	0.9849
	1.2750	1.5706	1.0057	0.0065	0.9877
	1.7000	1.3398	1.0897	0.0140	0.9787
	2.1250	1.5192	1.0067	0.0078	0.9853
AR73	**Mass of Sorbent (g)**	**k_2**	**q_e**	**SSE**	**R^2**
	0.4250	0.7216	1.2295	0.0133	0.9888
	0.8500	0.8108	1.2059	0.0093	0.9917
	1.2750	0.9097	1.1257	0.0148	0.9848
	1.7000	1.1104	0.9314	0.0144	0.9819
	2.1250	1.4682	0.8874	0.0056	0.9910

Table 5.13 Parameters of Pseudo-second Order Equation for the sorption of AG25, AO10, AO12, AR18 and AR73 onto chitosan with the Effect of different Masses at Room Temperature, Degree of Deacetylation (DD=53%), pH=4.00, dp=355-500 μm

5.6.4 The Modified-second Order Equation

The results for the pseudo-second order equation show that the acid dyes were adsorbed faster during the first hour of the experimental studies than the removal rate predicted. Therefore, the modified-second order equation was modified by incorporating the boundary condition of Ritchies's reaction kinetic model, in which the boundary condition was modified such that, at $t = 0$, $q = q_o$. As a result, a better fit

to the experimental data points would be obtained. The modified second order equation contains three parameters and they were determined by trial and error. Table 5.14 and 5.15 list the equation parameters of the modified second order equation with the effect of initial concentration and effect of sorbent mass, respectively, i.e. rate constant, k'_2 and β, equilibrium capacity, q_e, SSE and correlation coefficient, R^2.

By comparing the SSE and correlation coefficient of the pseudo-second order equation, the modified second order equation provides a closer fit to the experimental data of both the effect of initial concentration and the effect of sorbent mass. However, the values of rate constants and equilibrium capacities of both equations are very close to each other for some dyes and a better correlation of rate constants and equilibrium with the effect of initial concentration and sorbent mass were obtained for the pseudo-second order. Generally, the rate constants and equilibrium capacities can be expressed in term of initial concentration and are not shown here.

$$k'_2 = A_5 [C_o]^{B_5} \tag{5.10}$$

$$q_e = A_6 \ln[C_o] + B_6 \tag{5.11}$$

Concentration Effect						
AG25	Concentration (mM)	k'_2	q_e	β	SSE	R^2
	0.51	1.1581	0.5434	1.0334	0.0012	0.9945
	0.79	0.9528	0.6693	1.0525	0.0071	0.9768
	1.05	0.9391	0.6701	1.0695	0.0061	0.9814
	1.56	1.1345	0.7127	1.0271	0.0023	0.9944
	2.11	1.1960	0.8396	1.0557	0.0058	0.9886
AO10	Concentration (mM)	k'_2	q_e	β	SSE	R^2
	0.57	14.2034	0.2143	0.9972	0.0010	0.9904
	0.86	12.4699	0.3558	0.9991	0.0001	0.9969
	1.14	11.6694	0.4870	0.9994	0.0001	0.9959
	1.61	9.6503	0.6953	0.0009	0.0004	0.9936
	2.32	6.9844	0.9798	1.0016	0.0008	0.9955
A012	Concentration (mM)	k'_2	q_e	β	SSE	R^2
	0.36	7.4945	0.3338	0.9870	0.0009	0.9823
	0.77	2.1452	0.7891	1.0180	0.0028	0.9943
	1.05	1.0017	1.1298	1.0337	0.0051	0.9925
	1.55	0.5925	1.4992	1.0500	0.0145	0.9867
	2.05	0.5482	1.5911	1.0554	0.0179	0.9848
AR18	Concentration (mM)	k'_2	q_e	β	SSE	R^2
	0.26	12.6979	0.2681	0.9902	0.0007	0.9667
	0.51	4.8371	0.5346	1.0009	0.0021	0.9883
	1.01	1.5625	0.9115	1.0591	0.0077	0.9887
	1.55	1.3031	0.9848	1.0707	0.0133	0.9835
	2.06	1.2003	1.1122	1.0442	0.0114	0.9826
AR73	Concentration (mM)	k'_2	q_e	β	SSE	R^2
	0.51	3.2808	0.5252	1.0070	0.0017	0.9920
	0.76	1.4357	0.8063	1.0449	0.0034	0.9941
	1.03	0.8754	0.9815	1.0644	0.0079	0.9900
	1.51	0.6928	1.1133	1.0482	0.0088	0.9866
	2.04	0.6286	1.2537	1.0489	0.0093	0.9879

Table 5.14 Parameters of the Modified Second Order Equation for the sorption of AG25, AO10, AO12, AR18 and AR73 onto chitosan with the Effect of Initial Concentration at Room Temperature, Mass=1.7000g, Degree of Deacetylation (DD=53%), pH=4.00, dp=355-500 μm

Mass Effect						
	Mass of Sorbent (g)	k'_2	q_e	β	**SSE**	R^2
AG25	0.4250	0.4894	0.8802	1.0590	0.0079	0.9846
	0.8500	0.6256	0.8288	1.0674	0.0078	0.9841
	1.2750	1.0358	0.6885	1.0309	0.0022	0.9955
	1.7000	1.2668	0.5913	1.0670	0.0041	0.9897
	2.1250	1.0373	0.6426	1.0298	0.0015	0.9964
A012	**Mass of Sorbent (g)**	k'_2	q_e	β	**SSE**	R^2
	---	---	---	---	---	---
	0.8500	0.6413	1.8489	1.0082	0.0099	0.9951
	1.2750	0.5885	1.6642	1.0474	0.0219	0.9842
	1.7000	0.5485	1.5911	1.0554	0.0179	0.9848
	2.1250	0.5055	1.5013	1.0440	0.0146	0.9908
AR18	**Mass of Sorbent (g)**	k'_2	q_e	β	**SSE**	R^2
	---	---	---	---	---	---
	0.8500	1.7395	1.0292	1.0256	0.0070	0.9865
	1.2750	1.4773	1.0155	1.028	0.0058	0.9890
	1.7000	1.2003	1.1122	1.0442	0.0114	0.9826
	2.1250	1.4148	1.0185	1.0311	0.0067	0.9870
AR73	**Mass of Sorbent (g)**	k'_2	q_e	β	**SSE**	R^2
	0.4250	0.6591	1.2588	1.0228	0.0117	0.9901
	0.8500	0.7061	1.2475	1.0375	0.0051	0.9954
	1.2750	0.7582	1.1853	1.0499	0.0088	0.9910
	1.7000	0.8754	0.9815	1.0644	0.0079	0.9900
	2.1250	1.3247	0.9039	1.0400	0.0038	0.9939

Table 5.15 Parameters of the Modified Second Order Equation for the sorption of AG25, AO10, AO12, AR18 and AR73 onto chitosan with the Effect of different Masses at Room Temperature, Degree of Deacetylation (DD=53%), pH=4.00, dp=355-500 μm

5.7 Equilibrium Capacity of Sorbent

The equilibrium capacity of chitosan, q_e, increased as the initial concentraion of solution increased. When the initial concentration of solution was fixed at a constant level, the equilibrium capacity of the chitosan decreased as the mass of chitosan increased. This phenomenon is shown in Figure 5.13 (a) and (b), in which the kinetic

data are plotted onto the adsorption isotherm diagram – Redlich-Peterson isotherm in the form of an operating line. Figure 5.13 (a) shows that the operating lines are all parallel, i.e. same slopes, for the change of initial concentration of solution. However, the slopes of the operating lines vary based on the change of V/m ratios of each experimental run, when the initial concentration of solution is constant and the mass of chitosan is varied as shown in Figure 5.13 (b). The operating line can be extended to intersect with the Redlich-Peterson equilibrium curve. The intercept points of the two lines are at the saturation capacity of chitosan, namely, at $t = \infty$. By comparing the equilibrium capacities obtained previously from both isotherms and kinetics studies, the equilibrium capacity values from the kinetic equation are lower than those obtained from the adsorption isotherm. The relationship between the equilibrium sorption capacities for chitosan are a good fit to the logarithm of the initial concentration as proved in previous sections:

$$q_e = A_x \ln[C_o] + B_y \tag{5.12}$$

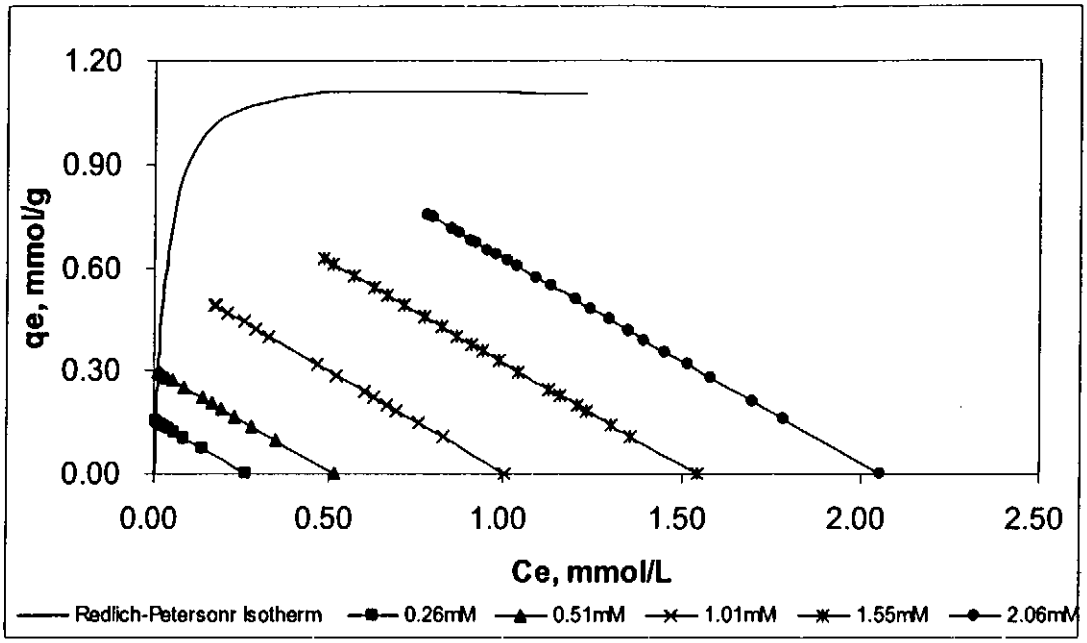

Figure 5.13 (a) Operating Lines and Redlich-Peterson Isotherm of Acid Red 18 onto Chitosan, Degree of Deacetylation =53%, pH=4.00, dp=355-500 μm

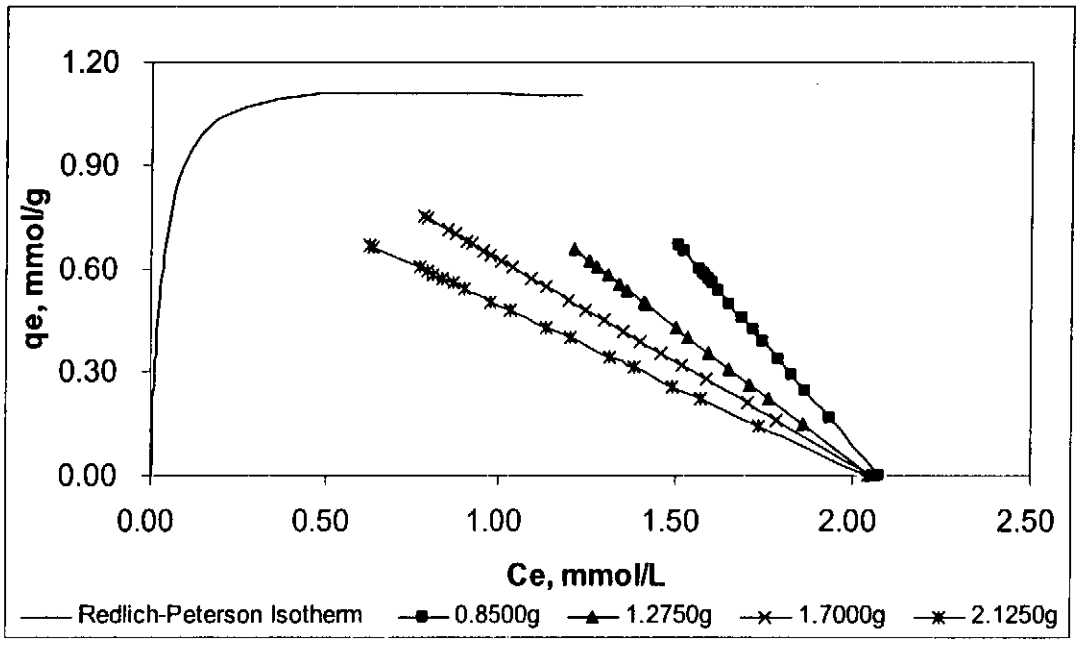

Figure 5.13 (b) Operating Lines and Redlich-Peterson Isotherm of Acid Red 18 onto Chitosan, Degree of Deacetylation =53%, pH=4.00, dp=355-500 μm

5.8 Determination of Sorption Kinetics

Figure 5.14 (a) shows that the pseudo-first order, the pseudo-second order, the modified second order and Elovich equation can be used effectively to describe the sorption of Acid Red 73 onto chitosan with initial concentration equal to 2.04 mmol/L. In this research, similar results were obtained for different acid dyes studies at different initial concentration and the mass of chitosan of each experimental runs. Since the sums of error squares and correlation coefficients of the equations are the different methods to evaluate the fitness of model to the experimental data, the direct comparison of different error methods cannot be used in this research. Alternatively, the applicability of kinetic models can be directly comparing by plotting the reciprocal of the rate Z=(dq/dt)-1 against t. Therefore, by differentiating the kinetic equation, Figure 5.14 (b) – (f) are the correlation between Z and t will be fitted into the differential form and the linearity of the Z-t plots represented the true kinetics of sorption of acid dyes onto chitosan. The reciprocal of the rate of different kinetic equation are as follows:

The pseudo-first order kinetic model:

$$Z_L = \frac{1}{q_e k_1 e^{-k_1 t}} \tag{5.13}$$

The pseudo-second order kinetic model:

$$Z_L = \frac{(1 + k_2 q_e t)^2}{q_e^{\,2} k_2} \tag{5.14}$$

The modified second order kinetic model:

$$Z_L = \frac{(\beta + k_2' t)^2}{q_e^2 k_2'} \tag{5.15}$$

The Elovich kinetic model:

$$Z_L = b(t + t_o) \tag{5.16}$$

Figure 5.14 (e) and (f) show perfect fit of the experimental data to the theoretical line of Elovichian kinetics for the effect of changing initial concentration and change of sorbent mass. However, Figure 5.14 (b) – (d) presented that the data points deviate form the theoretical line, which proved that there are not a full reaction kinetic model for the sorption of acid dyes onto chitosan.

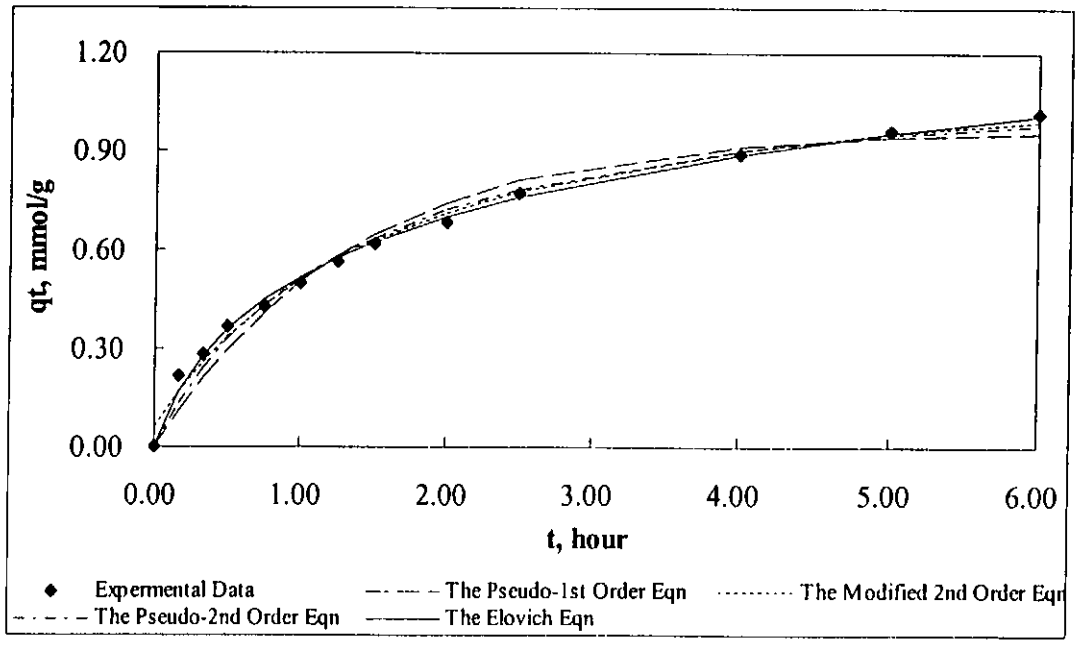

Figure 5.14 (a) Plots of Different Kinetic Models for the Sorption of Acid Red 73 onto Chitosan at Room Temperature, C_o = 2.04mM, Degree of Deacetylation = 53%, pH = 4.00, dp.=355-500 μm

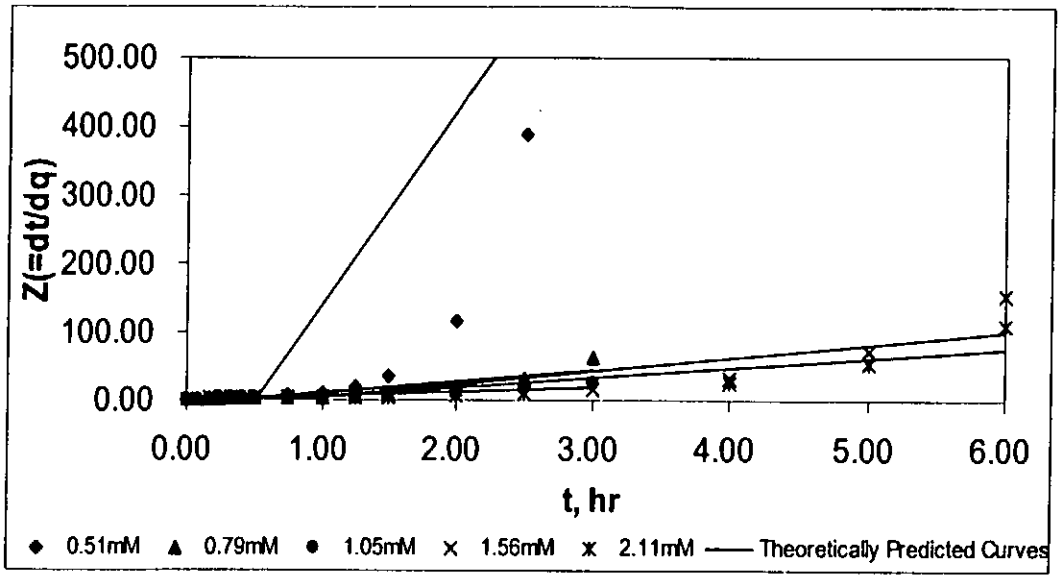

Figure 5.14 (b) Plots of the Reciprocal of the Rate against t for the Pseudo-first Order Equation for the Sorption of Acid Red 73 onto Chitosan for the Change of Initial Concentration

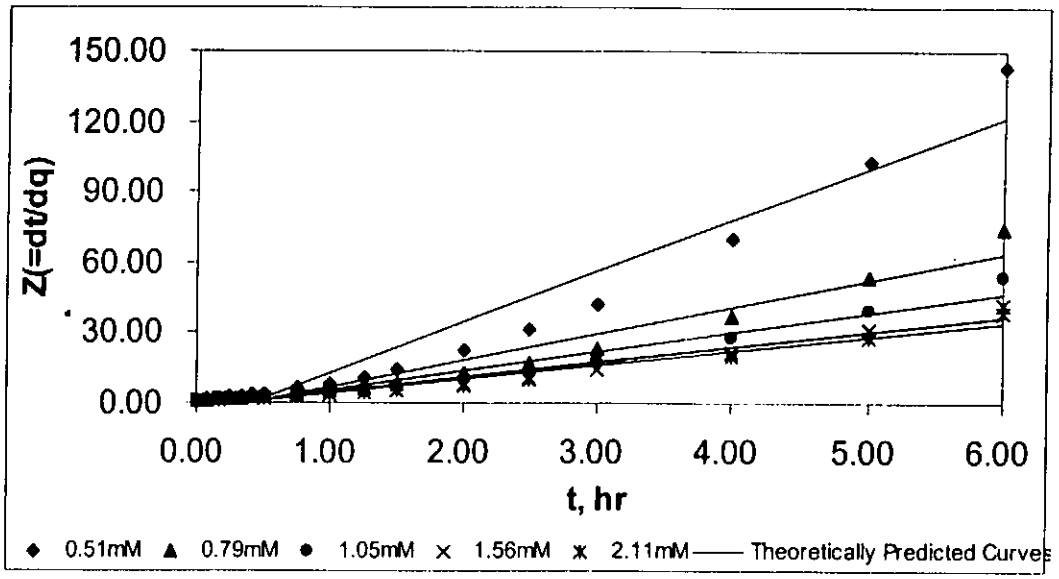

Figure 5.14 (c) Plots of the Reciprocal of the Rate against t for the Pseudo-second Order Equation for the Sorption of Acid Red 73 onto Chitosan for the Change of Initial Concentration

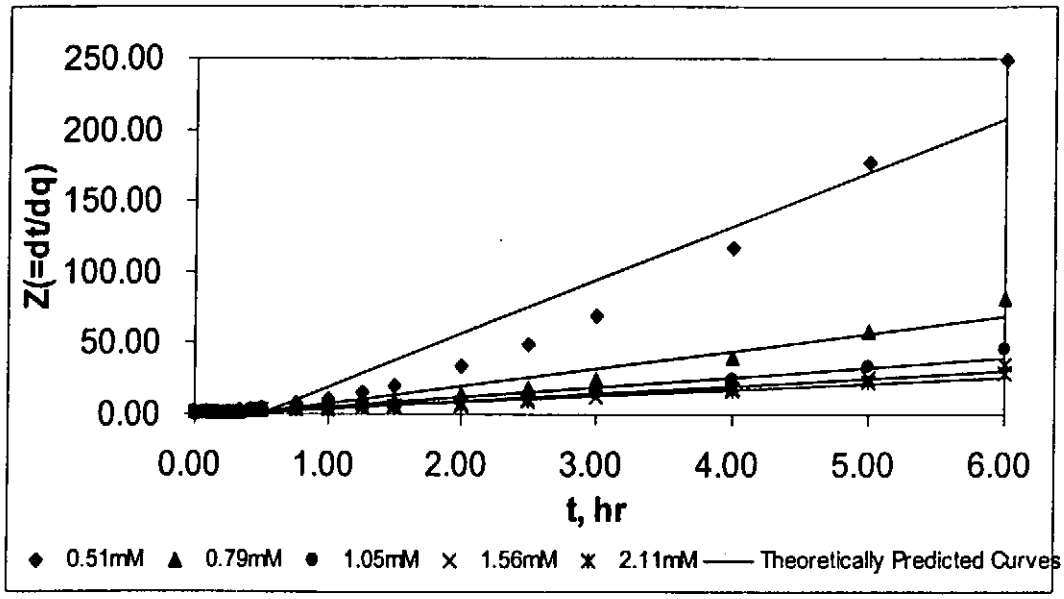

Figure 5.14 (d) Plots of the Reciprocal of the Rate against t for the Modified second Order Equation for the Sorption of Acid Red 73 onto Chitosan for the Change of Initial Concentration

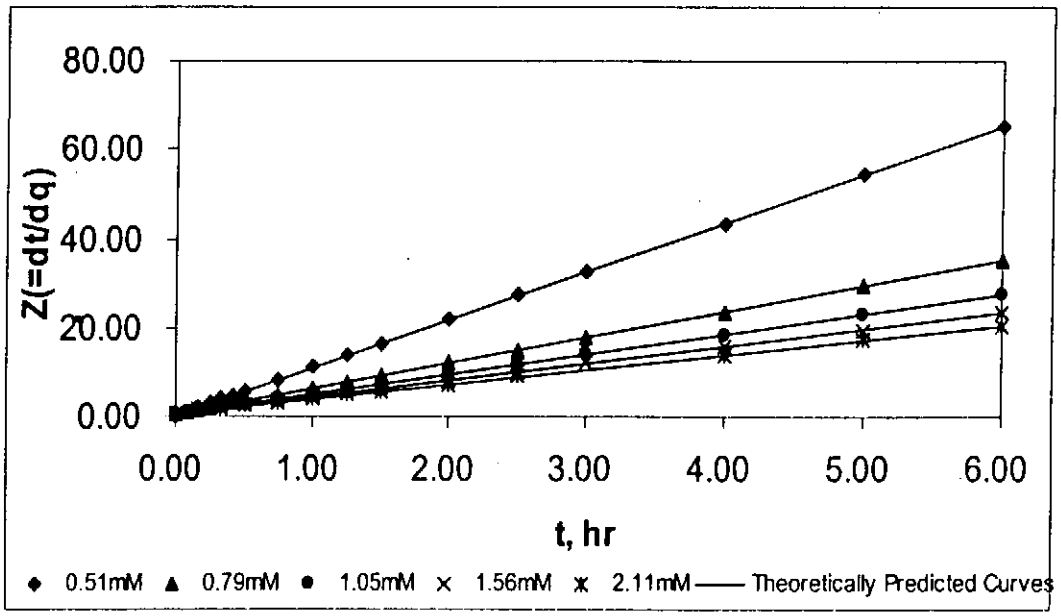

Figure 5.14 (e) Plots of the Reciprocal of the Rate against t for the Elovich Equation for the Sorption of Acid Red 73 onto Chitosan for the Change of Initial Concentration

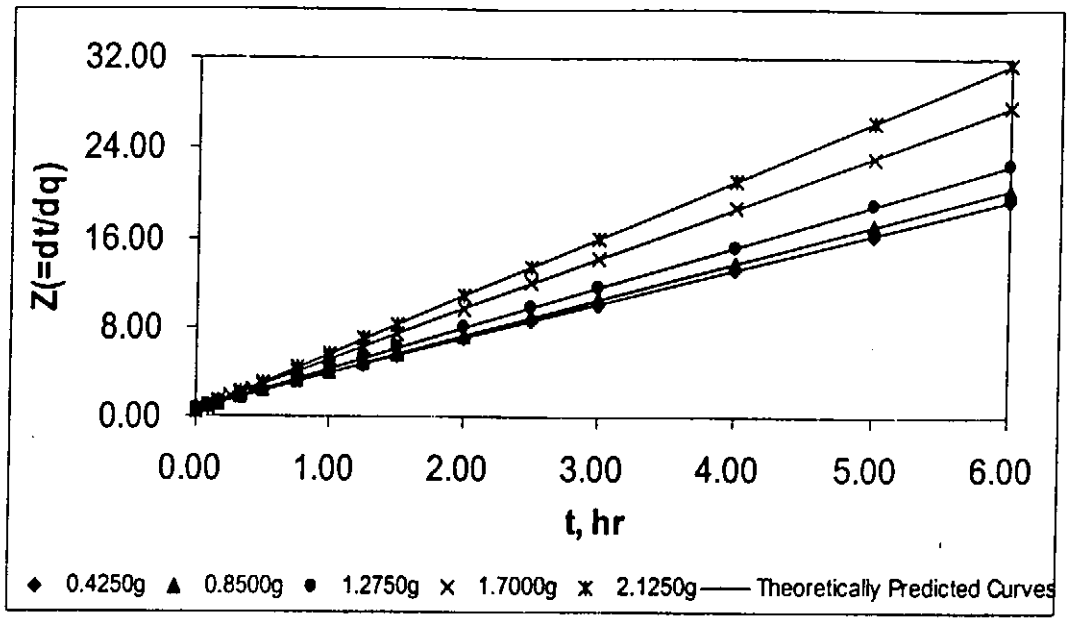

Figure 5.14 (f) Plots of the Reciprocal of the Rate against t for the Elovich Equation for the Sorption of Acid Red 73 onto Chitosan for the Change of Sorbent Mass

CHAPTER 6: CONCLUSIONS AND RECOMMENDATIONS

6.1 Conclusions

The performances of the chitosan as an adsorbent to remove acid dyes, namely, Acid Green 25, Acid Orange 10, Acid Orange 12, Acid Red 18 and Acid Red 73 from the aqueous solution have been investigated. Equilibrium isotherms and kinetic models have been measured for the sorption process.

The experimental isotherm data were analysed using Langmuir, Freundlich, Redlich-Peterson equations for each individual dye. Based on the Langmuir isotherm analysis, the monolayer adsorption capacities were determined to be 645.1, 922.9, 1006.3, 693.2 and 728.2 mg per g chitosan for Acid Green 25, Acid Orange 10, Acid Orange 12, Acid Red 18 and Acid Red 73, respectively. The difference in capacities may be due to the difference in the particle size of dye molecules and the number of sulfonate groups of each dye. Results demonstrated that monovalent and smaller dye particle having superior capacities due to increase in dye/chitosan ratio in the system, enabling a deeper penetration of dye molecules to the internal pore structure of chitosan. By comparing the correlation coefficients determined for each linear transformation of isotherm analysis, the Langmuir isotherm equation was found to provide the best prediction for the sorption of all five acid dyes for the entire concentration ranges.

Due to the inherent bias in using the correlation coefficient resulting from linearization, alternative single component parameters were determined by non-linear

regression employed in this study. Five error functions used were, The sum of the squares of the error (SSE); A hybrid fractional error function (HYBRID); Marquardt's percent standard deviation (MPSD); The average relative error (ARE) and The sum of the absolute errors (EABS). The values obtained from the error functions showed that contradicting results from linearization were obtained, in which, the Redlich-Peterson isotherm had the lowest error values and thus fit the experimental data better than Langmuir and Freundlich isotherm.

The effect of temperature on the equilibrium isotherm was significant. The monolayer adsorption capacities increase with increasing temperature from 25 °C to 60 °C and no further increment at 80 °C. This is possible due to the increase the mobility of the large dye ions and the maximum swelling within the internal structure of the chitosan at 60 °C.

The amount of dye adsorbed increased with decreasing particle sizes due to the inability of the large dye molecules to penetrate into the internal pore structure of chitosan and the increase in active surface areas exposd for adsorption of dyes onto the chitosan.

The effects of degree of deacetylation(DD%) were being evaluated in this study. The reformation of crystalline region within the chitosan due to increase in homogeneity of the internal structure of chitosan with higher DD% resulted in a decrease in overall monolayer equilibrium capacities.

Four kinetic models were studied for the sorption of acid dyes onto chitosan in this study. The experiment data were substituted to those kinetic models, which were the pseudo-first order, the pseudo-second order, the modified second order and the Elovich equation. The sorption kinetics of Acid Green 25, Acid Orange 10, Acid Orange 12, Acid Red 18 and Acid Red 73 onto chitosan can be fully correlated by the Elovich equation. The kinetic model was determined in accordance with the agreement between the rate equations and the differentiation of kinetic equations.

6.2 Recommendations

Based on the experimental results, chitosan has been proven to be an effective means for the removal of acid dyes from aqueous phase. Therefore, further studies should be extended to the application of this technique in different types of dyestuffs and examined the performance on actual dyeing wastewater. Furthermore, a continuous pilot scale reactor for the dye removal is needed as a next step to further develop.

The sorption isotherm of single component system can be successfully described here. However, the sorption process in the wastewater treatment process is usually in multi-component system. Therefore, the extended studies of sorption equilibrium isotherms for multi-component system, such as the Ideal Adsorbed Solution Theory (IAST) are significant to promote the utilization of chitosan to industry as another alternative for the treatment of dye wastewater.

For the sorption kinetics, the experimental data may be tested and correlated using a number of diffusion kinetic models, such as solid , pore and solid-pore diffusion models. The experimental results will be substituted to the diffusion kinetic models to determine the rate-limiting step of the sorption of dyes onto chitosan.

REFERENCES

Allen, S.J., Ph.D. Thesis, The Queen's University of Belfast Northern Ireland, U.K. (1981)

Allen S.J., Brown P., Mckay G. and Flynn O., "An evaluation of single resistance transfer models in the sorption of metal ions by peat". *Journal of Chemical Technology and Biotechnology*, vol. 54, pp.271-276. (1992)

Almas, K.A., Baradarajan A., Blair H., Decock P., Deiana S., Dessi A., Dubois B., Findon A., Kozlowski H., Mckay J., Micera G., Sastry C.A., Senstad C., Thome J.P., Van Daele J. and Venkatrao B., "Chitosan as a Tool for the Purification on Waters".

Annadurai G. and Krishnan M.R.V, "Batch Kinetic Studies on Adsorption of Reactive Dye using Chitosan". *Indian Journal of Environment Protection*, vol. 17, n 5, pp. 328-333. (1997)

Annadurai G., Chellapandian M. and Krishnan M.R.V, "Adsorption of Basic Dye from Aqueous Solution by Chitosan". *Indian Journal of Environment Protection*, vol. 17, n 2, pp. 95-98. (1997)

Annadurai G. and Krishnan M.R.V, "Batch Equilibrium Adsorption of Reactive Dye onto Natural Biopolymer". *Iranian Polymer Journal*, vol.6, n3, pp. 169-175. (1997)

Asfour H.M., Nassar M.M., Fadali O.A. and El-Geundi M.S., "Colour removal from textile effluents using hardwood sawdust as an absorbent". *Journal of Chemical Technology and Biotechnology*, vol. 35, pp.28-35. (1985)

Beydilli M.I., Pavlostathis S.G. and Tincher W.C., "Decolorization and toxicity screening of selected reactive azo dyes under methanogenic conditions". *Water Science Technology*, vol. 38, pp. 224-232. (1998)

Blair H.S., Ho T.C., "Studies in the adsorption and diffusion of ions in chitosan". *Journal of Chemical Technology and Biotechnology*, vol. 31, pp. 6-10. (1980)

Bolton J.R. and Cater S.R., "Homogeneous photodegradation of pollutants in contaiminated water: An introduction". In Helz G.R., Zepp R.G. and Crosby D.G., eds., *Aquatic and Surface Photochemistry*, Lewis Publisher, pp. 467-490. (1994)

Bulter J.A.V. and Ockrent C., "Studies in electrocapillarity. Part III, The surface tensions of solutions containing two surface containing two surface-active solutes". *Journal of Physical Chemistry*, vol. 34, pp. 2841-2845. (1930)

Carlough M., Hudson S. and Smith B., "Diffusion Coefficients of Direct Dyes in Chitosan". *Journal of Applied Polymer Science*, vol. 42, pp. 3055-3038. (1991)

Chang J.S. and Lin Y.C., "Fed-batch bioreactor strategies for microbial decolorization of azo dye using a Pseudomonas luteola strain". *Biotechnology Progress*, vol. 16, pp.979-985. (2000)

Chaudhuri S.K. and Sur B., "Oxidative decolorization of reactive dye solution using fly ash as catalyst". *Journal of Environmental Engineering*, vol. 126, pp. 583-594. (2000)

Cheung C.W. "MPhil. Thesis". The Hong Kong University of Science and Technology. (1999)

Cheremisinoff, P.N., *Hankbook of Water and Wastewater Treatment Technology*, New York, Marcel Dekker, Chapter 11, pp. 413-447. (1995)

Choy K.H.K "MPhil. Thesis". The Hong Kong University of Science and Technology. (1999)

Chu W. and Ma C.W., "Quantitative prediction of direct and indirect dye ozonation kinetics". *Water Research*, vol. 34, pp. 3153-3160. (2000)

Chu W. and Tsui S.M., "Photo-sensitization of diazo disperse dye in aqueous acetone". *Chemosphere*, vol.39, pp.1667-1677. (1999)

Cook M.M., "Sodium borohydride dye reduction in wastewater", *In Environmental Chemistry of Dyes and Pigments*, Reife A. and Freeman H.S., eds., John Wiley & Sons, Inc. New York, pp. 33-41. (1996)

Cooper P., "Removing color from dyehouse waste waters – a critical review of technology available", *Journal of Society of Dyers and Colourists*, vol.109, pp.97. (1993)

Coughlin R.W., Deshaies M.R. and Davis E.M. "Chitosan in crab shell wastes purifies electroplating wastewater". *Environmental Progress*, vol. 9, n. 1, pp.35-39. (1990)

Dubinin M.M. and Radushkevich L.V., "Equation of the characteristic curve of activated charcoal". *Chem. Zentr.*, vol. 1, pp. 875. (1947)

El-Geundi M.S., "Colour removal from textile effluents by adsorption techniques". *Water Research*, vol. 25, no. 3, pp. 271-273. (1991)

Freundlich, H.M.F., "Over the adsorption in solution". *Journal for Physical Chemistry*, vol. 57, pp. 385-470. (1906)

Furusawa, T. and Smith, J.M., "Fluid-particle and intraparticle mass transport in slurries, *Industrial Engineering and Chemistry Fundamentals*, vol. 12, pp. 197-203. (1973)

Ganesh R., Boardman G.D. and Michelsen D., "Fate of azo dyes in sludges", *Water Research*, vol.28, pp.1367-1376. (1994)

George A.F. Roberts, *Chitin Chemistry*, The Macmillan Press Ltd, (1992)

Grau P., "Textile industry wastewaters treatment". *Water Science and Technology*, vol.24, pp. 97-103. (1991)

Hamada K., Nishizawa M., Yoshida D. and Mitsuishi M., "Degradation of an azo dye by sodium hypochlorite in aqueous surfactant solutions". *Dyes and Pigments*, vol. 78, pp. 161-164. (1997)

Hsu Y.C., Yen C.H. and Huang H.C., "Multistage treatment of high strength dye wastewater by coagulation and ozonation". *Journal of Chemical Technology and. Biotechnology*, vol. 71, pp. 71-76. (1998)

Jain J.S. and Snoeyink V.L., "Adsorption from bisolute systems on active carbon". *Journal of Water Pollution Control Federation*, vol. 45, pp. 2463-2479.

Juang R.S. and Ju C.Y., "Kinetics of sorption of Cu(II) – Ethylenediaminetetracetic acid chelated anions on cross-linked, polyaminated chitosan beads". *Indian Engineering Chemical Research*, vol. 37, pp. 3463-3469. (1998)

Kim C.Y., Choi H.M. and Cho H.T., "Effect of deacetylation on sorption of dyes and chromium on chitin". *Journal of Applied Polymer Science*, vol. 63, n. 6, pp.725-736. (1997)

Knorr D., "Dye Binding Properties of Chitin and Chitosan". *Journal of Food Science*, vol. 48, pp. 36-41. (1983)

Lagergren, S., "About the theory of so-called adsorption of soluble substances". *Kungliga Svenska Vetenskapsakademiens. Handlingar*, Band 24, no.4, pp.1-39. (1898)

Langmuir, I., "The adsorption of gases on plane surfaces of glass, mica and platinum". *Journal American Chemical Society*, vol. 40, pp. 1361-1368. (1918)

Laszlo J.A., "regeneration of dye-saturated quaternized cellulose by bisulfite-mediated borohydride reduction of dye azo groups: An improved process for decolorization of textile wastewater". *Environmental Science and Technology*, vol. 31, pp. 3647-3653. (1997)

Lin S.H., and Lin C.M., "Treatment of textile waste effluents by ozonation and chemical coagulation". *Water Research*, vol. 27, pp. 1743-1748. (1993)

Low, M.J.D., "Kinetics of chemisorption of gases on solids". *Chemical Reviews*, vol. 60, pp. 267-312. (1960)

Marc S.R., "Asian textile dye makers are a growing power in changing market", *C&EN Northeast News Bureau*, pp.10-12. (1996)

Marquardt, D.W., "An algorithm for least-squares estimation of nonlinear parameters". *Journal of Society (Indian) Applied Mathematics*, vol. 11, pp. 431-441. (1963)

Marshall W.E., Champagne E.T. and Evans W.J., "Use of rice milling byproducts (hulls and bran) to removal ions from aqueous solution". *Journal of Environmental Science and Health Part A – Environmental Science and Engineering and Toxic and Hazardous Substance Control*, vol.28, pp. 1977-1992. (1993)

Marshall W.E., Champagne E.T., "Agricultural byproducts as adsorbents for metal ions in laboratory prepared solutions and in manufacturing wastewater". *Journal of Environmental Science and Health Part A – Environmental Science and Engineering and Toxic and Hazardous Substance Control*, vol.30, pp. 241-261. (1995)

Marshall W.E. and Johns M.M., "Agricultural by-products as metal adsorbents: Sorption properties and resistance to mechanical abrasion". *Journal of Chemical Technology and Biotechnology*, vol. 66, pp.192-198. (1996)

Mattheus F.A.G., "*Applications of chitin and chitosan*". Technomic Publication. (1997)

Mckay G. and Allen S.J., "Low-cost adsorbents in continuous processes". *Biosorbents for metal ions*, U.K., Taylor & Francis, Chapter 9, pp. 183-219. (1997)

Mckay G., Blair H.S. and Gardner J.R., "Adsorption of dyes on chitin. I. Equilibrium studies". *Journal of Applied Polymer Science*, vol. 27, pp. 3043-3057. (1982)

Mckay G., Blair H.S. and Gardner J.R., "Adsorption of dyes on chitin. III. Intraparticle diffusion processes". *Journal of Applied Polymer Science*, vol. 28, pp. 1767-1778. (1983)

Mckay G., El Geundi M. and Nassar M.M., "Equilibrium studies during the removal of dyestuffs from aqueous solutions using pith". *Water Research*, vol. 21, pp.1513-1520. (1987)

Mckay G., Otterburn M.S. and Aga J.A., "Fuller's earth and fired clay as adsorptions for dyestuffs equilibrium and rate studies". *Water, Air and Soil Pollution*, vol. 24, pp. 307-322. (1985)

Mckay G. and Porter J.F., "A comparison of Langmuir based models for predicting multicomponent metal ion equilibrium sorption isotherms on peat'. *Transactions of Institute of Chemical Engineering*, vol. 75, Part B, pp. 171-180. (1997)

Mckay G. and Porter J.F., "Equilibrium parameters for the sorption of copper, cadmium and zinc ions onto peat". *Journal of Chemical Technology and Biotechnology*, 69, pp. 309-320. (1997)

Mckay G., Ramprasad G. and Pratapa Mowli P., "Equilibrium studies for the adsorption of dyestuffs from aqueous solutions by low-cost materials". *Water, Air and Soil Pollution*. vol. 29, pp. 273-283. (1985)

Mckay G., Ramprasad G. and Pratapa Mowli P., "Desorption and regeneration of dye colours from low-cost materials". *Water Research*, vol. 21, n 3, pp. 375-377. (1986)

Michelson D.L., Fulk L.L., Woodly R.M. and Boardman G.D., "Adsorption and chemical pretreatment of reactive dye discharges". *Emerging Technologies in Hazardous Waste Management III*, pp.119-136. (1993)

Muzzarelli R.A.A., "*Chitin*". Pergamon Press, Oxford. (1977)

Okieimen F.E., Okundia E.U and Ogbeifan D.E., "Sorption of cadmium and lead ions on modified groundnut (Arachis hypogea) husks". *Journal of Chemical Technology and Biotechnology*, vol. 51, pp. 97-103. (1991)

O'Neill C., Hawkes F.R., Esteves S.R.R., Hawkes D.L. and Wilcox S.J., "Anaerobic and aerobic treatment of a simulated textile effluent". *Journal of Chemical Technology and Biotechnology*, vol. 74, pp. 993-999. (1999)

O'Neill C., Hawkes F.R., Hawkes D.L., Lourenco N.D., Pinheiro H. and Delee W., "Colour in textile effluents – sources, measurement, discharge consents and simulation: a review". *Journal of Chemical Technology and Biotechnology*, vol.74, pp. 1009-1018. (1999)

Perineau F., Molinier J. and Gaset A.,"Adsorption of ionic dyes on wool carbonizing waste". *Water Research*, vol. 17, pp. 559-567. (1983)

Peter A.T. and Freeman H.S., *Physico-chemical principles of color chemistry*, Blackie Academic & Professional, London. (1996)

Philippe C.V., Roberto B. and Willy V., "Treatment and reuse of wastewater from the textile wet-processing industry: review of emerging technologies". *Journal of Chemical Technology and Biotechnology*, vol. 72, pp.289-302. (1998)

Poulios I. And Tsachpinis I., "Photodegradation of the textile dye Reactive Black 5 in the presence of semiconducting oxides". *Journal of Chemical Technology and Biotechnology*, vol.74, pp.349-357. (1999)

Radke C.J. and Prausnitz J.M., "Thermodynamics of multi-solute adsorption from dilute liquid solutions". *AIChE Journal*, vol. 18, no.4.

Ravi Kumar M.N.V., Rajakala Sridhari T., Durga Bhavani K. and Pradip Kumar Dutta, "Trends in Color Removal from Textile Mill Effluents". *Colourage*, pp. 25-34. (1998)

Redlich, O. and Peterson, D.L., "A useful adsorption isotherm". *Journal of Physical Chemistry*, vol. 63, pp.1024-1026. (1959)

Ritchie, A.G., "Alternative to the Elovich equation for the kinetics of adsorption of gases on solids". *Journal of Chemical Society-Faraday Transactions*, vol. 73, pp. 1650-1653. (1977)

Safarik I., "Removal of organic polycyclic compounds from water solutions with a magnetic chitosan based sorbent bearing copper phthalocyanine dye". *Water Research*, vol. 29, n1, pp. 101-105. (1995)

Sheindorf C., Rebhun M. and Sheintuch M., "Organic pollutants adsorption from multi-component systems modeled by Freundlich type isotherm". *Water Research*, vol. 16, pp. 357-362. (1982)

Shimizu Y., Kono K., Kim I.S. and Takagishi T., "Effects of added metal ions on the interaction of chitin and partially deacetylated chitin with an azo dye carrying hydroxyl groups". *Journal of Applied Polymer Science*, vol. 55, pp. 255-261. (1995)

Smith B., Koonce T., Hudson S., "Decolorizing Dye Wastewater Using Chitosan". *American Dyestuff Reporter*, Oct., pp.18-36. (1993)

Sopa C., Munsin T. and Thongchai P., "Anaerobic decolorization of reactive dyebath effluents by a two-stage UASB system with tapioca as a co-substrate". *Water Research*, vol. 34, pp. 2223-2232. (2000)

Sarasa J., Roche M.P., Ormad M.P., Gimeno E., Puig A. and Ovelleiro J.L., "Treatment of a wastewater resulting from dyes manufacturing with ozone and chemical coagulation". *Water Research*, vol. 32, pp. 2721-2727. (1998)

Smith B., Koonce T. and Hudson S., "Decolorizing dye wastewater using chitosan". *American Dyestuff Reporter*, Oct., pp. 18-36. (1993)

Suen, S.Y., "A comparison of isotherm and kinetic models for binary-solute adsorption to affinity membranes." *Journal of Chemical Technology and Biotechnology*, vol. 65, pp. 249-257. (1996)

Stefancich S., Delben F. and Muzzarelli R.A.A., "Interaction of soluble chitoans with dyes in water. I. Optical evidence". *Carbohydrate Polymers*, vol. 24, pp. 17-23. (1994)

Tang W.Z. and Chen R.Z., "Decolorization kinetics and mechanisms of commercial dyes by H_2O_2/Iron powder system". *Chemosphere*, vol. 32, pp. 947-958. (1996)

Toth J., "State equations of the solid-gas interface layer". *Acta. Chem. Acad. Hung.*, vol.69, pp. 311-317. (1971)

Trotman, E.R., *Dyeing and chemical technology of textile fibers*, Chapter 12, 4th Edition, London, England. (1970)

Tunay O., Kabdasli I., Eremektar G. and Orhon D., "Color removal from textile wastewaters", *Water and Science Technology*, vol.34, pp.9-16. (1996)

Ungarish, M. and Aharoni, C., "Kinetics of chemisorption, deducing kinetic laws from experimental date". *Journal of Chemical Society-Faraday Transactions 1*, vol. 77, pp. 975-985. (1981)

Vandevivere P.C., Bianchi R.and Verstracte W., "Treatment and reuse of wastewater from the textile wet-processing industry: Review of emerging technologies", *Journal of Chemical Technology and Biotechnology*, vol.78, pp. 289-302. (1998)

Walker G.M. and Weatherley L.R., "Adsorption of acid dyes on to granular activated carbon in fixed beds". *Water Research*, vol. 31, pp. 2093-2101. (1997)

Wu T., Lin T., Zhao J., Hidaka H. and Serpone N., "TiO_2-assisted photodegradation of dyes. 9. Photooxidation of a squarylium cyanine dye in aqueous dispersions under visible light irradiation". *Environmental Science Technology*, vol. 33. pp.1379-1387. (1999)

Yoshida H., Fukuda S., Okamoto A. and Kataoka T., "Recovery of direct dye and acid dye by adsorption on chitosan fiber – Equilibria". *Water Science and Technology*, vol. 31, pp. 1667-1676. (1991)

Yoshida H., Okamoto A. and Kataoka, T., "Adsorption of acid dye on cross-linked chitosan fiber: Equilibria". *Chemical Engineering Science*, vol. 48, n12, pp. 2267-2272. (1993)

Yoshida H. and Takemori T., "Adsorption of direct dye on cross-linked chitosan fiber: Breakthrough curve". *Water Science and Technology*, vol. 35, n7, pp. 29-37. (1997)

Young L. and Yu J., "Ligninase-catalysed decolorization of synthetic dyes". *Water Research.*, vol. 31, pp. 1187-1193. (1997)

Zepp R.G. and Cline D.M., "Rates of direct photolysis in aquatic environment". *Environmental Science Technology*, vol. 11, pp. 359-366. (1997)

Zollinger H., *Color chemistry: syntheses, properties, and applications of organic dyes and pigments.* Weinheim, Neq York. (1991)